Novel Degradable Polymeric Materials for Biomedical and Antibacterial Applications

Dissertation

Zur Erlangung des Doktorgrades der Naturwissenschaften (Dr. rer. nat)

dem Fachbereich Chemie

der Philipps-Universität Marburg

vorgelegt von

Dipl.-Chem. Yi Zhang

aus Peking V.R. China

Marburg/Lahn 2012

Vom Fachbereich Chemie der Philipps-Universität Marburg als Dissertation am angenommen.

Erstgutachterin: Prof. Dr. Seema Agarwal
Zweitgutachter: Prof. Dr. Joachim H. Wendorff

Tag der mündlichen Prüfung: 11. 09. 2012

Die vorliegende Arbeit entstand auf Anregung und unter Leitung von

Frau Prof. Dr. Seema Agarwal

am Institut für Makromolekulare Chemie
der Philipps-Universität Marburg

For my parents

Table of Contents

Chapter I: Introduction and Aim

1.1 Degradable Polymers

Biodegradable polymers have a huge field of applications, from agricultural over daily life usage to the biomedical area.[1–3] The global production of biodegradable polymers increases annually. In 2008 174,000 metric tons were produced. In 2011 this value tripled. In 2015 the production will probably increase to 714,000 metric tons (Figure 1).

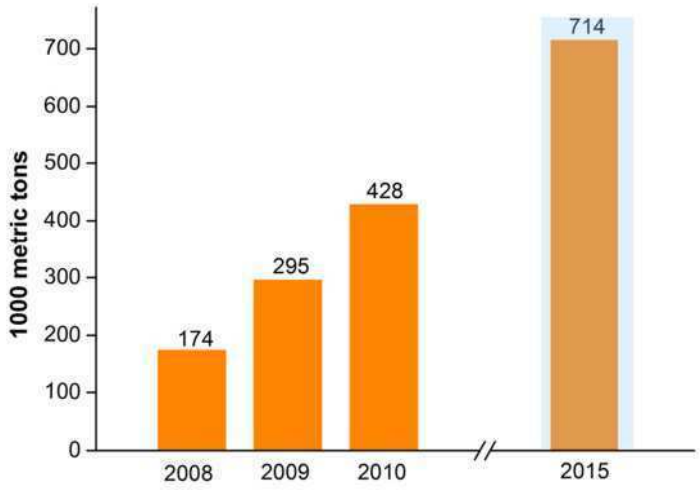

Figure 1: Global production capacity for bioplastics according to the European bioplastics source.[4]

The growing need for biodegradable polymers is mainly caused by suitable degradation kinetics for different applications.[5] In terms of application biodegradable polymers can be divided into two major groups: the medical and the ecological applications.[6] For example the poly(lactic-*co*-glycolic acid) (PLGA) and collagen are used for scaffolding applications. In this case the biodegradability kinetics of the scaffold polymer should correlate with the growth velocity of the tissue regeneration. Biodegradable polymers like polyhydroxyalkanoates (PHAs) can also be used as potential carrier to deliver drugs to

infected body parts in an effective and non-invasive way.[7] The copolymer *hy*-PEI-*g*-PCl-*b*-PEG is used for DNA transfection.[8] For these kinds of usage the biodegradable polymer should be stable for a certain time in a physiological environment until it can serve its purpose. Eventually the polymer is supposed to degrade completely to leave no foreign materials in the body. Biodegradable polymers for ecological applications like Ecoflex® (BASF) and Ecoflex® starch blends are used as food package, in agriculture and forestry. Ecoflex® film can be 100% degraded in compost.[9] Some typical biodegradable polymers are classified and shown in Figure 2.

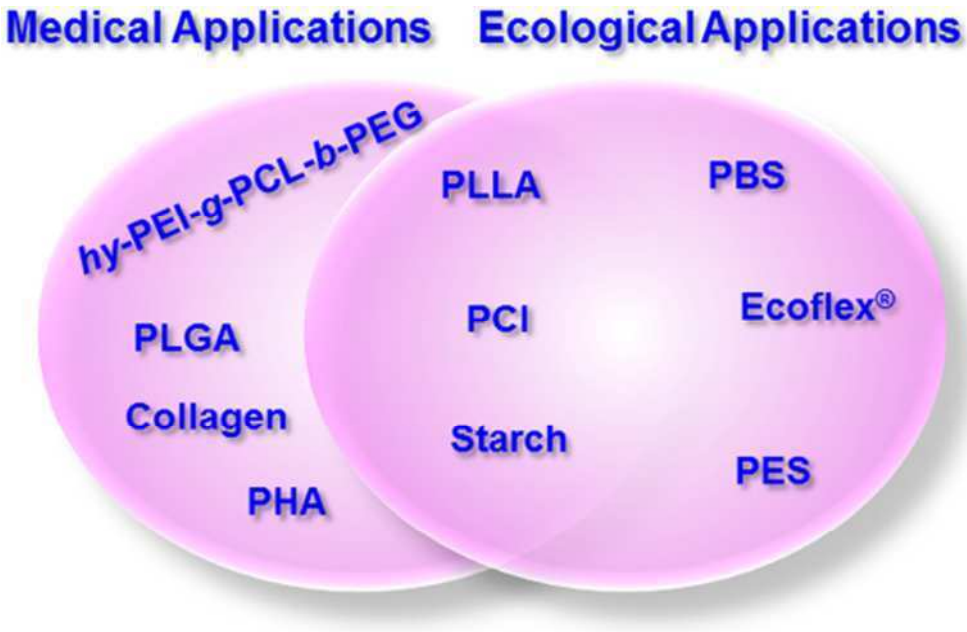

Figure 2: Application fields of biodegradable polymers. PHA: polyhydroxyalkanoates: *hy*-PEI-*g*-PCl-*b*-PEG: *hyper-branched*-polyethylenimine-*grafted*-polycaprolacton-*co*-polyethylenglycol; PLGA: poly(L-lactic-*co*-glycolic acid); PLLA: poly(L-lactide); PCl: polycaprolacton; PBS: poly(butylene succinate); PES: poly(ethylene succinate).

In order to synthesize suitable degradable polymers for different applications it is important to understand the relationship between polymer architecture and degradation mechanism. Most saturated carbon backbone in a polymer is not degradable, but polymers like polyesters, polyamides are degradable. This illustrates the importance of heteroatoms in the main chain in

order to open degradation pathways. Hence to synthesize degradable polymers it is necessary to introduce functional groups into the polymer chain.[10]

Cyclic ketene acetals are intensively investigated in the synthesis of degradable polymers. In the 1970's *Bailey's* group synthesized for the first time the cyclic ketene acetal 2-methylene-1,3-dioxepane (MDO) with an exo-methylene group, which readily undergoes radical ring-opening polymerisation.[11] Under ideal reaction conditions polyesters are formed by this radical ring-opening polymerization. Furthermore other cyclic ketene acetals, like 5,6-benzo-2-methylene-1,3-dioxepane (BMDO), were also synthesized and investigated for ring-opening polymerization (ROP) reactions (Figure 3a). In *Agarwal*'s group the homopolymerisation and copolymerization of cyclic ketene acetals are intensively studied to introduce ester groups in a polyvinyl polymer backbone by radical polymerization (Figure 3b).[12] This radical copolymerisation with cyclic ketene acetats gives the opportunity to incorporate ester groups in ordinary plastics, which until today are considered inert against biological degradation. (Figure 3c).

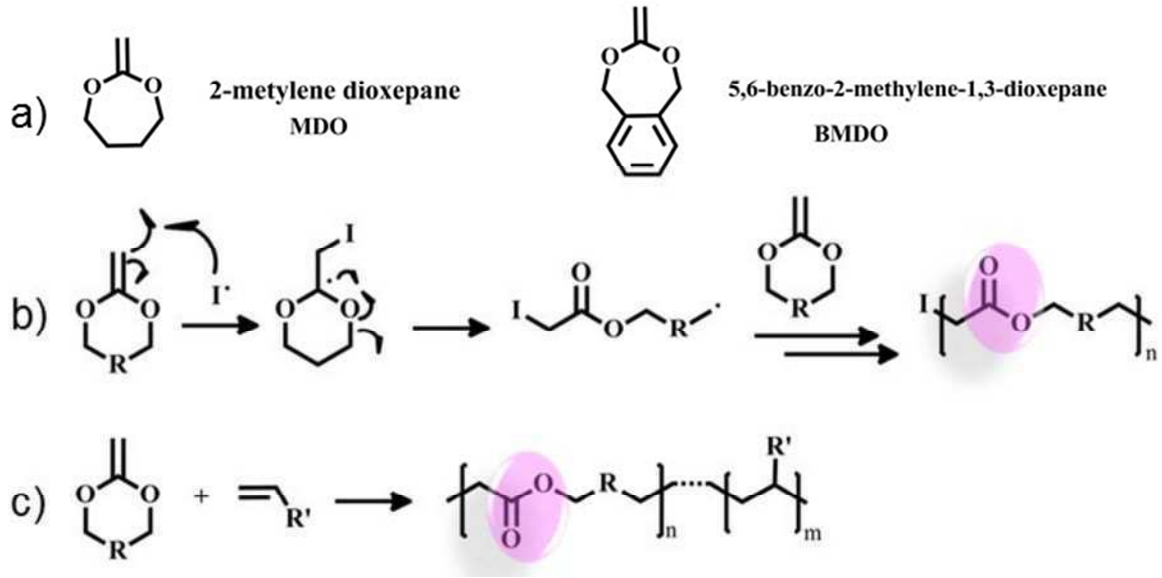

Figure 3: a) MDO and BMDO structures; b) radical ring-opening polymerization of cyclic ketene acetals; c) copolymerization of vinyl monomers and cyclic ketene acetals.

1.2 Deoxyribonucleic Acid (DNA) Transfection

1.2.1 Gene Therapy

Genes are the basic physical and functional units of heredity, which are carried on chromosomes.[13] Cancer and many genetic diseases are caused by genetic disorders which means that the encoded proteins are unable to carry out their normal functions. Gene therapy is a promising method to treat these genetic defects by transferring functional genetic material as a pharmaceutical agent into specific cells of the patient.[14,15] For this treatment the functional genes have to be delivered into the eukaryotic cells to replace the mutated gene. After the correction of the abnormal gene, gene expression can be observed.

1.2.2 Gene Carriers

The major challenge for gene therapy is the delivery of sufficient DNA into specific target cells to achieve the desired gene expression.[16] DNA can be delivered into the cell nucleus via specific carriers, two major groups of these carriers are the viral gene carriers and the non-viral gene carriers (Figure 4).[17]

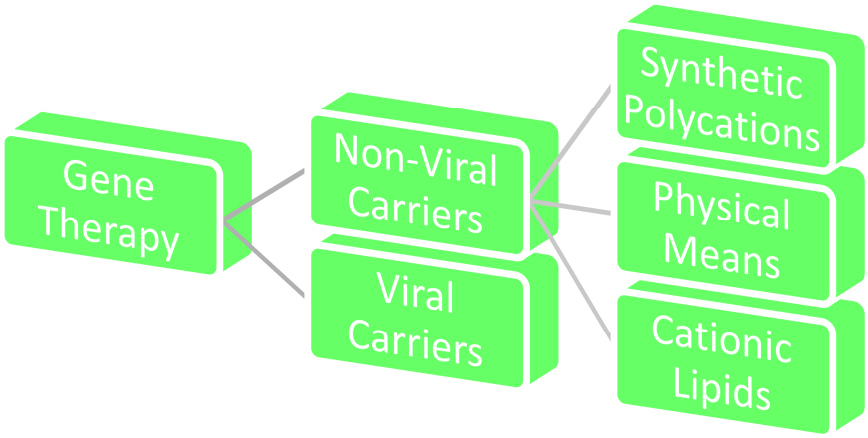

Figure 4: Classification of the gene carriers for gene therapy.

a) Viral Gene Carriers

Since viruses are the simplest life form and only consist of ribonucleic acid (RNA) and a protein shell; they can be used to transport functional DNA into eukaryotic cells. A virus generally attaches itself onto the surface of a target cell and introduces its RNA into the host cell by an injection mechanism. The disadvantages of viral gene carriers are the high cost, high immunogenicity and safety concerns.[18]

b) Non-Viral Gene Carriers

In contrast to the viral gene carriers, the non-viral gene carriers have the advantages of low-toxicity, non-immunogenicity and feasibility to be produced on a large scale. Non-viral gene carriers can be divided into three main groups, physical means, cationic lipids and synthetic polycations for gene transfection (Figure 4).[19–22]

Synthetic Polycations. Non-viral gene delivery systems based on synthetic polycations have recently attracted significant attention because of easy up-scaling, storage stability, high safety and low cost.[23,24]

A good polymeric gene carrier works as follows (Figure 5). First the cationic polymer forms a complex with the negatively charged DNA, which is named polyplex. The polyplexes are based on electrostatic interactions between the phosphate groups of the DNA and the positively charged polycation. A suitable polycation DNA carrier protects the DNA from degradation in the physiological environment and provides an easy cellular uptake into the eukaryotic cells. Cells prefer small polyplexes with a positive zeta potential. Inside the cell the polymer releases the DNA near or inside the cell nucleus, so the DNA can be transcribed and translated. After the translation of the gene the gene translation is successful. The gene expression can be detected.

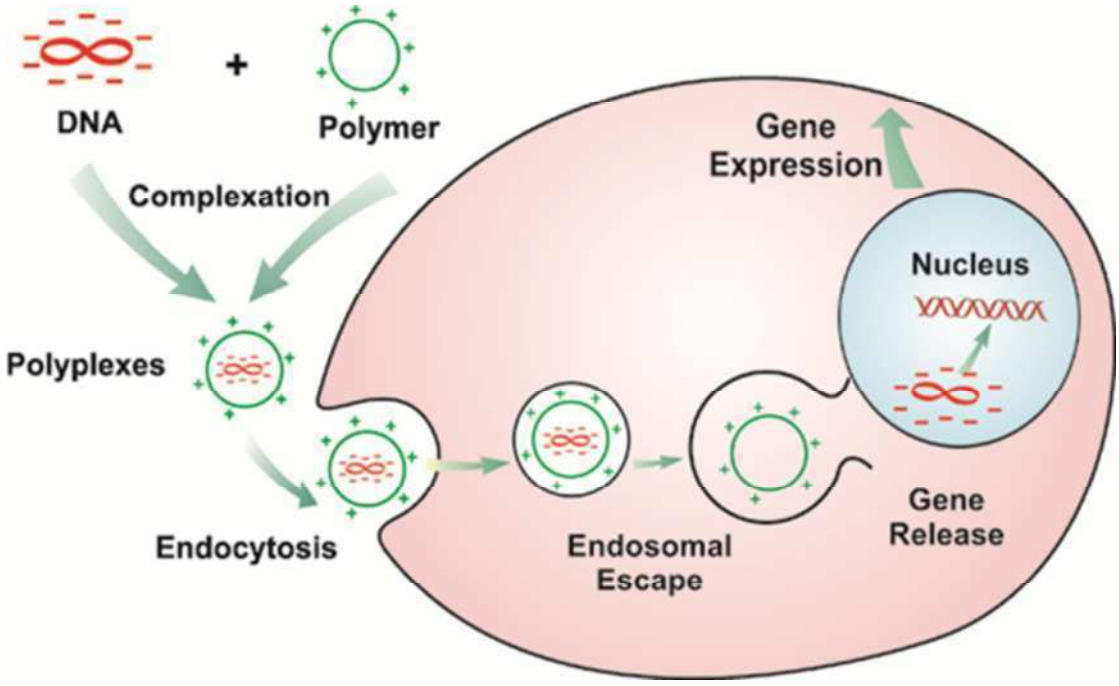

Figure 5: DNA transfection mechanism using a cationic polymer as carrier.

In the last few years, polyethylenimine (PEI) has become a gold standard for non-viral gene delivery due to its high transfection efficiency.[25] The main drawback of PEI is the high cytotoxicity and non-degradability. Recently a lot of attention is being focused on the reduction of the polymer carriers' cytotoxicity, the immunogenicity and increase the biodegradability and the transfection efficiency. For example *Kwon* and coworkers have shown a biodegradable hybrid recombinant block copolymer p[Asp(DET)]$_{53}$ELP(1–90), which possesses a thermo-responsive elastin-like polypeptide (ELP) segment and a diethylenetriamine (DETA) modified poly-L-aspartic acid segment, for gene delivery (Figure 6).[26]

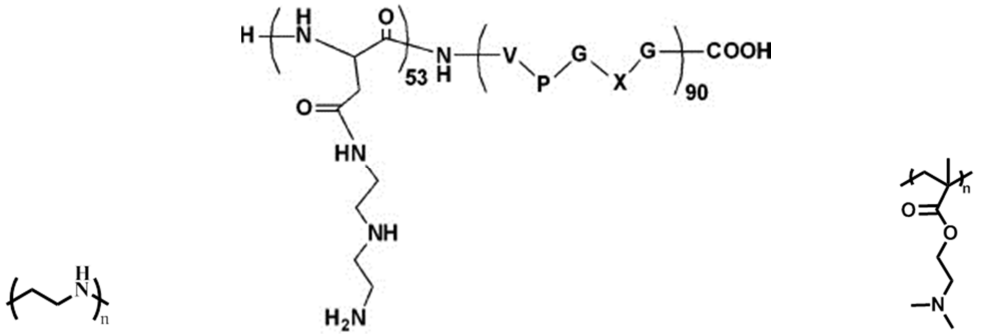

Figure 6: Chemical structure of linear PEI, p[Asp(DET)]$_{53}$ELP(1–90) and PDMAEMA (left to right).[26]

Kissel and coworkers have demonstrated a series of amphiphilic copolymers of *hy*-PEI-*g*-PCL-*b*-PEG, which are biodegradable. They showed that the transfection efficiency of this copolymer depends on the grafting density of the PCL-*b*-PEG chains (Figure 7).[27]

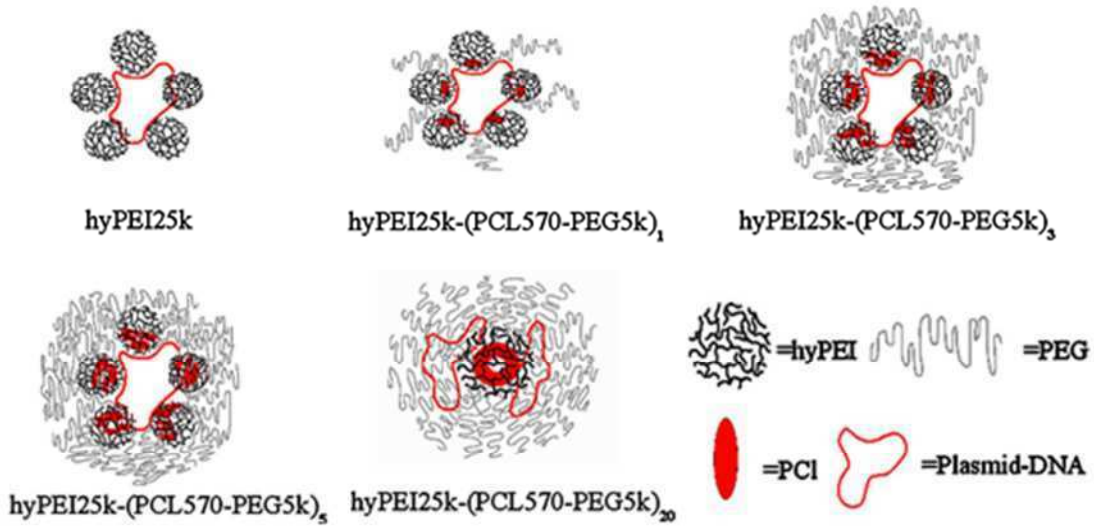

Figure 7: Polyplexes of amphiphilic copolymer *hy*-PEI-*g*-PCL-*b*-PEG grafted with different density of the PCL-*b*-PEG chains.[27]

Poly*(N,N*-dimethylaminoethyl methacrylate) (PDMAEMA) and its copolymers are recently also intensively investigated as alternative non-viral carrier to PEI and PEI based copolymers. *Zhong* and his colleagues presented a triblock copolymer poly-(dimethylaminoethyl methacrylate)-SS-poly(ethylene glycol)-SS-poly-(dimethylaminoethyl methacrylate) (PDMAEMA-SS-PEG-SS-PDMAEMA) which is able to form reversibly shielded DNA polyplexes for gene transfection.[28] Figure 8 shows schematically the PDMAEMA-SS-PEG-SS-PDMAEMA triblock copolymer's ability to effectively condense DNA into partially shielded nano-sized polyplexes and the uptake by a cell. In the cells the disulfide bonds cleave and result in rapid deshielding and DNA release into the cytoplasm and cell nucleus.

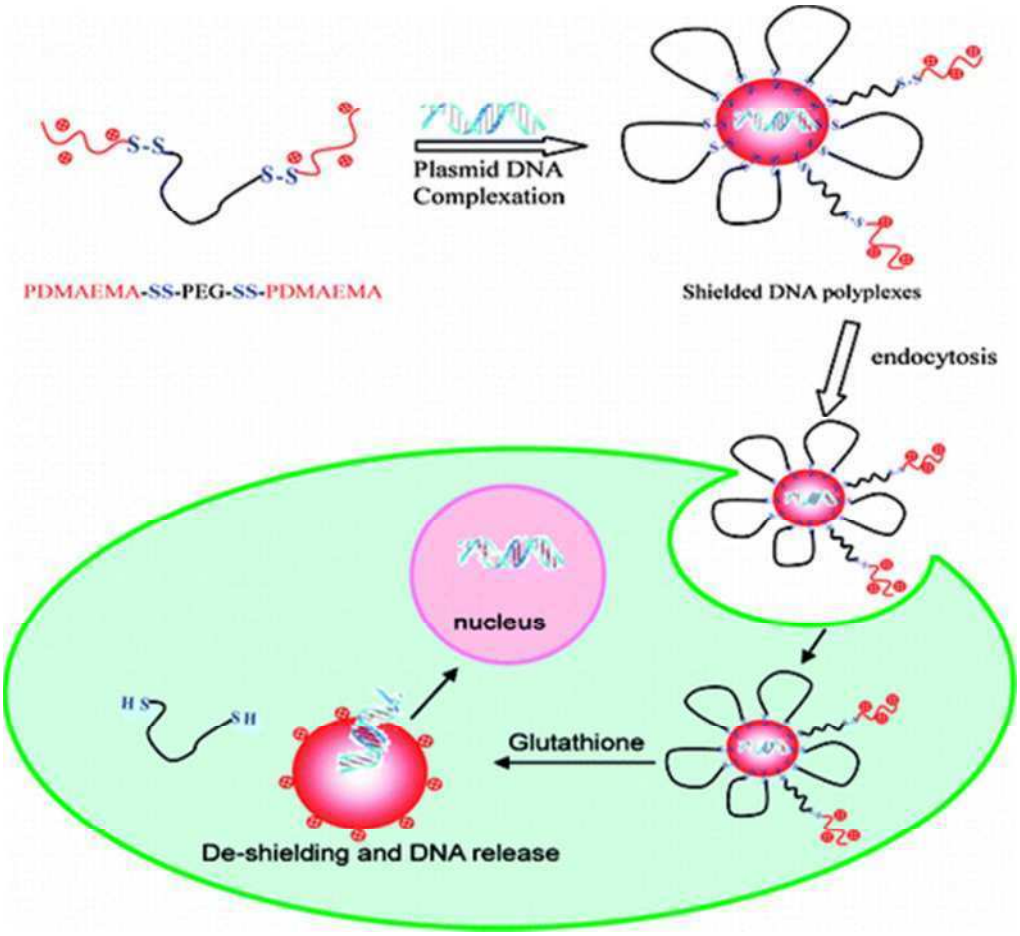

Figure 8: (PDMAEMA-SS-PEG-SS-PDMAEMA) triblock copolymer for the gene transfection procedure.[28]

1.2.3 Detection Method for Gene Transfection Efficiency – Luciferase Assay

The DNA transfection efficiency can be determined by the luciferase assay.[29] This assay uses the bioluminescence of the oxidizing enzyme firefly luciferase from the firefly *Photinus pyralis* to yield an easily detectable signal (Figure 9). First a firefly luciferase sequence containing fragment of a plasmid is used. After successful transfection, the DNA-fragment is transcribed and translated into the enzyme luciferase. After cell lysation luciferin is added as the substrate, which at first undergoes an ATP-mediated (adenosine triphosphate) activation. This activated AMP-derivative (adenosine monophosphate) is subsequently oxidized to oxyluciferin. After that oxyluciferin, which in this reaction is formed in an excited electronic state, emits a photon while returning to its ground state. Photon emission can be easily detected and quantified. The measured light intensity is directly proportional to the protein expression level.

Figure 9: Illustration of the luciferase assay.

1.2.4 Detection Method of Polyplex Stability – Sybr Gold Assay and Heparin Assay

a) Sybr Gold Assay

The Sybr Gold assay is the most sensitive assay to quantitatively measure the condensation ability of a polymer/DNA complex. Sybr Gold is a dye which has the ability to bind to free DNA forming a Sybr Gold/DNA complex, which absorbs blue light and emits green light.[30] In contrast, the Sybr Gold cannot bind to already complexed DNA as in a polyplex (Figure 10). The sensitivity of this dye is 25 to 100 fold increased in comparison to ethidiumbromide.[31] It has furthermore a very weak background signal (ratio 1:1000), so the detected fluorescence signal can be directly correlated to the amount of free DNA.

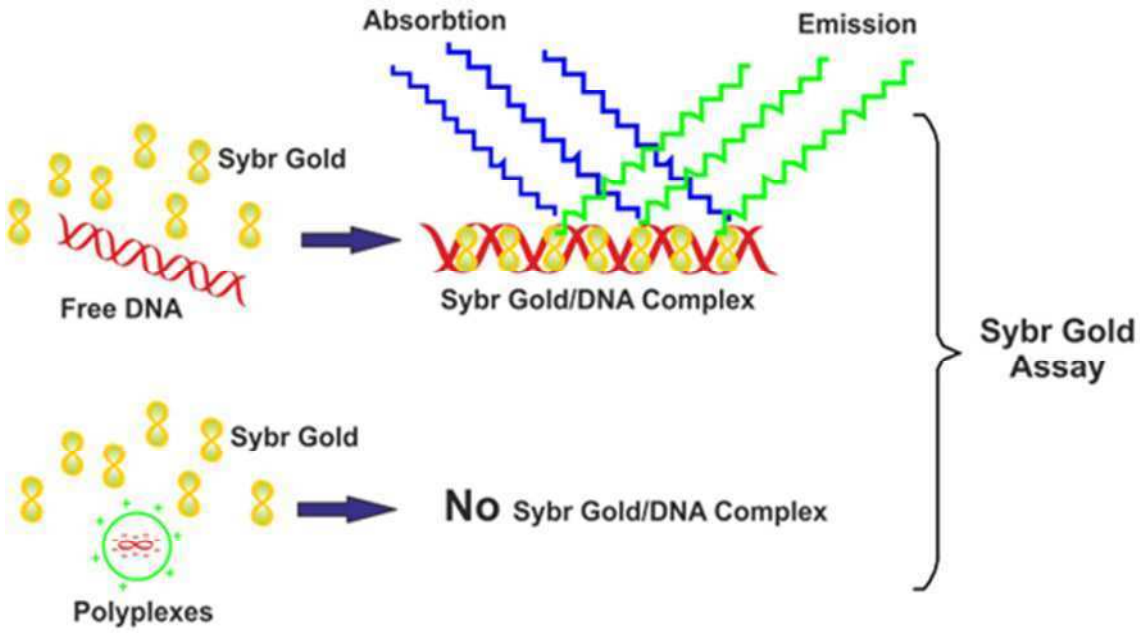

Figure 10: Illustration of the Sybr Gold assay.

b) Heparin Competition Assay

Heparin is a glycosaminoglycan with a sulfonic acid group, which is medically used as a blood anticoagulant. It has a high negative charge density as shown in Figure 11.[32,33] Since certain *in vivo* polymers as well the cell surfaces in general are negatively charged, it can simulate the *in vivo* environment in a simple assay.

In this assay Heparin is used to compete with the DNA for the affinity to the polymer. Figure 11 shows the competing reactions between Heparin and the DNA. The binding of Heparin to the polymer sets the DNA free. The amount of released DNA, which can be quantified by the change in the fluorescence intensity determined with the Sybr Gold assay, correlates with the stability of the DNA/polymer complex.

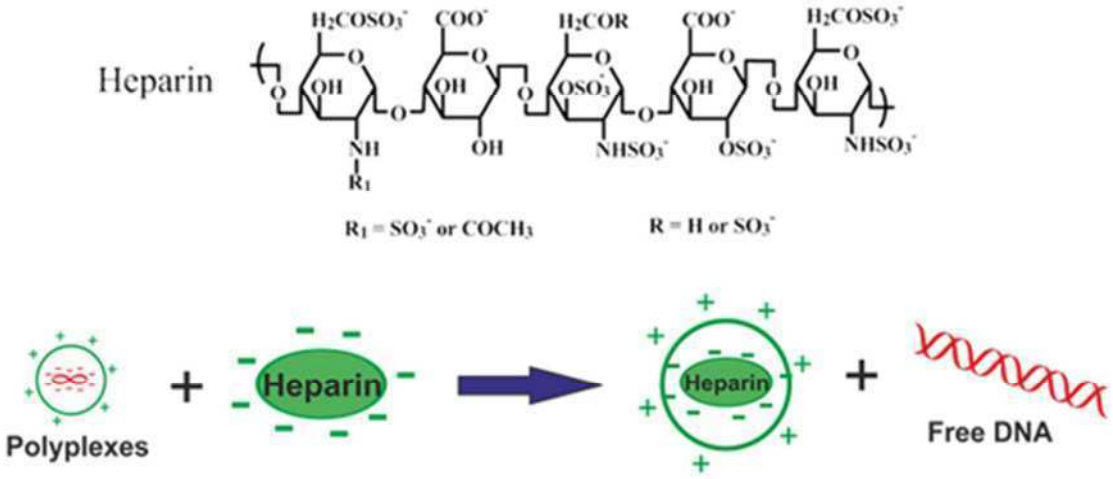

Figure 11: Illustration of the Heparin competition assay.

1.2.5 Cytotoxicity Test Using 3-(4,5-Dimethylthiazol-2-yl)-2,5-Diphenyltetrazolium Bromide (MTT) Methods

The MTT assay method is an established cell viability test method which is used for the cytotoxicity test.[34] This test is a colorimetric assay which measures the activity of enzymes that reduce MTT to formazan dyes which have a purple color. This reaction is shown in Figure 12, the tetrazole yellow ring is reduced to form the formazan purple in living cells.

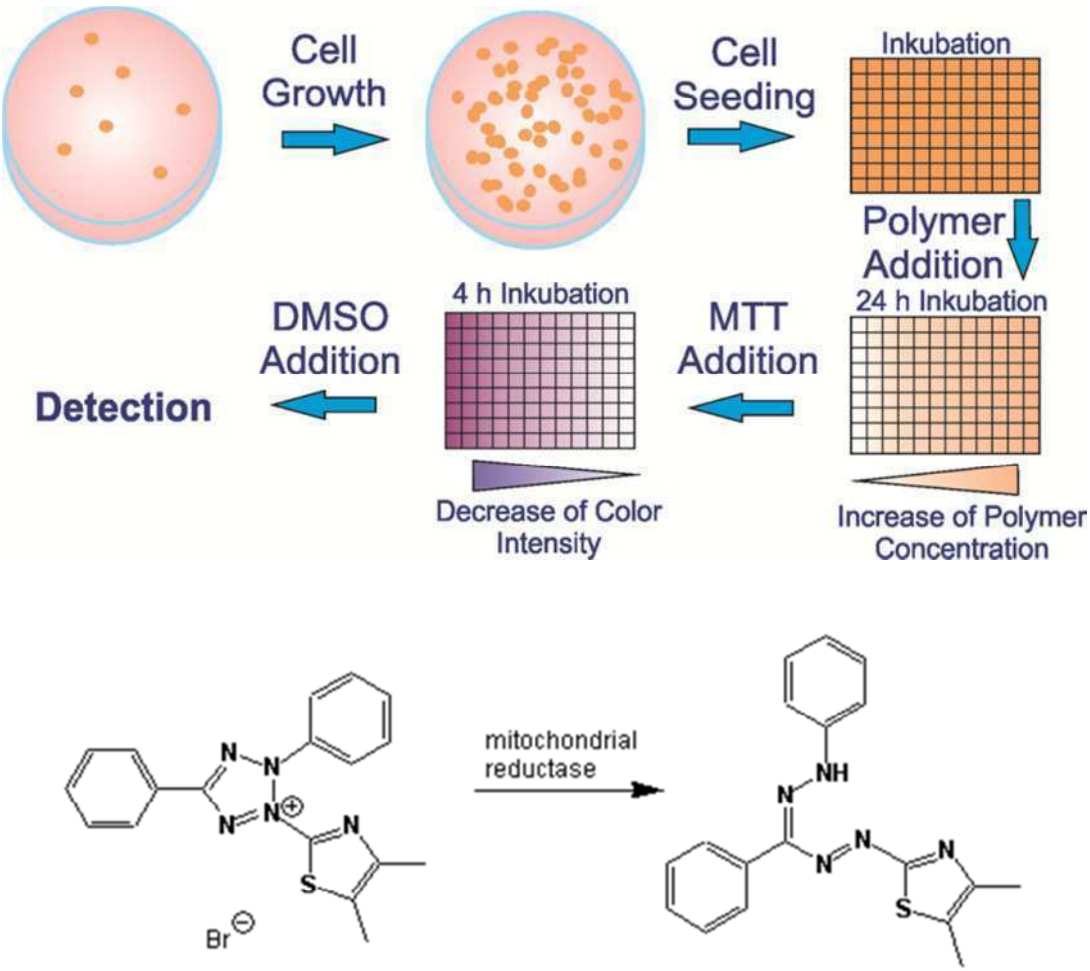

Figure 12: Illustration of the MTT test and the MTT reaction.

The test procedure was performed as follows. First the cells needed one to two weeks to grow. Then the cells were counted and seeded into a 96-well plate. About 8000 cell were placed in each well. After 24 h incubation of the cells in the well plate, the medium was exchanged and polymer solutions with different concentrations were added into the wells. After a further incubation for 24 hours, MTT was added into each well. Then the reaction shown in Figure 12 can occur. The living cells produce an enzyme, which can reduce the MTT (yellow) to the formazan (purple). Finally, the absorbance of this colored solution can be quantified by measuring at a certain wavelength (between 500 and 600 nm) with a spectrophotometer.

1.3 Sustained Drug Delivery

1.3.1 General Introduction of Sustained Drug Delivery

Drug delivery methods were developed very fast in the last few years. Conventional drug delivery methods conventioned are drops, pills, ointments and intravenous solutions. Recently a number of polymers have been developed as new drug delivery systems. Drug delivery carriers are used to minimize drug degradation and loss as well as to increase drug biocompatibility.[35] An optimization of drug loading and release properties, a long shelf life and low cytotoxicity are the important factors for drug delivery systems. Recently it has been shown that colloidal drug carriers like micelles, vesicles and nanoparticles are very promising drug delivery systems.[36] Figure 13 shows the most common colloidal drug carrier methods.

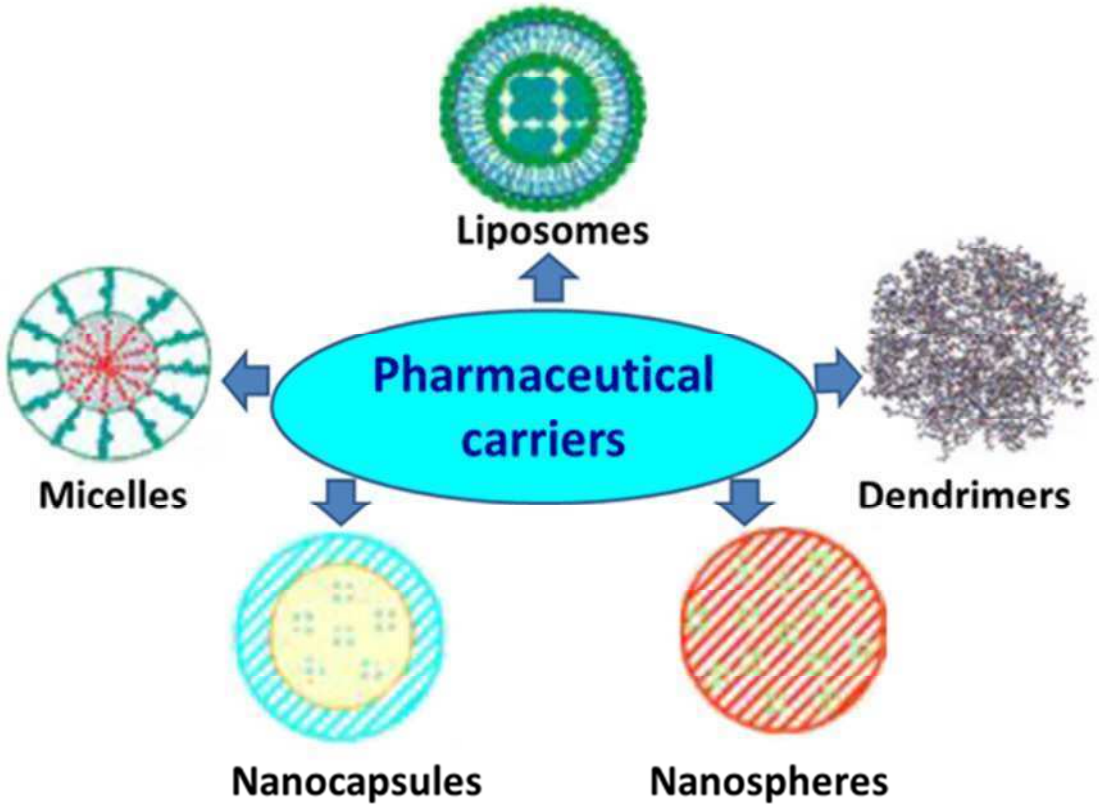

Figure 13: Illustration of the common pharmaceutical carriers.[37]

a) Micelles as Drug Carriers

In this case amphiphilic block copolymers are used to form micelles by self-assembly with a size between 5 and 50 nm in an aqueous solution.[38] The drugs can be physically entrapped in the core of the micelles. The hydrophilic blocks of the micelles can form hydrogen bonds with the aqueous phase, so that a tight shell around the micelle core is formed. This shell can prevent recognition by the reticuloendothelial system. Therefore preliminary elimination of the micelles from the bloodstream cannot occur.[37] The hydrophobic part of the micelle (inside) can protect the drug against hydrolysis and degradation.

The advantage of this system is the easy modification of the chemical composition. The size of the micelles can be readily controlled by the amphiphilic block length.

b) Dendrimers as Drug Carriers

Dendrimers are nanometer sized (1-100 nm) three dimensional highly branched polymers, which have attracted a lot of attention as controlled and targeted drug delivery systems. Dendrimers are known as well defined, mono disperse polymers which can bear various modificable surface groups.[39] The structure of dendrimers consists of an initiator core, branched repeating units and functional end groups on the outmost layer. Due to the structural configuration, a high drug loading by different techniques can be performed. The drug can for example be loaded directly by using the covalent conjugation to the surface functional groups or using a ionic interaction of the adsorption onto the surface or by exploiting the hydrophobic character inside of the branching clefts.[40] All these unique properties make the dendrimers a potent platform for both hydrophobic and hydrophilic drugs.[40]

c) Liposomes as Drug Carriers

Liposomes are spherical vesicles which are composed of one or more phospholipid bilayers with a drug containing aqueous core. They are able to encapsulate both hydrophilic and hydrophobic drugs. Due to the double layer, liposomes can protect the drug from the external environments.[41]

d) Polymeric Nanoparticles as Drug Carriers

Polymer nanoparticle carriers (including nanospheres and nanocapsules) are based on random or block copolymers which form nanoparticles with a size between 3 and 200 nm. The nanosphere carriers are a physically uniformly dispersed matrix system for the drug.[42] The naonocapsule encapsulates the drug in the core of the hollow spheres. The naonocapsules and the nanoparticles are able to protect the drug against enzymatic degradation. Some carriers are also able to control the drug release rate.[43,44] The drug release can occur by reservoir diffusion and material diffusion. It can also be facilitated by chemical control, in which the nano carrier polymer degrades for drug cleavage from a polymer chain Figure 14.[45]

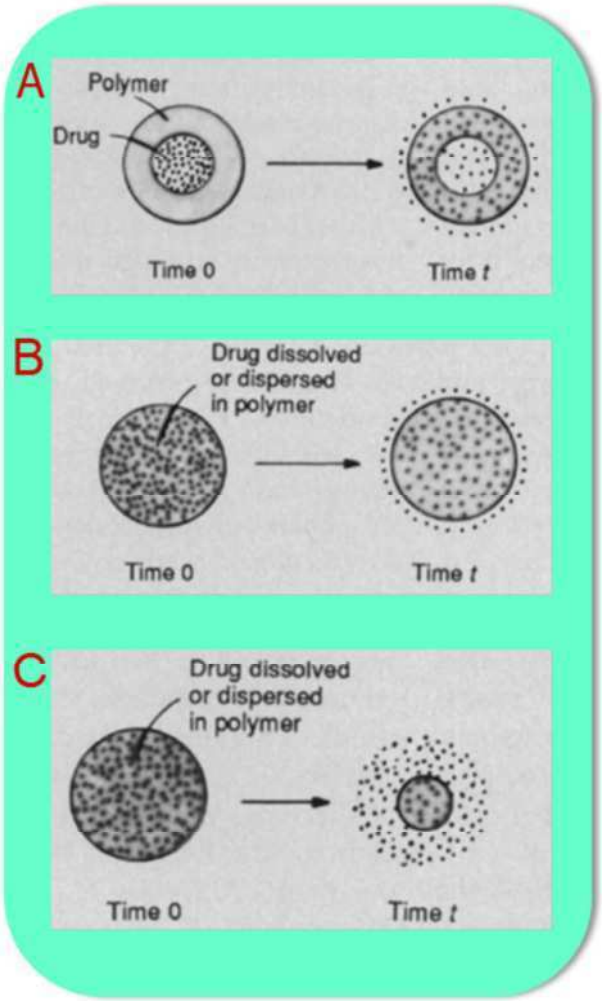

Figure 14: Polymer release mechanisms. A) common release mechanism diffusion through a polymer shell; B) drug uniformly distributed through the polymeric matrix; C) drug released by chemical mechnisms such as degradation of the polymer.[45]

In this work a degradable nanoparticle polymer carrier was synthesized and characterized.

1.4 Aim of This Thesis

The aim of this thesis is to synthesize degradable polymers for gene transfection, for sustained drug delivery and for antibacterial applications. To achieve these aims, cyclic ketene acetals like BMDO and MDO have been copolymerized with appropriate functional vinyl monomers like HEMA and DMAEMA using radical polymerization chemistry.

Chapter II: Degradable Polymers for DNA Transfection

2.1 Introduction

Gene therapy is a very promising approach for the potential treatment of genetic and inherited diseases.[14,15] Substantial research has already been carried out in the last few decades on the development of gene delivery vectors.[46–48] In spite of the high transfection efficiency of viral gene vectors, there is an ever increasing amount of number of literature on the use of non-viral gene delivery vehicles for gene therapy. This is to overcome the basic drawbacks of viral vectors which are immune response, limitations in the size of inserted DNA, difficulty in large scale pharmaceutical grade production etc.[17] Some non-viral DNA delivery systems include pure plasmid DNA, lipoplexes (DNA complexed with cationic lipids), polyplexes (nucleic acid complexes with polycations and encapsulated DNA in degradable polymer matrices). For example, cationic polymers show the ability to form polyplex with DNA by electrostatic interactions due to its polyanionic character.[19,49–52] An example of a frequently studied polycation for this purpose is polyethyleneimine (PEI), a gold standard with buffering properties (at physiological pH only 25% of the amine groups are protonated) but with the major drawback of cytotoxicity (half maximal inhibitory concentration (IC_{50}) = ~ 8 µg/ml).[53] Recently, attention has been given to poly(*N,N*-dimethylaminoethyl methacrylate) (PDMAEMA) as a non-viral gene delivery system with buffering capacity and less cytotoxicity (IC_{50} = ~ 40µg/ml) (pKa = 7.5). This polymer is prepared by radical polymerization of the corresponding vinyl monomer. It was shown for the first time in 1996 by Hennink et al. that PDMAEMA is an interesting vector for designing of a gene transfection system.[54]

PDMAEMA contains tertiary amines for the complexation of DNA and reaches 90% of the transfection efficiency of PEI (branched PEI 25 kDa). Since then, several aspects of this transfection reagent have been modified i.e. the role of molecular weight, polyplex size and transfection parameters, pH, ionic strength, temperature, viscosity, polymer/plasmid-DNA (p-DNA) ratio and the presence of stabilizers on transfection efficiency of PDMAEMA.[55–59] Despite so much research, the key problem of polycations like PEI and PDMAEMA is their non-biodegradable nature, notable toxicity and the need for further improvement of transfection efficiency.

Vinyl polymers like PDMAEMA, which can be easily synthesized by radical polymerization, could be further designed to meet these requirements. Recently, *Oupicky* et al. reported PDMAEMA copolymers with reducible –S-S- disulfide linkages using reversible addition fragmentation transfer (RAFT) polymerization with comparable cytotoxicity and gene transfection efficiency like homo PDMAEMA for the first time.[60] Unfortunately, no data (*in vivo* or *in vitro*) regarding biodegradation behavior was provided.

To solve the non-degradability issue of PDMAEMA, we recently showed the possibility of forming a degradable and less toxic PDMAEMA by introducing ester linkages into the PDMAEMA backbone**.** We consider radical-ring-opening polymerization of cyclic ketene acetals a promising method for introducing degradable ester linkages into the polymer backbone, which can be used to develop new gene transfection systems. Cyclic ketene acetals are the isomers of the corresponding cyclic lactones and can undergo radical addition at the vinyl double bond with subsequent ring-opening leading to the formation of polyesters. Free-radical copolymerization of cyclic ketene acetal 5,6-benzo-2-methylene-1,3-dioxepane (BMDO), with *N, N*-dimethylaminoethyl methacrylate (DMAEMA) can lead to the formation of degradable PDMAEMA with ester linkages in the backbone.[61] The polymers were not

soluble in water, therefore quaternization with alkyl bromide was carried out. Regardless of copolymer composition, all of the polymers were less cytotoxic than PEI and showed very high cell viability. Unfortunately, the system showed poor transfection efficiency which could be due to the strong interactions between the positively charged units and DNA. Therefore, further improvement was implemented in this system by designing a polymer avoiding quaternization of PDMAEMA. Small poly(ethylene glycol) (PEG) hydrophilic blocks were introduced onto degradable PDMAEMA units to enhance water solubility and reduce the cytotoxicity.[62,63] Again, simple free radical chemistry with cyclic ketene acetal 2-methylene-1,3-dioxepane (MDO) and BMDO als monomer was used for this purpose and a poly(ethylene oxide) (PEO) macro-azo-initiator was used. The success of this concept is highlighted in this work by giving details about synthesis, cytotoxicity, polyplex formation and gene transfection.

2.2 BMDO based Polymers for DNA Transfection

Zhang, Yi; Zheng, Mengyao; Kissel, Thomas; Agarwal, Seema. *Biomacromolecules* **2012**, *13*, 313-322.[64]

2.2.1 Experimental Part

Materials. PEO macro-azo-initiator (WAKO Company M_n = 24 kDa, PEG block = 6000 g/mol) and bromoethane (Acros, 99%) were used as received. DMAEMA (Acros) was passed through a basic alumina column to remove the inhibitor. Demethylformamide (DMF), chloroform, pentane and methanol were distilled before use. BMDO was synthesized according to our previous report.[65] Luciferase-Plasmid (pCMV-Luc) (LotNo.: PF461-090623) was amplified by The Plasmid Factory (Bielefeld, Germany). DMEM low glucose medium contains 1g/L glucose and different inorganic salts and vitamins and amino acids to reach a neutral pH 7.0-7.5 and osmolarity of 280-350 mOsmol/kg. All other chemicals were obtained from Sigma–Aldrich (Steinheim, Germany) and used as received.

Instrumentation. ^{1}H (400,13 MHz) and ^{13}C (100,21 MHz) spectra were recorded on a Bruker DRX-400 spectrometer. Tetramethylsilane was used as internal standard. The molecular weight of the polymers were measured with size exclusion chromatography at 25 °C with 1 liner PSS suprema Max 1000 Å column and a differential refractive index detector (SEC curity RI, PSS). 0.3 mol/L formic acid in water was used as an eluent at a flow rate of 0.5 mL/min. An SEC curity 1100 (PSS) pump was used for the experiment. Linear poly 2-vinylpyridine was used for calibration. The injected volume was 100 µL and the polymer concentration was 1 mg/mL.

Copolymerization of DMAEMA and BMDO with PEO Azo-initiator (general procedure). As an example for polymerization reactions, the procedure for the synthesis of

sample 4 is described below. All of the sample names and monomer feed ratios are shown in Table 1 and Table 2.

The monomer BMDO (0.99 g, 6.1 mmol) was dissolved in DMAEMA (0.1 mL, 0.59 mmol) in a predried Schlenk tube under an argon atmosphere. The reaction mixture was degassed by three freeze-pump-thaw cycles. The PEO azo-initiator with PEG 6000 block (0.41 g, 6.8×10^{-2} mmol) was added to the still frozen solution. The Schlenk tube was closed, evacuated and refilled with argon three times. This reaction mixture was placed immediately in a preheated oil bath at 70 °C for 24 h. Then the Schlenk tube was taken out of the oil bath and shock cooled in an ice bath. The reaction mixture was diluted with chloroform and precipitated in 200 mL of pentane which yielded a white precipitate. This white polymer was washed with a small amount of water then dissolved in chloroform and precipitated in pentane again. This procedure was repeated twice and then purified by dialysis (MWCO 20kDa) against water. The final copolymer was dried under a vacuum at 40 °C for 48 h.

Quaternization Reaction of Poly(PEO-*co*-(BMDO-*co*-DMAEMA)) Copolymers. 200 mg copolymer (samples 1-4) were dissolved in 20 mL chloroform at room temperature in a flask. 0.5 mL methanol and 2 mL ethylbromide were added to the copolymer solution. The flask was placed in a preheated oil bath at 45 °C for 40 h. Afterwards, the solvent was evaporated using a rotary evaporator. The residue was dissolved again in methanol and precipitated in pentane. This product was then purified by repeatedly dissolving in methanol and precipitating in pentane. The final product was dried at 40 °C under vacuum for 48 h.

Hydrolytic Degradability. In general, 100 mg copolymer was dissolved in a flask containing 10 mL of 5 wt.% KOH in distilled water. This mixture was kept at room temperature for 48 h. Then, 10 mL 10 wt.% HCl was added. This mixture was extracted with chloroform. The

aqueous phase was dried with a freeze dryer for 3 days. The remaining solid was than characterized with NMR spectroscopy.

Enzymatic Degradability and Degradation in Buffer. 200 mg copolymer was solved in phosphate buffered saline (PBS) buffer (0.1 M, pH = 7.4) and Lipase from Pseudomonas Cepacia (10 mg/mL) with a 0.2 mg/mL NaN_3 solution. This mixture was then placed at 37 °C with shaking for different time. Then the mixture was dried with a freezer dryer for 5 days. The remaining solid was also characterized with NMR spectroscopy and GPC.

Cell Culture. L929 mouse fibroblasts cells (human adenocarcinoma) for MTT assay and luciferase assay were seeded at a density of $5.0 \cdot 10^3$ cells$\cdot$cm^{-2} in dishes (10 cm diameter, Nunclon Dishes, Nunc, Wiesbaden, Germany). The incubation condition was at 37 °C in a humidified 8.5% CO_2 atmosphere (CO_2-Incubator, Integra Biosciences, Fernwald, Germany).[66] The medium was exchanged every 3 days. Cells were split after 5 days when confluence was reached.

Cytotoxicity Test using MTT Assay. The cell viability test (MTT assay) was performed according to the method of Mosmann.[67] Polymer solutions were prepared in a serum supplemented tissue culture medium (Dulbecco's modified Eagle's medium, supplemented with 10% serum, without antibiotic) containing $2 \cdot 10^{-3}$ M glutamine and was sterile filtered (0.2 µm, Schleicher&Schüll, Dassel, Germany).

24 h before the MTT assay, L929 cells (8000 cells/well) were seeded into 96-well plates (Nunc, Wiesbaden, Germany). On the day of MTT assay, the culture medium was replaced by 200 µL of a serially diluted polymer medium solution with a different concentration. After a further 24 h of incubation at 37 °C, the cell culture medium was replaced with 200 µL medium containing 20 µL sterile filtered MTT (3-(4,5-dimethyl-thiazol-2-yl)-2,5-diphenyl

tetrazolium bromide) (Sigma, Deisenhofen, Germany) stock solution in phosphate buffered saline (PBS) (5 mg/mL) in each well. The final concentration of MTT in each well was 0.5 mg/mL. After a 4 h incubation at 37 °C in the dark, the medium was removed and 200 µL of DMSO was added in each well to dissolve the purple formazane product. The measurement was performed spectrophotometrically with an ELISA reader (Titertek Plus MD 212, ICN, Eschwege, Germany) at wavelengths of 570 nm and 690 nm. The calibration of the spectrometer to zero absorbance was performed using a culture medium without cells and to 100% absorbance was performed using control wells containing standard cell culture medium but without polymer. The relative viability (%) related to the control wells containing the cell culture medium without polymer was calculated by the following equation:

$$\text{Relative cell growth} = ((A\ 570)\ \text{test} - (A\ 690)\ \text{test}) / ((A\ 570)\ \text{control} - (A\ 690)\ \text{control}) \quad (1)$$

Hyperbranched poly(ethylenimine) (hy-PEI 25kDa, BASF, Germany) was used as a positive control. The IC_{50} was calculated using the Boltzman sigmoidal function from Microcal Origin1 v 7.0 (OriginLab, Northampton, USA). It shows the polymer concentration, which inhibits growth of half of the cells relative to non-treated control cells. The calculation of IC50 was fitted logistically by the Levenberg-Marquardt methods of least-squares minimization for nonlinear equation under the default conditions using by the following equation:

$$Y = Y_0 + (Y_m - Y_0)/[1+(C/C_0)] \quad (2)$$

where C_0 is the IC_{50} dose, Y is the optical density in a well containing a particular polymer/extract of concentration C. Y_0 and Y_m are the optical density corresponding to 0% viability and 100% viability, respectively.

To observe the cell viability qualitatively, we also used 0.4% trypan blue solution to stain died cells, which were incubated with 0.03 mg•mL^{-1} polymers for 4 h and 24 h. After removing the medium in each well, cells were washed with 200 µL PBS buffer and incubated for another 20 min in 0.4% trypan blue solution. After that, cells were washed again with PBS buffer and observed with microscopy. The blue color shows the dead cells in well plate. This picture is shown in the supporting information.

Preparation of Nanoparticles for Samples 3 and 4. Nanoparticles of the samples 3 and 4 were prepared by a solvent displacement technique.[68] 10 mg polymer was dissolved in 1 mL of acetone or acetonnitrile. Under magnetic stirring, 0.5 mL of the obtained solution was injected with an injection needle (0.6•30 mm) into 5 mL of distilled water at a constant flow rate (8.0 mL/min). After the injection, the suspension was stirred for about 2 h under reduced pressure to remove the organic solvent. The resulting suspension contained 1 mg/mL polymer concentration.

Preparation of Polyplex with Copolymer. A 5% glucose solution and p-DNA (plasmid-DNA) for physicochemical-experiments was used for the polyplex formation. 5% glucose is an isotonic solution. In the buffer-solutions, the surface charges of the polymers are reduced due to the higher ionic strength, and the polyplexes aggregates to larger agglomerates due to the lack of repulsion.[62] In terms of dimension, complex formation in a glucose solution is most suitable for transfection.[27] All solutions were filtered with 0.20 µm pore sized filters (Nalgener syringe filter, Sigma–Aldrich, Taufkirchen, Germany). 50 µL of p-DNA solution (40 ng/µL) were placed in a micro centrifuge tube. The volume of a 1 mg/mL (based on hy-

PEI 25 kDa) polymer stock solution (samples 1, 2 and 5-8) or suspension (samples 3, 4) required for a certain Nitrogen/Phosphorus-ratio (N/P ratio) was calculated by following equation:[63]

$$V_{DNA} = (C_{copolymer} \times 10\ \mu L \times 330) / (C_{DNA} \times 157 \times N/P) \quad (3)$$

$C_{copolymer}$ = concentration of the stock copolymer

C_{DNA} = concentration of the stock DNA solution

A certain amount of polymer stock solution was diluted with buffer-solution to a final volume of 50 µL in a micro centrifuge tube. The 50 µL polymer aliquots were mixed with 50 µL diluted p-DNA aliquots and then incubated for 30 min at room temperature for complexation and equilibrium formation.

Zeta Potential and Size Measurements. The zeta potential and size measurements of the polyplexes were monitored with Malvern Zetasizer Nano ZS (Marvern Instrument, Worcestershire, UK). The viscosity (0.88 mPa•s) and the refractive index (1.33) of distilled water at room temperature (RT) was used for data analysis. The measurement angle was 173° in backscatter mode. This polyplex solution was prepared and incubated at RT for 30 min before measurement. Subsequently, zeta-potential measurements were performed with the same samples after diluting 50 µL of polyplexes with an additional 500 µL of 5% glucose solution to a final DNA concentration of 1.82 ng/µL and a final volume of 550 µL. A low volume cuvette (100 µL) was used for the size measurements, and the measurements of zeta potential were carried out in the standard clear capillary electrophoresis cell at room temperature. Three samples were prepared for each N/P ratio, and three measurements were performed on each sample. Each measurement of size consisted of 15 runs for 10 sec. Each

measurement of zeta potential consisted of 60 runs, which was set to automatic optimization by the software.

Confocal Laser Scanning Microscopy (CLSM). 24 h before of the cell uptake experiment, L929-cells were seeded into 8 well-chamberslides (Lab-Tek, Rochester, NY, USA) at a seeding density of 50,000 cells/well. in a DMEM low glucose (PAA, Cölbe, Germany) medium, which contained 10% fetal calf serum (Cytogen, Sinn, Germany) . Before complexation with the copolymer, p-DNA was at first labeled with YOYO-1 (Invitrogen, Karlsruhe, Germany) at a weight ratio of 1:15 at room temperature for 30 min in the dark to protect fluorescent markers. The YOYO-1 labeled p-DNA was condensed with polymer at N/P 15 in a 5% glucose solution, and the polyplexes were incubated for another 20 min at room temperature. 25 µL polyplex solution containing 0.5 µg p-DNA and 375 µL medium with 10% FCS were added in each well. The well-chamberslides were incubated for 4 h at 37 °C in a humidified 8.5% CO_2 atmosphere. After incubation, the cells were washed with a 0.5 mL PBS buffer and then fixated by 20 min of incubation with 0.1 mL of 4% paraformaldehyde in PBS. 30 µL of a 6 µg/mL DAPI solution (Invitrogen, Karlsruhe, Germany) was diluted with 1 mL a PBS buffer. Then 100 µL DAPI solutions were filled into each chamber for 20 min of incubation in the dark. Afterwards, the cells were washed again three times with a 0.5 mL PBS buffer before being fixated with Fluorsafe (Calbiochem, San Diego, USA) and covered with a No.1.5 thickness cover slip (Menzel Gläser, Braunschweig, Germany). The CLSM measurements were performed with a 385 nm long pass filter and a band pass filter of 505-530 nm in the single-track mode (Axiovert 100M and CLDM 510 Scanning Device; Zeiss, Oberkochen, Germany). The excitation of YOYO-1 labeled DNA was performed with a 488 nm argon laser while the excitation of DAPI-stained chromosomal DNA was performed with an enterprise laser with an excitation wavelength of 364 nm.

***In Vitro* Transfection.** L929 cells were seeded with a density of 30000 cells/mL in 96-well-plates (Nunc, Wiesbaden, Germany) 24 h before transfection. Each well contained 6000 cells in 0.2 mL medium. The preparation of the polyplex solution was described above. 25 μL of polyplex solution and 175 μL of the medium (10% serum content) were placed in each well (0.5 μg p-DNA content). The well plates were incubated for 4 h at 37 °C under an 8.5% CO_2 atmosphere. After 44 h, the cell medium was exchanged, and the cells were lysed in a 100 μL cell culture lysis buffer (Promega, Mannheim, Germany) for 15 min at 37 °C. The quantification of lucifaerase activity was determined by injecting a 50 μL luciferase assay buffer, containing 10 mM luciferin (Sigma-Aldrich, Taufkirchen, Germany), into 25 μL of cell lysate. The relative light units (RLU) were measured with a plate luminometer (LumiSTAR Optima, BMG Labtech GmbH, Offenburg, Germany). The protein concentration was determined using a Bradford BCA assay (BioRad, Munich, Germany). The measurement of the transfection activity was performed according to the protocol provided by Promega (Madison, WI, USA).

Sybr Gold Assay. The polymer/p-DNA complexes were prepared at N/P = 0.25, 0.5, 1, 2, 4, 6, 8, 10 in 96 well-plates as described. 200 μL dilutions of polymers containing 0.5 μg DNA for the Syber Gold assay were performed in a water solution. After 20 min of incubation at room temperature, 20 μL of diluted Sybr Gold solution (5 μL stock solution was diluted in 12.5 mL water) was added to each well and incubated for another 20 min. Sybr Gold is light sensitive, and this experiment should be protected from direct light as much as possible. The fluorescence was directly detected using a fluorescence plate reader (BMG Labtech, Offenburg) at 495 nm excitation and 537 nm emission. Origin 7.0 software was used to draw the figure.

Heparin Competition Assay. Briefly, polyplexes were prepared in solutions at different N/P-ratios like the Sybr Gold assay. Additionally, a 20 µL Heparin (150 000 IU/g, Serva, Pharm., USPXV2, Merck, Darmstadt, Germany) solution with a concentration of 0.5 mg/mL was added into a 200µL polyplex solution in each well of the 96-well plate (Perkin Elmer, Rodgau-Jügesheim), where each well contained 0.5 µg p-DNA. After a 20 min incubation of the Heparin at 25°C, 20 µL of the diluted Sybr Gold solution (Invitrogen, Karlsruhe, Germany) were added. The measurement was performed in the same manner as for the Sybr Gold assay.

Statistical analysis. The statistical analysis was conducted in quadruplicate per group. Statistical evaluation was done using the program Sigma Stat 3.5. The One way ANOVA with Bonferroni t-test was performed for all the transfection and MTT data.

2.2.2 Results and Discussion

Synthesis. Free radical polymerization of cyclic ketene acetal BMDO and vinyl monomer DMAEMA was performed with different monomer ratios in the feed at 70 °C for 24 h. PEO macro-azo-initiator with PEO 6 kDa block was used to start the reaction. The molecular weight of the PEO azo-initiator was 24 kDa. A schematic illustration of the reaction is given in Scheme 1.

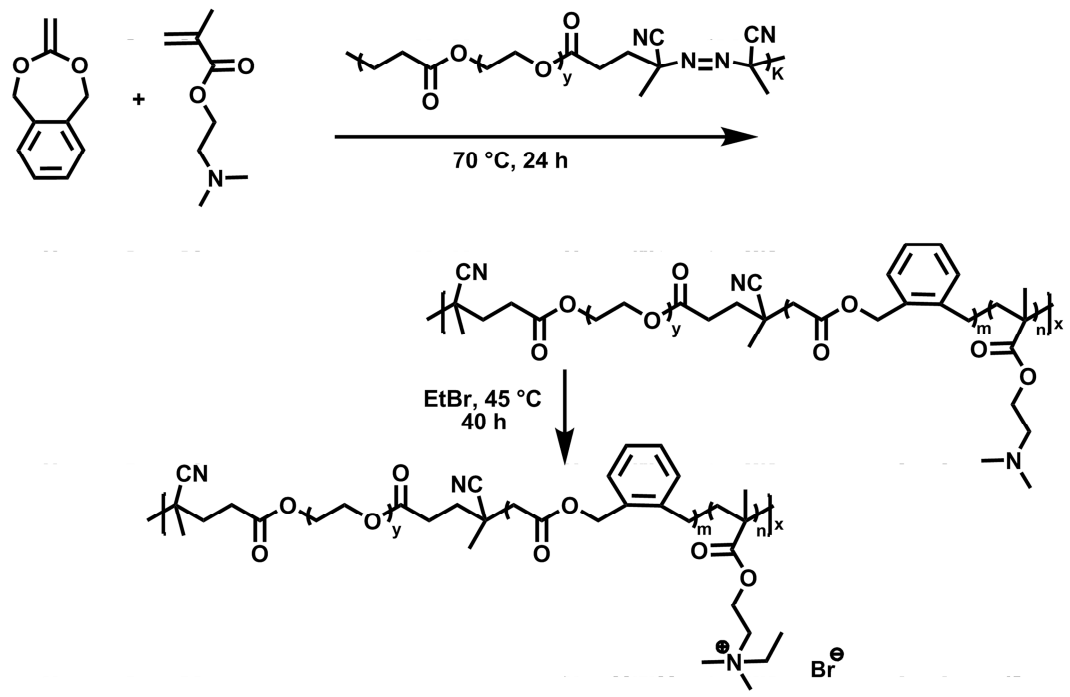

Scheme 1: Synthesis route for the formation of the poly(PEG-*co*-(BMDO-*co*-DMAEMA)) and poly(PEG-*co*-(BMDO-*co*-DMAEMA))•EtBr.

The copolymer composition was determined by NMR. In the ^{1}H NMR spectrum, the characteristic peaks from both comonomers (BMDO and DMAEMA) and the PEG block from initiator were seen. The peak assignments are given in Figure 15. The signal at 3.6 ppm resulted from the PEG block (-OCH_2- peak numbers 21, 22 in Figure 15). The 2.2 ppm signal

could be assigned to the two methyl groups of DMAEMA (peak 8 in Figure 15). Aromatic signals and –OCH_2- of BMDO were seen around 7 and 5 ppm, respectively (peaks 5 and 1 in Figure 15). In the ^{13}C NMR (not shown here), there was no peak observed around 110 ppm. This proved that the complete ring opening mechanism of BMDO formed ester units.[65,69] Peaks 1, 8, 21 and 22 were used to determine the final copolymer composition. Different copolymers with varied amounts of ester units could be synthesized by simply changing the amount of BMDO in the feed (Table 1).

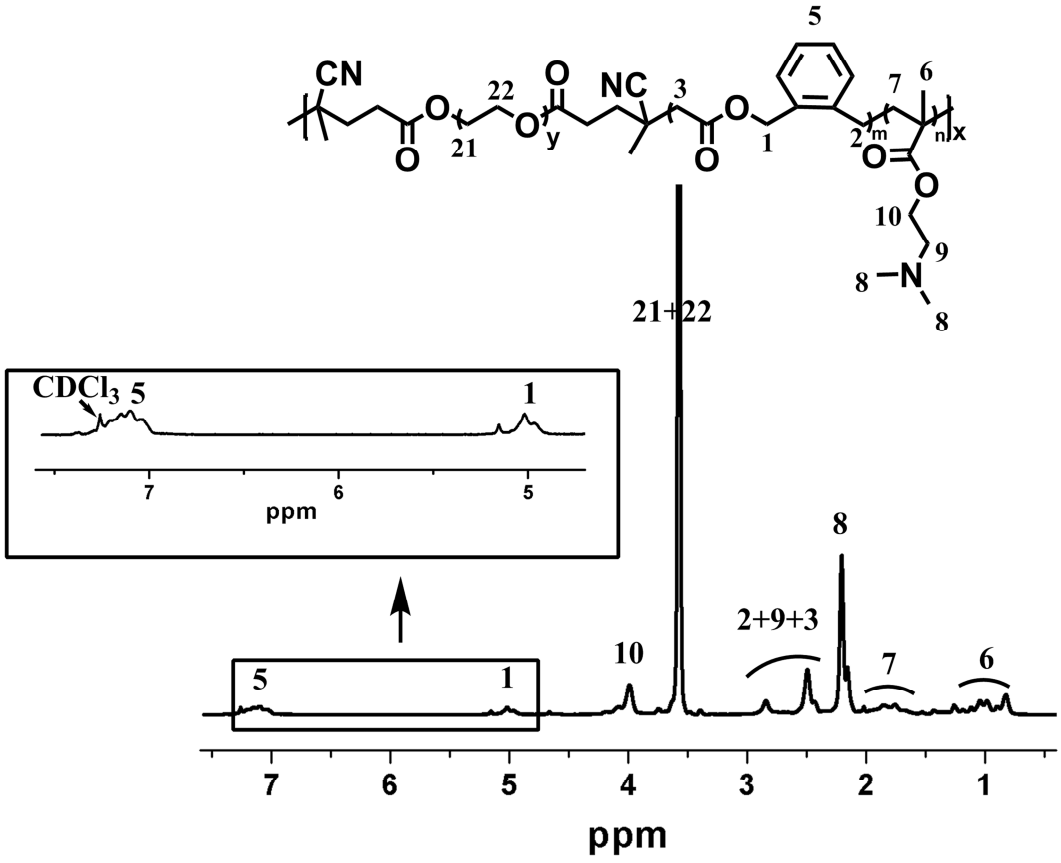

Figure 15: ^1H NMR spectrum of the copolymer p(PEG-*co*-poly(BMDO-*co*-DMAEMA)) with 4 mol% BMDO in the feed (Sample 2, Table 1).

Table 1**:** Synthesis of the p(PEG-*co*-poly(BMDO-*co*-DMAEMA)) copolymers with PEO macro-azo-initiator at 70 °C for 24 h.

Sample Name	Feed ratio molar ratio BMDO:DMAEMA	Poylmer composition molar ratio BMDO:DMAEMA	Yield [%]	Solubility maximum [mg/mL]
1[a]	0 : 100	0 : 100	43	2.1 (water) [b]
2	10 : 90	4 : 96	70	2.0 (water) [b]
3	50 : 50	16: 84	45	0.5 (water) [b]
4	90 : 10	45: 55	32	280 (acetonitile)

[a] This reaction was carried out for 50 min; [b] under ultrasound.

The presence of PEG blocks from the initiator in the polymer chains increased the hydrophilicity of these new copolymers and showed an improvement in the solubility behavior in water. In our previous work, the random copolymer poly(BMDO-*co*-DMAEMA) showed limitations for use as a gene transfection system due to insolubility in water and water miscible solvents like acetonitrile.[61] The quantitative data are shown in Table 1 and Table 2. The use of a PEO macro-azo-initiator led to improved solubility of all of the copolymers both in water and acetonitrile, even with high amounts of BMDO (Table 1).

The copolymers (Samples 1-4; Table 1) were further quaternized with ethylbromide via SN_2 substitution. The properties of quaternized polymers are tabulated in the Table 2. After quaternization, the solubility of the copolymer was further improved significantly. All copolymers (even the polymer with BMDO: DMAEMA 45 : 55 molar ratio) could be solved in water immediately.

Table 2: Quaternization reaction of the p(PEG-*co*-(BMDO-*co*-DMAEMA)) with ethyl bromide at 45 °C for 40 h.

Sample Name (quaternized)	Copoylmer composition molar ratio BMDO:DMAEMA	Reactant sample	Quaternization Yield [%]	M_n [kDa]	M_w[a] [kDa]	Solubility Max. [mg/mL]
5	0 : 100	1	100	54	322	320 (water)
6	4 : 96	2	100	46	127	300 (water)
7	16 : 84	3	100	26	67	220 (water)
8	45 : 55	4	92	13	36	200 (water)

[a] M_n, M_w were determined with water GPC.

The ^{1}H NMR spectrum after the quaternization reaction showed the shifting of peaks 8 and 9 to a lower magnetic field (Figure 16). The addition of the ethyl groups (-CH_2-) and –CH_3 protons 23, 24 in Figure 16) was also observed at a high magnetic field. The degree of quaternization was calculated using the integrals of the two methyl groups on the nitrogen atom of DMAEMA. The quaternization reaction for most of the polymers was quantitative (Table 2)**.** The molecular weight and yield of the copolymer decreased with the increase of BMDO content. The copolymers showed molecular weights between 13 kDa and 60 kDa. The polydispersity of the polymers was high. This could be due to the formation of different multiblock copolymers with PEG block and block of a copolymer of BMDO-*co*-DMAEMA or amphiphilic nature of the block copolymers. Poly(PEG-*co*-(BMDO-*co*-DMAEMA•EtBr))

copolymer contained a hydrophilic part, PEO, a hydrophobic part, BMDO, and the positivly charged PDMAEMA-EtBr. This combination is a challenge for the column system and could lead to broad signal.

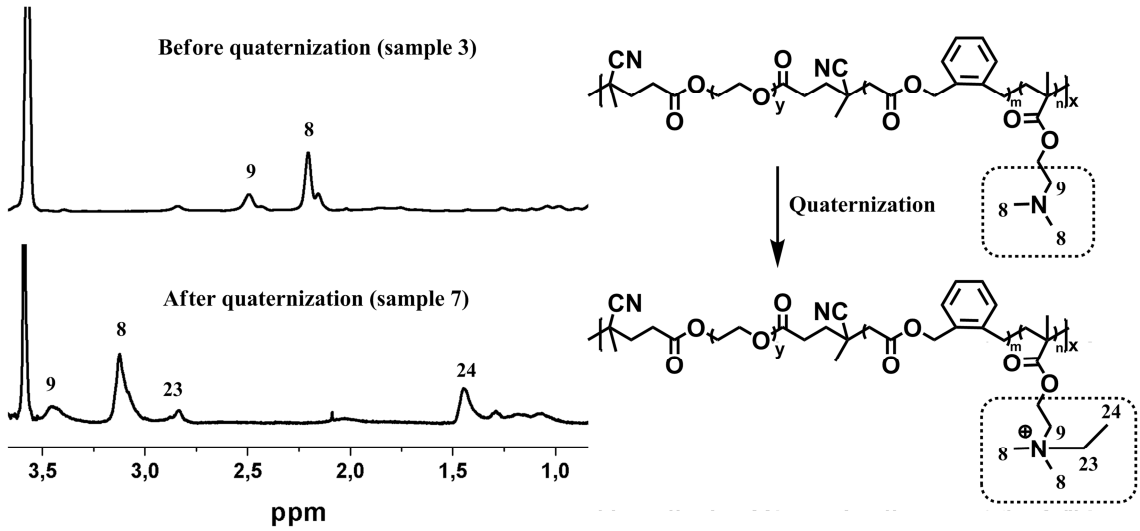

Figure 16: Comparison of NMRs of sample 3 and sample 7 (molar ratio of DMAEMA:BMDO is 15:85) before and after quaternization reaction.

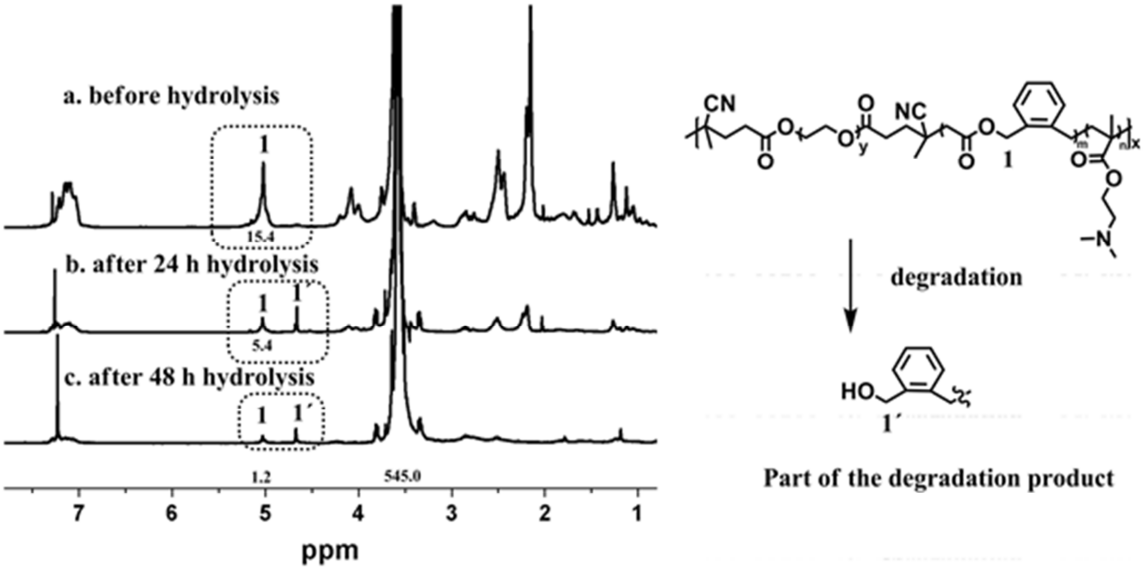

Figure 17: ^{1}H NMR spectrum in $CDCl_3$ before and after hydrolysis of poly(PEG-*co*-(BMDO-*co*-DMAEMA)) (sample 4): a) before hydrolysis of the copolymer with molar ratio of BMDO:DMAEMA = 45:55; b) after 24 h hydrolysis in 5 wt.% KOH solution; c) after 48 h hydrolysis in 5 wt.% KOH solution.

Degradability Study. The hydrolytic degradation behavior of the new copolymers was studied under basic (pH = 9), physiological (pH = 7.4) and enzymatic conditions. The degradation rate was determined by comparing peak integrals before and after hydrolysis as shown for sample 4 (Figure 17). Proton 1 at 5 ppm showed the characteristic proton peak in proximity to the ester bond of BMDO units. In Figure 17, the reduced intensity of the proton 1 signal after 24 h degradation could be observed. After 24 h, around 65% and after 48 h, nearly 93% of the ester bond was hydrolyzed.

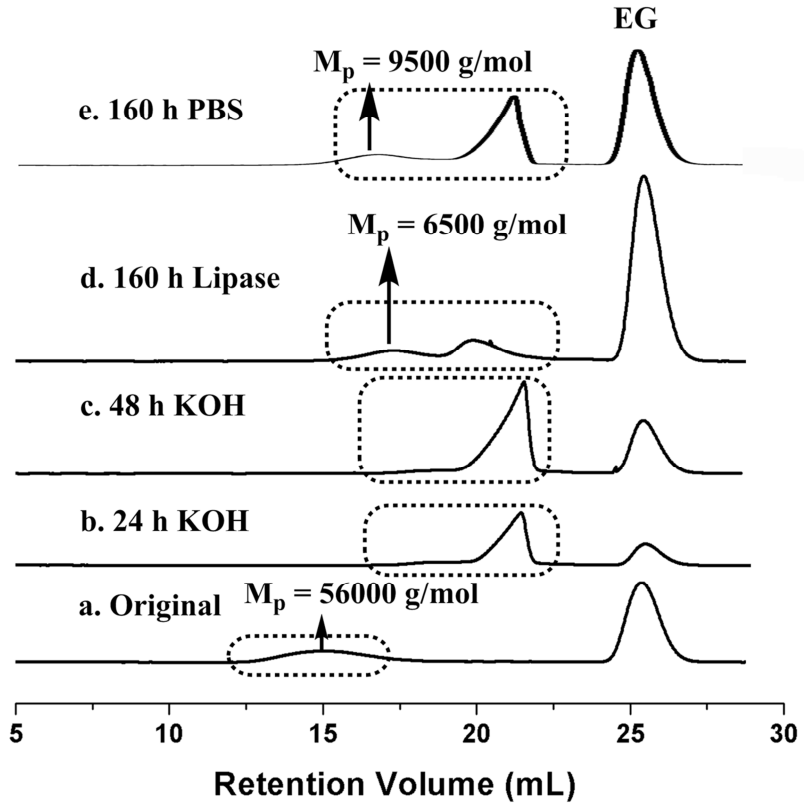

Figure 18: GPC overlays of poly(PEG-*co*-(BMDO-*co*-DMAEMA)) (sample 7, mol ratio of BMDO:DMAEMA = 16:84) a) GPC result before basic hydrolysis; b) after 24 h of basic hydrolytic degradation with 5 wt.% KOH; c) after 48 h of basic hydrolytic degradation with 5 wt.% KOH; d) after 160 h degradation with 10 mg/mL Lipase (from Pseudomonas cepacia) solution. e) after 160 h degradation with phosphate buffered saline (PBS) (0.1M, pH 7.4)

For the quaternized polymer (samples 5-8), the decrease of molecular weight could be observed directly via GPC. The molecular weight of the basic and enzymatic degradation products of sample 7 are shown in Figure 18. The overlay of the GPC results showed a shift in the retention volume. After 24 h of basic hydrolysis, the synthesized block copolymer was completely degraded to the low molecular weight range, which was already in the exclusion volume of the column. A significant signal in the oligomer range around 6 kDa was seen. This was the molecular weight of the PEG block left over after degradation. The SEC results showed also a clear shift to the small molecular range after 160 h degradation with both an

enzyme (Lipase from Pseudomonas cepacia) and PBS buffer at 37 °C. The molecular weight of the degradation product under PBS buffer condition is slightly higher than under the enzymatic condition. A bimodal molecular curve was obtained after degradation. Because of the bimodality of the GPC curve, the M_p value of the curve was determined for comparison. The higher M_p is around 6500 g/mol. This also showed the molecular weight of the PEG block. The smaller molecular weight is already out of the resolution range of the column. Sample 7 had the least ester content and could still be rapidly degraded to oligomers because of the random addition of BMDO in the polymer.

Cytotoxicity Test Using MTT Assay. The cytotoxicity of all of the synthesized copolymers was tested using L929 cells. The cell viability of the synthesized copolymer was compared with a PEI 25 kDa as the standard. A polymer concentration between 0.01 mg/mL and 1 mg/mL was tested. The cell viability is shown logarithmically (Figure 19, A)**.** The IC_{50} values are shown in a bar diagram (Figure 19, B). The statistical analysis shows the "probability of obtaining a test statistic" (P value) to be smaller than 0.001. Sample 4 shows the highest cell viability so we compared all the MTT result with sample 4. The statistical analysis shows also a small p value, smaller than 0.001. All of the synthesized copolymers have higher IC_{50} values than PEI 25 kDa, especially the unquaternized copolymers (samples 1-4). For example, sample 4 showed an IC_{50} value of 0.18 mg/mL, which was 22 times higher than PEI 25 kDa. All of the quaternized copolymers (samples 5-8) have higher cell viability than the unquaternized copolymers because of the more positively charged surface. Sample 8 showed an IC_{50} value of 0.12 mg/mL, which was 15 times higher than PEI 25 kDa.

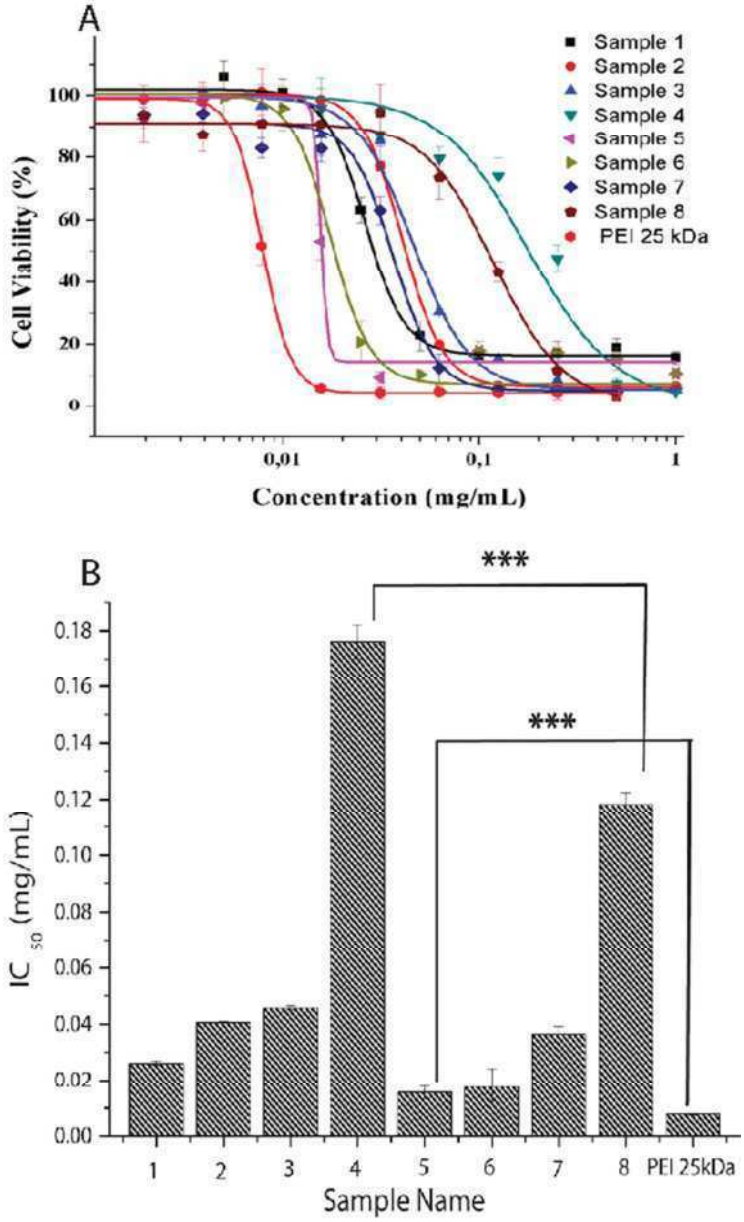

Figure 19: A) Cytotoxicity of polymer study by MTT assay. L929 cells were incubated with polymers of different composition for 24 h; B) IC_{50} doses for different poly(PEG-*co*-(BMDO-*co*-DMAEMA) polymers and the standard PEI 25kDa.*** means a P value smaller than 0.001.

The micrographs showed the cell morphology comparison after 4 h and 24 h treatment with 0.03 mg/mL of the polymer samples 6-8 and PEI 25 kDa (Figure 20)**.** The micrographs of the L929 cells demonstrate the higher viability of the cells treated with the BMDO copolymer as opposed to those treated with PEI. Sample 6 (pictures a and e) and PEI 25 kDa (pictures d and h) showed comparable cell morphology, while samples 7 and 8 showed higher cell density

and viability. After 20 further hours of incubation, the viability in all cases decreased, but the differences between samples 7 and 8 as opposed to samples 6 and PEI remained. Whereas for sample 6 and the PEI 25kDa, the cell viability was almost zero after 24 h, sample 7 showed a reduced viability and sample 8 showed a minimal decrease in viability. All of these results clearly show significantly reduced toxicity of the polymers compared to the accepted gold standard PEI 25kDa.

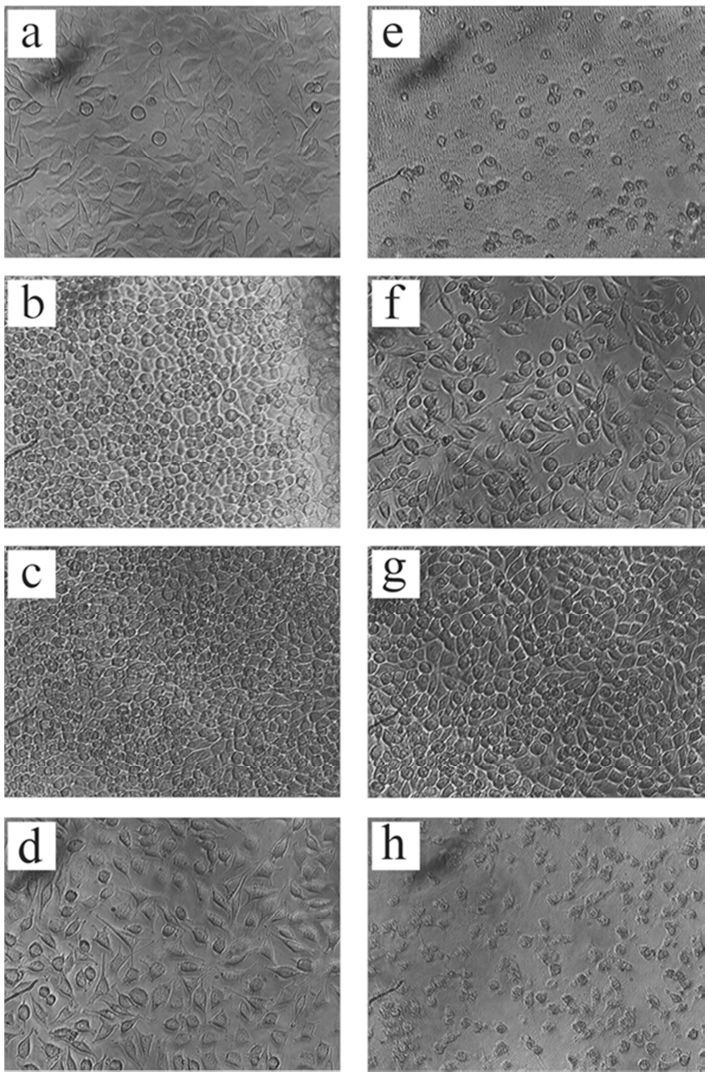

Figure 20: 40×Micrographs of the L929 cells, which were incubated with polymers for 4 h and 24h, respectively. The concentration of the polymers was 0.03 mg/mL. a) with sample 6 for 4 h; b) with sample 7 for 4 h; c) with sample 8 for 4 h; d) with PEI 25 kDa for 4 h; e) with sample 6 for 24 h; f) with sample 7 for 24 h; c) with sample 8 for 24 h; d) with PEI 25 kDa for 24 h.

Quantitative data of MTT assay for 4 h polymer treatment as a percentage curve are shown in supporting information. To assess the cell viability qualitatively, we also used 0.4% trypan blue solution to stain died cells. The same result could be observed like using bright field microscope. This experiment results are showing in the supporting information.

Zeta Potential and Size Measurements. The hydrodynamic diameters of the polymer with a p-DNA complex at different N/P ratio were measured at room temperature (Figure 21). This size measurement was performed for all of the stable polyplexes at N/P ratios between 0 and 20. It has been reported that the acceptable size of polyplex for endocytosis are less than 250 nm.[70,71]

The polydispersities of the polyplexes were all smaller than 0.3. All of the polyplex sizes were less than 250 nm, and had already reached this size at an N/P ratio of 5. The size of the polyplex depends on the N/P ratios and the polymer composition. With the increase of the N/P ratio, the polyplex size decreased. With the increase of the PEG and BMDO part, the polyplex size decreased as expected. That can be explained by the shielding effect of PEG.[70] According to the hydrodynamic size of the polyplexes, these copolymers are suitable candidates for gene transfections.

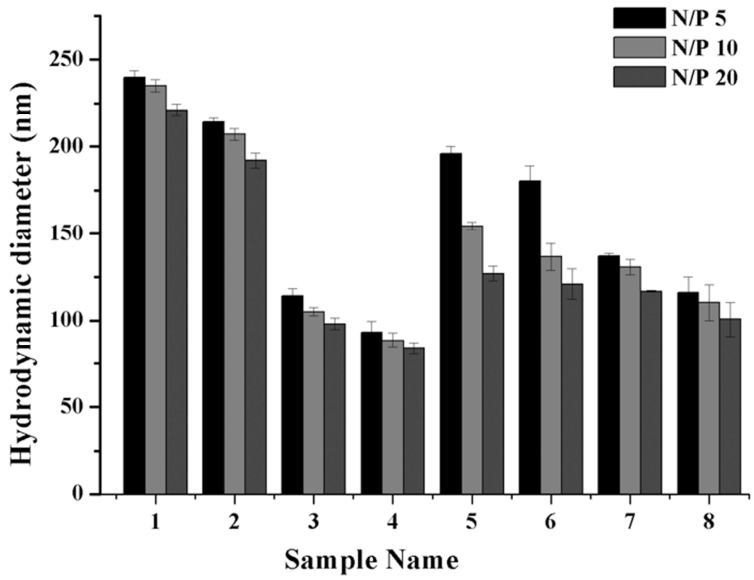

Figure 21: Size of polyplexes formed with plasmid DNA (samples 1-8) at different N/P ratios by DLS (dynamic light scattering) measurement.

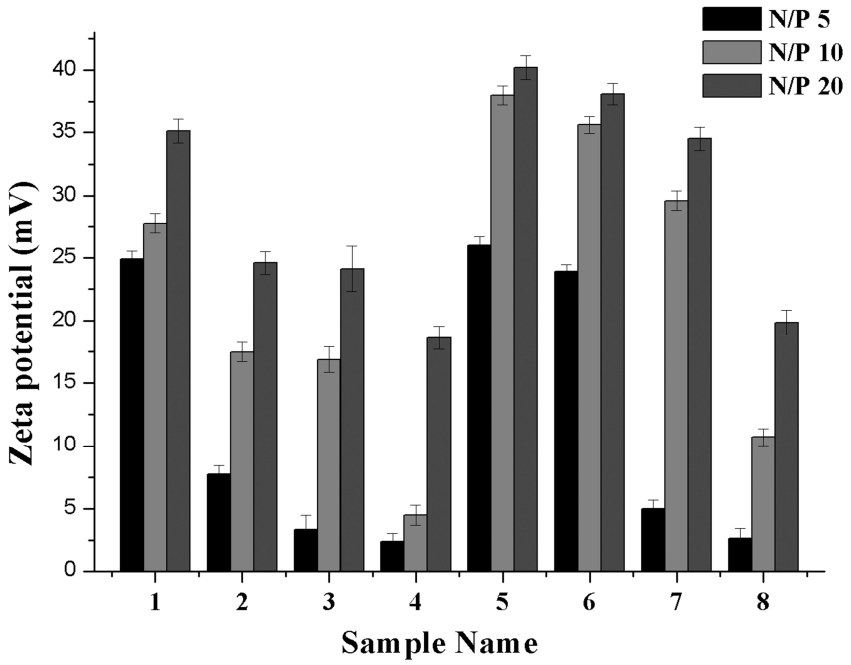

Figure 22: The zeta potential of polyplexes (samples 1-8 with plasmid DNA) at different N/P ratios. Values are the means of 6 runs.

The zeta potential of the polyplex was determined at the N/P ratios of 5, 10, and 20 (Figure 22). The zeta potential increased with the increasing N/P ratio. The polyplex with

quaternized polymer poly(PEG-*co*-(BMDO-*co*-DMAEMA))•EtBr showed higher zeta potential than the unquaternized polymer poly(PEG-*co*-(BMDO-*co*-DMAEMA)). All of the p-DNA polyplexes had positive surface charges which are considered to facilitate uptake by negatively charged cell membranes.[71,72]

Confocal Laser Scanning Microscopy (CLSM). To observe the cell uptake differences between unquaternized polymers and quaternized polymers, the unquaternized/quaternized pair: sample 3 and sample7 was used for CLSM. CLSM images of the L929 cells incubated with fluorescence labeled copolymer p(PEO-*co*-(BMDO-*co*-DMAEMA)) DNA complexes for 4 h are shown in Figure 23. The CLSM graph showed obviously cell uptake of these two polymers not only into the cell cytosol, but also into the cell nucleus. But compared with unquaternized sample 3, quaternized sample 7 showed meanwhile higher cytotoxicity because of the higher surface charges. Therefore, we assumed that the quaternized polymers can condense the p-DNA very well but the transfection efficiency of these polymers was still limited because they were too toxic. On the other hand, the interaction between p-DNA and quaternized polymers was too strong and it was therefore difficult for the quaternized polymers to release the p-DNA in the cell nucleus.

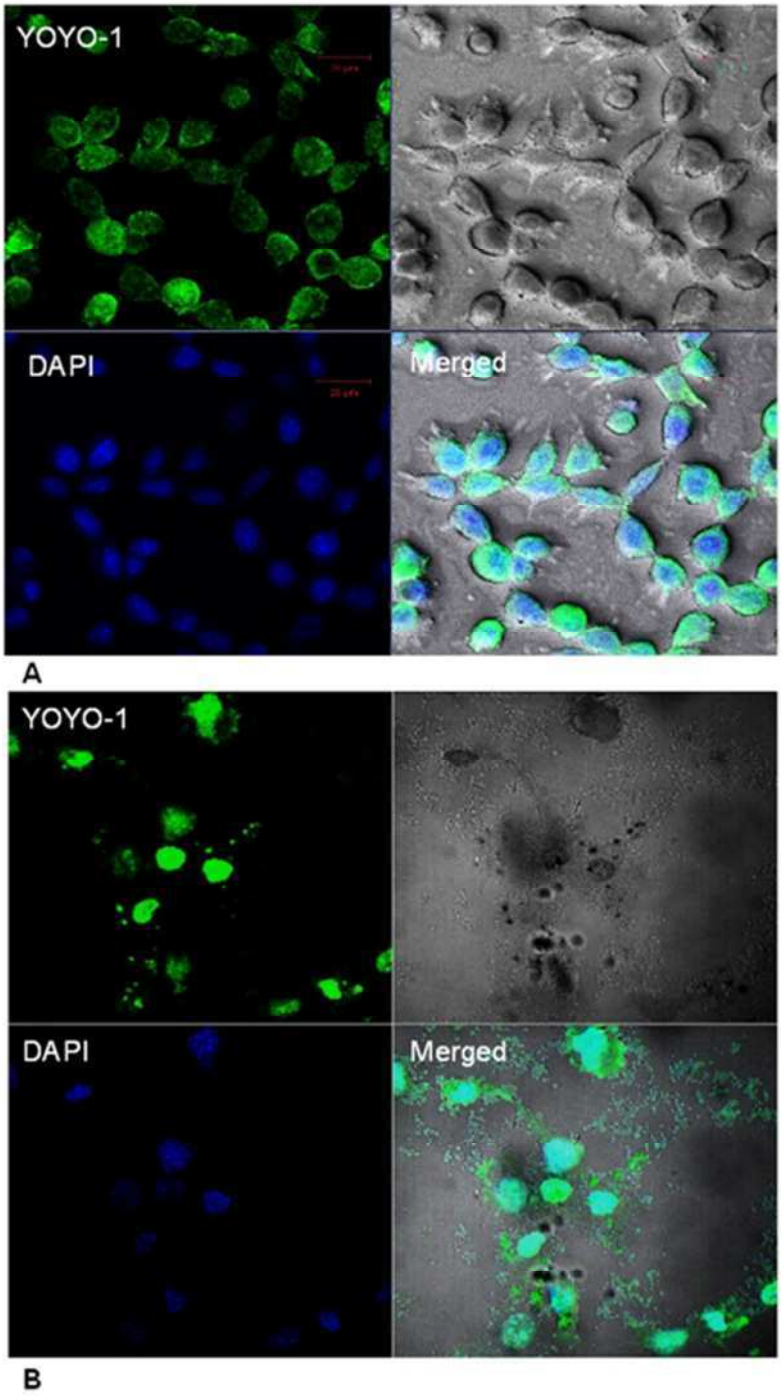

Figure 23: Cell uptake study using CLSM with L929 cells for A: sample 3 and B: sample 7. Plasmid DNA were labeled with YOYO-1 (green); cell nucleus were labeled with DAPI (blue). The cells were incubated with pDNA/p(PEG-*co*-(BMDO-*co*-DMAEMA)) complexes at N/P ratio 10 for 4 h. The sample 3 showed significantly cell uptake of complexes into the cell nucleus and also the cell cytosol; the quaternized sample 7 showed obviously cytotoxicity, although the cell uptake of complexes into the cell nucleus was also observed.

***In Vitro* Transfection**. Transfection experiments with plasmid-DNA were performed with all the DMAEMA based polymers (samples 1-8) (Figure 24). PEI 25kDa was used as the positive control for this experiment. First we compared the synthesized polymer transfection effiency with PEI 25kDa. Then we compared the transfection effiency at N/P 5 for all the samples. The statistical analysis for the unquaternized polymers shows the P value to be smaller than 0.01, which indicated a relative good test results.

All of the unquaternized polymers (samples 1-4) showed successful transfection and the same tendency. The p-DNA transfection efficiency increased with the increasing of N/P ratio until a best N/P ratio and decreased after the best transfection efficiency was reached. At N/P 1, almost no polymers showed significant transfection, even PEI 25kDa, because at N/P 1, the p-DNA could not be condensed completely within the polycations. Surprisingly, sample 2 with the 4% BMDO began to show low transfection while the other polymers were silent. Samples 1 and 2 have the advantage of a higher DEMAEMA concentration and, therefore, the higher density of positive charges for condensing the negatively charged p-DNA. Compared to samples 3 and 4, they showed a better transfection in the luciferase experiment. However, sample 1 only showed a good transfection efficiency at a higher N/P 20 because the polyplexes of this polymer with p-DNA were larger than the others and the size was only less than 230 nm if the N/P ratio was over 10. Compared to samples 1, 2 and 4, sample 3 showed the best transfection at N/P 5, which is a standard for animal testing, at which the polymers were not yet so toxic. The particle size of the polyplex with sample 3 was also relatively low and was even under 120 nm at N/P 5. Additionally, sample 3 had a lower surface charge than samples 1 and 2, which offers a long term circulation in the blood in the *in vivo* experiment. The ester bond in BMDO could be degraded under basic and enzymatic condition. Sample 3 had a higher BMDO content than samples 1 or 2, which means more potential

biodegradability than sample 1 or 2. Therefore, although the *in vitro* luciferase assay showed no greater p-DNA transfection efficiency with sample 3 than samples 1 and 2, we believe that sample 3 will be a highly potent gene delivery agent.

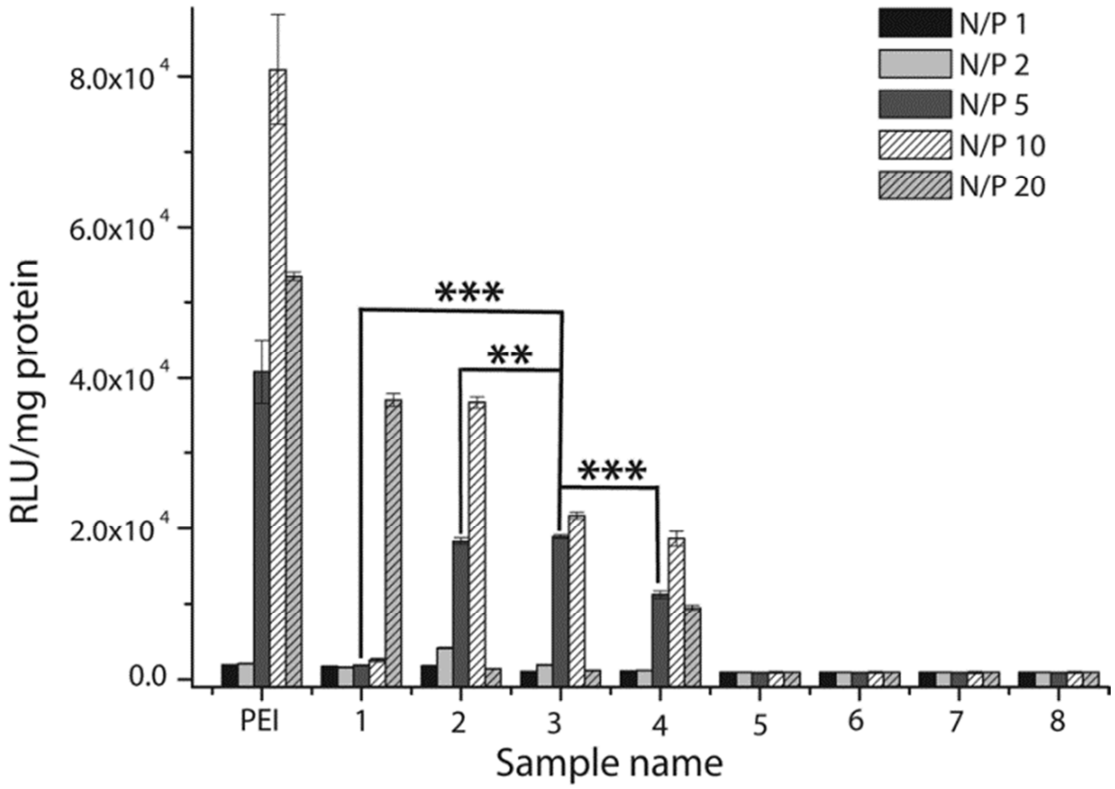

Figure 24: Transfection result of plasmid-DNA-polymer-complexes with L929 cells at different N/P ratio. ***means a P value smaller than 0.001, ** means a P value smaller than 0.01.

It is known that the molecular weight, rigidity and charge density of the pDMAEMA influence the transfection efficiency.[73] . All of these physical properties could be regulated to balance the protection and release of the DNA. Among these factors, the stability of polyplexes was believed to play a more important role than others.[74] The stability of the polyplex is dependent on the charge density of the polymer. Because the polyplexes of plasmid DNA were formed via electrostatic interaction between polymer and plasmid, the polymer with relative high positive charge density can condense the plasmid into more stable

complex with positive charged surface.

The CLSM result showed that all of the quaternized copolymer polyplexes (samples 6-8) reached the cell nucleus. The cytotoxicity of the quaternized polymers was higher than the unquaternized polymer due to the higher density of the positive charges on the polymer surface. A high density of positive charges on the polymer surface may cause very strong electrostatic interactions, which may lead to polyplexes that are too stable to release plasmid DNA into the cytosol or into the cell nucleus, therefore no expression of the target gene could be observed. That could be the reason for the completely negative transfection results for the quaternized polymer samples. The quaternized samples had a much higher charge density than the unquaternized samples. That led to a much more stable complex with DNA and higher toxicity of the polymers. To analyze the stability of the polyplexes, a further Sybr Gold and Heparin competition assay was performed.

Sybr Gold and Heparin Competition Assay.

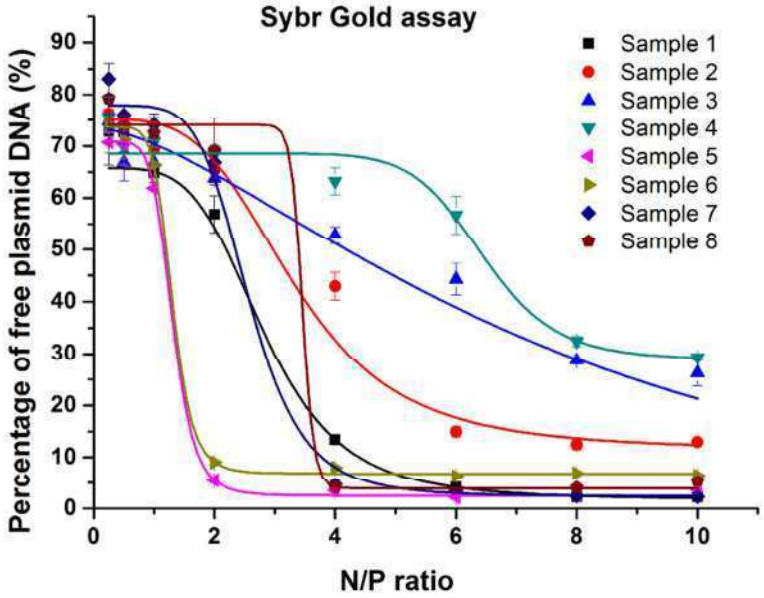

Figure 25: Complexation behavior of p(PEG-*co*-(BMDO-*co*-DMAEMA) (samples 1-8) measured by Sybr Gold intercalation of residual free plasmid DNA increaseing N/P ratio.

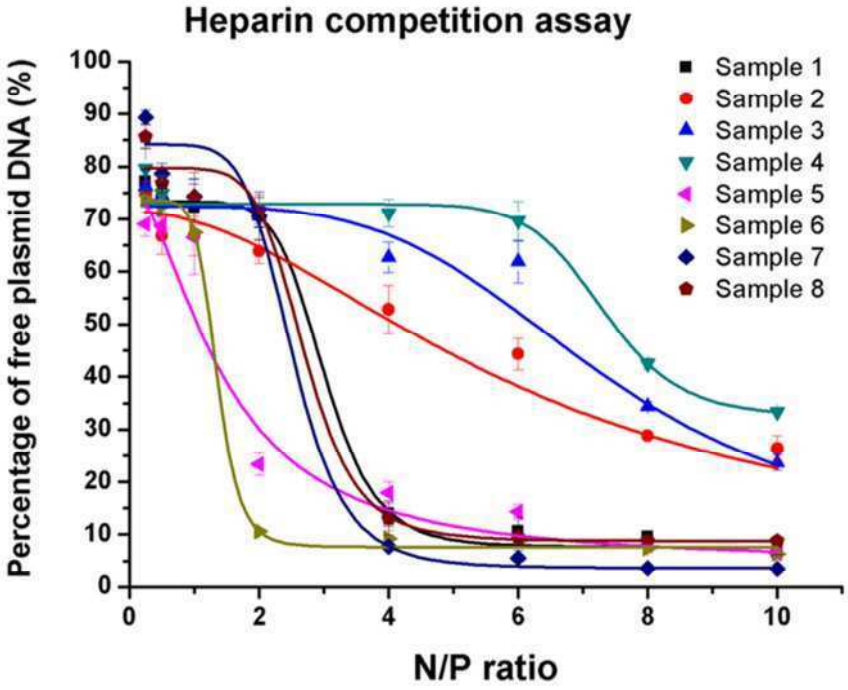

Figure 26: Release profiles of plasmid DNA from polyplex of samples 1-8 by increasing N/P ratio.

The Sybr Gold assay showed the different condensation abilities of the polymers with plasmid-DNA. The affinity of plasmid-DNA with a polymer was increased by increasing the DEMAEMA content, and plasmid DNA could be condensed very well from N/P 6 with all of the quaternized polymers (samples 5, 6, 7, 8) (Figure 25). Compared to the quaternized polymer, the condensation ability with plasmid DNA of the unquaternized polymers was lower. However, sample 1 also showed good condensation with plasmid DNA up to N/P = 6 because of the high DEMAEMA content, although it was unquaternized and had a less positive surface charge. The other unquaternized polymers (samples 2, 3, 4) could not completely reach a complete p-DNA condensation with an increasing N/P ratio, especially sample 4. The stability of polyplexes against competing polyanions is also an important parameter for a gene delivery system, especially for *in vivo* experiment, because the stability of the polyplexes can be strongly weakened by the presence of serum in blood.[75] The process of gene material complexation within polycations is entropy driven and can be significantly impaired by the presence of other polyions like Heparin.[76] Differences in the stability against polyions were found to follow the same trend as the Sybr Gold assay, but the polyplexes formed with quaternized copolymers were less impaired by Heparin (Figure 26). That means the condensation of the plasmid DNA with quaternized copolymers was complete. The plasmid DNA was very difficult to be released if delivered into the nuclei. Therefore, no successful transfection was observed in the *in vitro* transfection experiment for the quaternized polymers, in contrast to the successful transfection with unquaternized polymers (Figure 27).

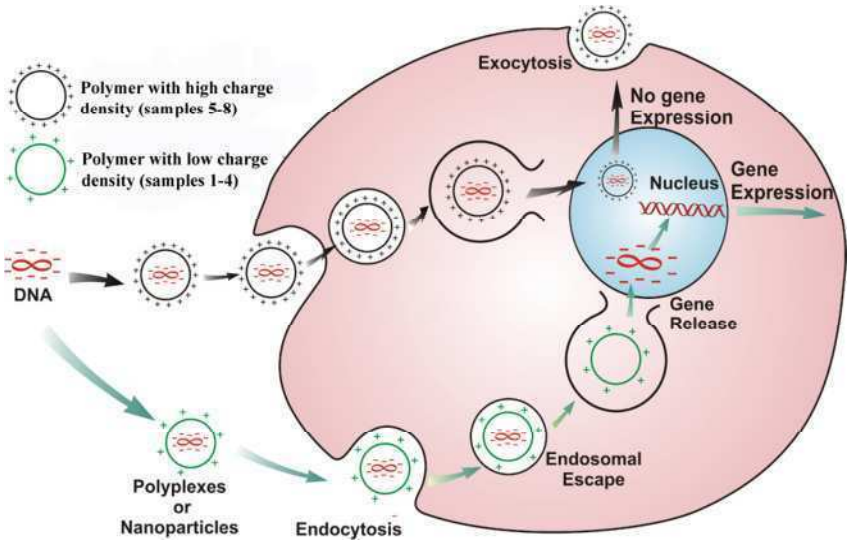

Figure 27: *In vitro* pDNA transfection mechanism with the synthesized polymer p(PEG-*co*-(BMDO-*co*-DMAEMA) (samples 1-4) and p(PEG-*co*-(BMDO-*co*-DMAEMA)•EtBr (samples 5-8).

2.2.3 Conclusion

Novel degradable and biocompatible poly(PEG-*co*-(BMDO-*co*-DMAEMA) for gene transfection were successfully synthesized via free radical polymerization. The solubility and the IC_{50} values of the copolymers were significantly improved by bringing hydrophilic PEG blocks into the polymer backbone. The toxicity of all the polymers was much lower than the positive control PEI. The unquaternized copolymers showed a higher cell viability than the quaternized copolymers as well as positive results in p-DNA transfection.

2.3 MDO based Polymers for DNA Transfection

This work was done in cooperation with prof. Dr. Achim Aigner. Transfection studies were carried out in his laboratory.

2.3.1 Experimental Part

Materials. PEO macro-azo-initiator (M_p = 24 kDa, PEG block = 6 kDa g/mol and PEG block 2 kDa g/mol) was purchased from WAKO Chemicals (Neuss, Germany). *N,N*-dimethylaminoethyl methacrylate (DMAEMA) (Acros Organics / Fisher Scientific, Nidderau, Germany) was destabilized by removing the inhibitor through a basic alumina column to remove the inhibitor. Bromoethane (99%; Acros Organics / Fisher Scientific) was used as received. DMF, chloroform, pentane and methanol were purchased from BASF (Ludwigshafen, Germany) and distilled prior to use. MDO was synthesized according to our previous report.[12,69]

The ovarian carcinoma cell line SKOV-3 was purchased from ATCC/LGC Promochem (Wesel, Germany). The luciferase plasmid (pGL3 control) was obtained from Promega (Mannheim, Germany), and the luciferase plasmid (pCMV-Luc) (Lot No.: PF461-090623) was ordered from The Plasmid Factory (Bielefeld, Germany).

Instrumentation. One dimension NMR ^{1}H (400, 13 MHz) and ^{13}C (100, 21 MHz) spectra were recorded on a Bruker DRX-400 spectrometer. Tetramethylsilane was used as internal standard.

For the elementary analysis (CHN), the polymer was burnt in an excess of oxygen. The corresponding products water (H_2O), carbon dioxide (CO_2) and nitric oxide (NO) were

collected and weighted. From the weight of the corresponding products the composition of CHN of the sample could be calculated.

For bromine analysis, Schoendinger oxidation was performed, followed by the titration with silver nitrate ($AgNO_3$). The measurement of the weight of AgBr allows the calculation of the bromine content in the corresponding sample.

Thermo gravimetric (TGA) measurements were done on a TGA/SDTA 851e (Mettler Toledo). Differential scanning calorimetry (DSC) measurements were performed on a DSC 821e unit (Mettler Toledo). 8-15 mg of the sample were heated in an alumina crucible with a rate of 5 K/min. The temperature program consisted of two heating and cooling cycles from -100 °C to 250 °C.

For the good water soluble samples, the molecular weight and the polydispersity of the synthesized polymers were measured by size exclusion chromatography at 25 °C, using a linear PSS suprema Max 1000 Å column, a differential refractive index detector (SEC curity RI, PSS) and a SECcurity 1100 (PSS) pump. 0.3 mol/L formic acid water solvent was used as eluent at a flow rate of 0.5 mL/min. Linear polyvinylpyridin was used as standard for calibration. The inject volume of the GPC system was 100 µL and the polymer concentration was 1 mg/mL. Ethylene glycol served as internal standard.

Sample T7, which showed limited solubility in water, was measured with DMF LiBr GPC.

The DMF GPC was measured at 25 °C with a 50 × 8 mm^2 pre-column and three linear 10 µm polyester columns (GRAM, PSS) 300 × 8 mm^2. The inject volume was 50 µL and the polymer concentration was 1 mg/mL. An RI Detector 2300 (KNAUER) and a pump (AGILENT) system was used in this system. Destilled DMF containing 5 g/L LiBr served as eluent at a

flow rate of 1 mL/min. PMMA was used for calibration, and toluene served as internal standard.

Copolymerization of MDO and DMAEMA with PEO Macro Initiator. As an example for polymerization reactions, the conditions for sample T3 are described as follows: The monomer MDO (3.5 mL, 31 mmol) and DMAEMA (0.57 mL, 3.3 mmol) were filled in a pre-dried Schlenk tube with a magnetic stir bar under argon atmosphere. This reaction mix was degassed by three freeze-pump-thaw cycles. The PEO macro-azo-initiator with PEG 2000 block (0.69 g, 1 mol-%) was added to the still frozen reaction mixture. The Schlenk tube was evacuated and backfilled with Argon three times. This reaction mixture was placed immediately in a preheated oil bath on a magnet heater at 70 °C for 24 h. Subsequently, the Schlenk tube was taken out of the oil bath and fast cooled in an ice bath. The reaction mixture was diluted with $CHCl_3$ and precipitated in 200 mL cold pentane, yielding a pale yellow precipitate. This pale yellow polymer was washed with a small amount of water and then dissolved in chloroform and precipitated in pentane again. This procedure was repeated twice, and the product was then further purified by dialysis against water. The final polymer product was dried under vacuum at 40 °C for 48 h.

The polymer structure was determined by NMR spectroscopy. Details on the feed ratio, the composition of the copolymers with regard to the monomers and the corresponding copolymer names are given in Table 3.

Quaternization Reactions with EtBr. 500 mg copolymer (T1-T3, S1-S3) were dissolved in 40 mL chloroform at room temperature in a round bottom flask with a magnetic stir bar. Ethane bromide was used as quaternization reagent.[61] 1.5 mL methanol and 5 mL ethane bromide (excess) were added to the reaction mixture. The flask was placed in a preheated oil bath at 45 °C and stirred for 40 h. Afterwards, most of the solvent was evaporated in a rotary

evaporator at 45 °C. The residue was dissolved again in 3 mL methanol and precipitated in cold pentane. This product was purified by repetitive solving in methanol and precipitating in pentane twice. The final polymer was dried at 40 °C under vacuum for 48 h.

Hydrolytic Degradability. In general, 100 mg the polymer was dissolved in a flask containing 15 mL of 5 wt.% KOH in distilled water on a magnetic stirrer. After stirring of the mixture at room temperature for 24 h, 10 mL 10 wt.% HCl was added for neutralization, prior to extraction of this neutral mixture with chloroform. The chloroform phase was dried under vacuum for 3 days. The molecular weight of the remaining solid was than characterized by GPC measurement.

Preparation of Polyplexes from the Copolymers. Complexes were prepared in ddH_2O at various polymer/nucleic acid mass ratios, as indicated in the figures. To this end, 10 mg/ml polymer stock solutions in 1:1 acetonitrile / ddH_2O (S1 - S3, T1 - T3) or in ddH_2O (S5 - S7, T5 - T7) were prepared. The polymer solution was pipetted directly into a 0.1 mg/ml DNA stock solution in water, and ddH_2O was added to adjust to the final complexation volume (30 µl, 60 µl or 90 µl for the complexation of 1 µg, 2 µg or 3 µg DNA, respectively), mixed briefly, incubated for 30 min at room temperature, and briefly vortexed again directly prior to use.

Size Measurement and Zeta Potential Measurement. The zeta-potential and the average particle sizes of the polyplexes obtained at different N/P ratios were determined by dynamic light scattering using a Malvern Zetasizer Nano ZS (Malvern Instruments, Worcestershire, UK). The viscosity (0.88 mPa•s) and the refractive index (1.33) of destilled water at room temperature (RT) was determined and used as reference. The measurement angle was 173° in backscatter mode. The polyplex solution was incubated at room temperature for 30 minutes prior to measurement in a low volume cuvette (100 µL). Three samples were prepared for

each polymer/DNA ratio and three measurements were performed on each sample. Each measurement of size was performed for 15 runs at 10 sec each. The particle mean diameter (Z-Ave) and the width of the fitted Gaussian distribution were calculated with the DTS V. 5.10 software. Each measurement of zeta-potential consisted of 60 runs, which was set to automatic optimization by the software. Again, the DTS V. 5.10 software was used to calculate the average z-potential values from the data of multiple runs.

Determination of DNA Complexation Efficacy. To determine the efficacy of polymer/DNA complex formation, DNA was [^{32}P]-labeled using the ReadyPrime kit from Amersham (Freiburg, Germany) according to the manufacturer's protocol, with 25 ng DNA and 50 µCi α-[^{32}P]dCTP. Purification was performed using Micro Bio-Spin Chromatography Columns (BioRad Laboratories, CA) by applying the solution onto pre-centrifuged (2 min, 1,000 x g) P-6 columns and subsequent centrifugation at 1,000 x g for 4 min for recovering the labelled nucleic acids in the flowthrough. Prior to complexation, the labeled DNA was mixed with 25 µg unlabeled DNA. The complexation was performed as described above, with 200 ng DNA per complex and polymer/DNA mass ratios as indicated in the figure (0.001 - 1000). Samples were then mixed with loading buffer, and loaded onto 1% agarose gels. Electrophoresis was performed at 100 mV for 1 h, and DNA bands were analysed by autoradiography in a Cyclone Plus Phosphoimager (Perkin-Elmer, Fremont, CA). Percentages of nucleic acid complexation were calculated based on the quantity of free DNA relative to completely complexed (100%) samples.

Determination of Transfection Efficacy and Cytotoxicity. For transfection experiments, cells were cultivated in IMDM medium (PAA, Cölbe, Germany) supplemented with 10 % fetal calf serum (Gibco / Life Technologies, Darmstadt, Germany) under standard conditions (37°C, 5% CO_2 in a humid atmosphere). DNA transfection was performed in serum-

containing medium (IMDM/10% FCS), essentially as described previously.[77] Briefly, cells were seeded at 4 x 10^4 cells/well in 24-well plates, and after 1 d cultivation in serum-containing medium, polymer/DNA complexes prepared as described above were added at the amounts detailed in the figures. Luciferase activity was determined 48 h after DNA transfection, using the luciferase assay kit from Promega (Mannheim, Germany) according to the manufacturer's protocol. Briefly, the medium was aspirated and the cells were lysed in 100 µl lysis buffer. In a luminometer tube, 25 µl substrate was mixed with 10 µl lysate, and chemiluminescence was determined immediately in a luminometer (Berthold, Bad Wildbad, Germany).

Cell viabilities in the presence of the polymers were determined as described previously.[61] Briefly, cells were seeded in 96-well plates at 2000 cells/well and treated with a polymer at the concentration indicated in the figure. Numbers of viable cells were determined using a colorimetric assay, which is based on the cleavage of the tetrazolium salt WST-1 by mitochondrial dehydrogenases, according to the manufacturer's protocol (Cell Proliferation Reagent WST-1, Roche Molecular Biochemicals, Basel) with each value representing the mean of triplicate wells.

2.3.2 Results and Discussion

Synthesis and Characterization of P(PEG-*co*-(MDO-*co*-DMAEMA))

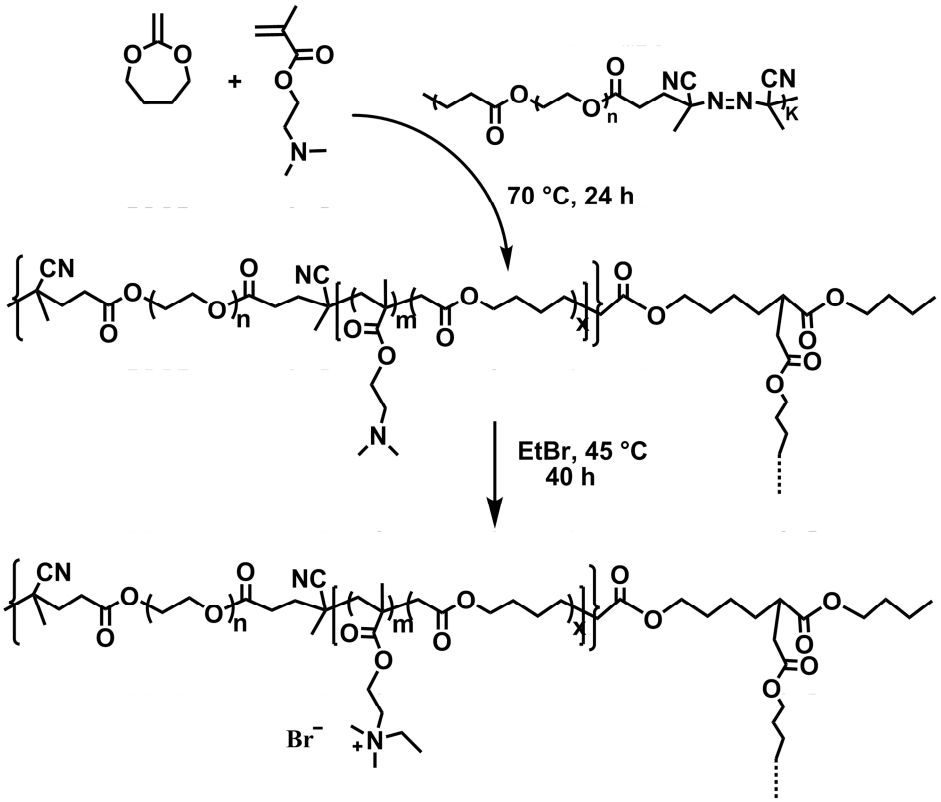

Scheme 2: Synthesis route for the poly(PEG-*co*-(MDO-*co*-DMAEMA)) and poly(PEG-*co*-(BMDO-*co*-DMAEMA))•EtBr.

First, the monomer MDO was synthesized through a previously reported three step reaction method.[12,78] A free radical polymerization of MDO and DMAEMA was performed with two kinds of PEO macro-azo-initiators, one with PEG 2 kDa block length and the other one with PEG 6 kDa block length. Both kinds of PEO macro-azo-initiators have a molecular weight of 24 kDa and contain PEG blocks which are connected with azo groups (Scheme 2). As set of p(PEG-*co*-(MDO-*co*-DMAEMA)) copolymers with different monomer ratios was synthesized. Copolymer names and reaction details are shown in Table 3.

Table 3: Details and properties of the various p(PEG-co-poly(MDO-co-DMAEMA)) copolymers synthesized with PEO macro-azo-initiator at 70 °C for 24 h. Copolymers T1-T4 contain PEG 2000 blocks, copolymers S1-S4 contain PEG 6000 blocks.

Copolymer name	**Feed ratio molar ratio MDO:DMAEMA**	**Composition mol% MDO:DMAEMA**	**Yield %**	**Soluble in**
T1	0:100	0:100	80	Acetonnitrile
T2	50:50	10:90	66	Acetonintrile
T3	90:10	57:43	59	Acetone
T4	100:0	100:0	50	$CHCl_3$
S1	0:100	0:100	68	H_2O
S2	50:50	22:78	62	Acetonnitrile
S3	90:10	51:49	52	Acetone
S4	100:0	100:0	40	$CHCl_3$

The structural characterization of the polymers was done by NMR spectroscopy. A representative ^1H NMR spectrum of the polymer product (T3) with 57 mol-% of MDO in the initial feed (Sample T3, Table 3) is shown in Figure 28, and a comparison of copolymers with various MDO:DMAEMA ratios is presented in Figure 29**.**

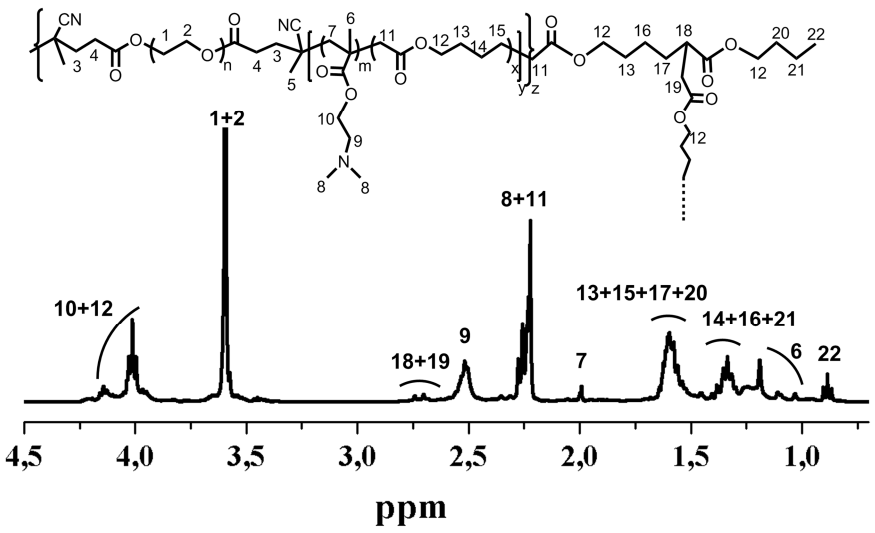

Figure 28: ^{1}H NMR spectrum of copolymer p(PEG-*co*-poly(MDO-*co*-DMAEMA)) with 90 mol-% MDO in the feed ratio (copolymer T3; see Table 3).

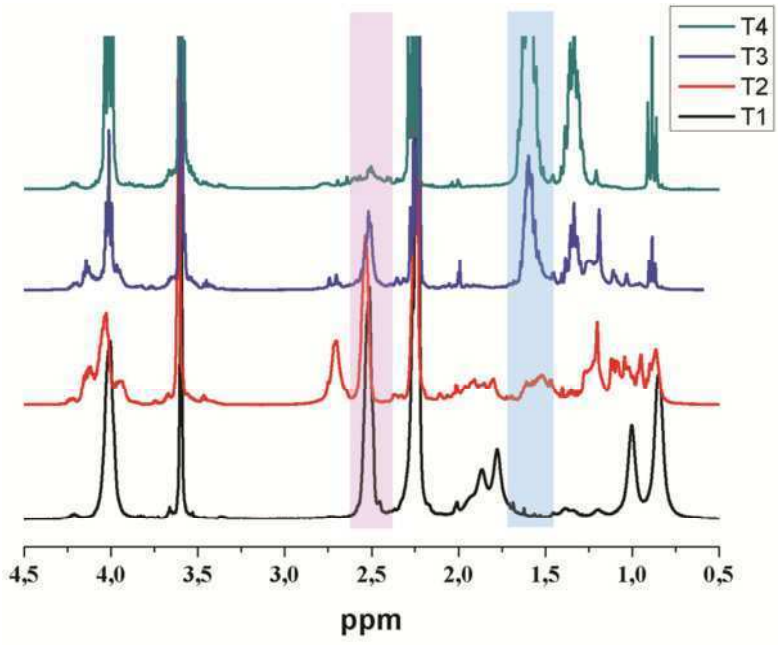

Figure 29: ^{1}H NMR spectrum overlay of various p(PEG-*co*-poly(MDO-*co*-DMAEMA)) copolymers (T1-T4; see Table 3).

The solubility of the polymer in water and water miscible solvents determines the conditions of polyplex formation with DNA. The addition of PEG blocks in the copolymer increased the solubility of the polymer in water or water miscible solvents. The solubility was better for

polymers made with PEG 6 kDa initiator (samples S1-S4) as compared to the polymers made with PEG 2 kDa (T1-T4), and decreased with higher MDO content (Table 3).

To improve the solubility and increase the charge density of the polymers, a quaternization reaction of nitrogen atoms was performed with EtBr at 45 °C for 40 h. The sample names, molecular weights and solubilities of the polymers are shown in Table 4. The quaternization ratio was determined by a ^{1}H NMR method (Figure 30). After 40 h, more than 90% of the nitrogen in the polymer was quaternized. All the obtained quaternized cationic polymers containing DMAEMA were water soluble. A further increase in water solubility was observed with decreasing MDO amounts in the composition and higher PEG block length. Sample T7 was soluble in water after ultrasound treatment for 5 minutes.

Table 4: Details and properties of the various quaternized p(PEG-*co*-poly(MDO-*co*-DMAEMA)) copolymers (quaternization performed with ethyl bromide at 45 °C for 40 h).

Quaternized copolymer name	**Composition mol% MDO:DMAEMA**	**Educt sample name**	**Yield %**	**Soluble in**	**M_n kDa**	**M_w kDa**
T5	0:100	T1	95	H_2O	31	104
T6	10:90	T2	92	H_2O	25	110
T7	57:43	T3	90	H_2O[a)]	12[b)]	24[b)]
-	100:0	T4	-	$CHCl_3$	11	34
S5	0:100	S1	93	H_2O	58	145
S6	22:78	S2	91	H_2O	55	150
S7	51:49	S3	95	H_2O	23	80
-	100:0	S4	-	$CHCl_3$	3	9

[a)]soluble under ultrasound; [b)]measured with DMF LiBr GPC.

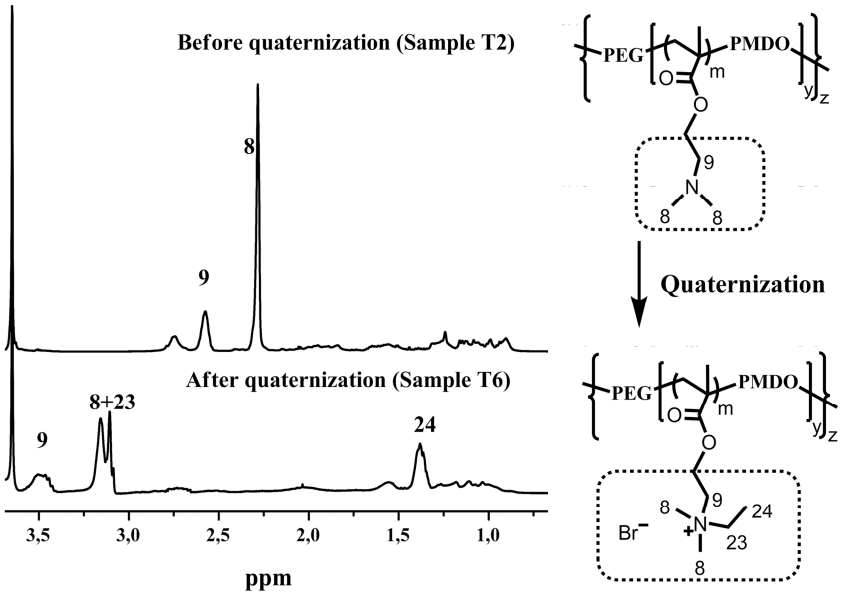

Figure 30: Comparison of NMR spectra of copolymer T2 and its quaternized counterpart (copolymer T6).

The unquaternized block copolymers (T1-T3, S1-S3) were stable up to about 250 °C, as determined by thermo gravimetric analysis. The differential scanning calorimetric thermogram for the PEO macro-azo-initiator showed a single melting peak at 42 °C. The second heating cycle of the synthesized polymers is shown in Figure 31**.** For the MDO-containing copolymers, a melting peak at around 50 °C was determined. These polymers showed different crystallinity, dependent on the PEO macro-azo-initiator length. An increase in the area under the melting peak (melting enthalpy) was obtained with the higher PEG block length in the copolymer composition. More specifically, copolymers with PEG 2000 block as initiator (T2, T3, T4) showed a melting enthalpy smaller than 30 J/g, while for copolymers with PEG 6000 block as initiator (S2, S3, S4) melting enthalpies higher than 30 J/g were

determined. The percentage of crystallinity was calculated based on the known melting enthalpy of 100% crystalline PEG (189 J/g [79]). Only samples with PEG 2000 block (T2, T3, T4) showed T_g (glass transition temperature) in the second heating cycle. The glass transition temperature of copolymers increased with decreasing amounts of DMAEMA in the copolymers 50°C, 55°C and 60°C for the samples T2, T3 and T4, respectively.[80]

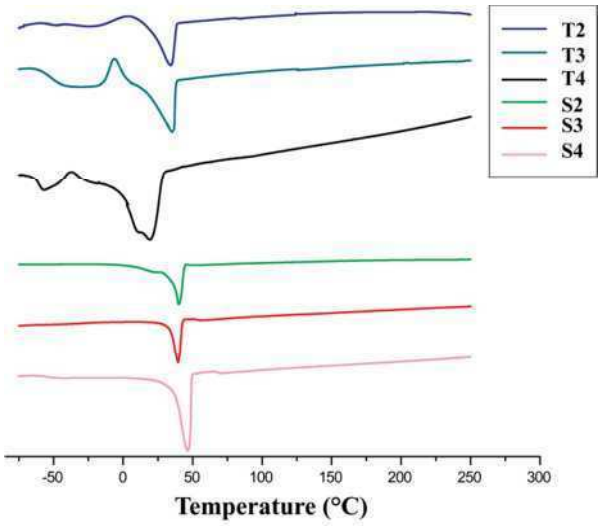

Figure 31: Differential scanning calorimetry (DSC) thermograms of the various p(PEG-*co*-(MDO-*co*-DMAEMA)) copolymers (second heating cycle of the unquaternized copolymers T2-T4, S2-S4).

The hydrolytic degradation behavior of the polymers was analyzed at basic pH, with the decrease of the polymer molecular weight being monitored via GPC. As a representative example, the molecular weight of sample T6 before and after degradation is shown in Figure 32. The overlay of the GPC results shows the difference in the retention volumes, indicating that polymer T2 was completely degraded from 25 kDa down to the PEG blocks and small

molecules. Comparable to T6, all MDO-containing polymers showed complete degradation under these conditions (data not shown).

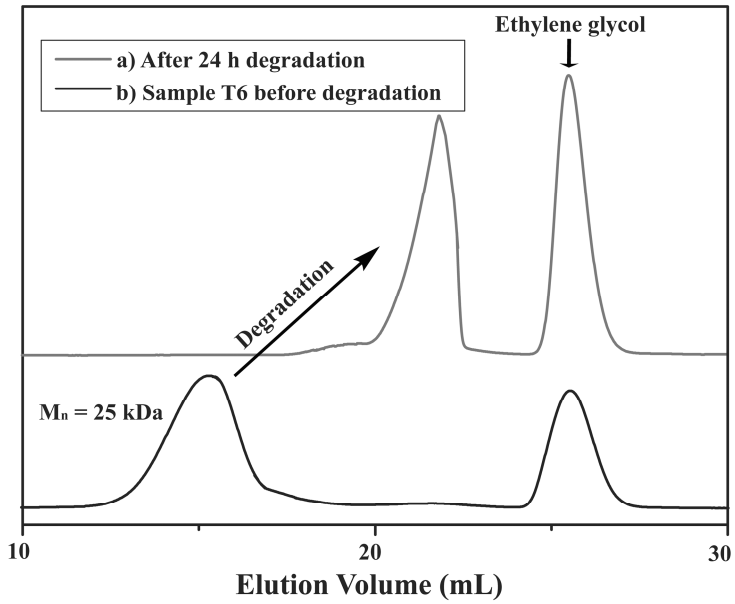

Figure 32: GPC overlays of poly(PEG-*co*-(MDO-*co*-DMAEMA)) (copolymer T6, mol ratio of MDO:DMAEMA = 10:90) a) GPC result before basic hydrolysis; b) after 24 h of basic hydrolytic degradation with 5 wt.% KOH.

Upon complexation of DNA, zetasizer measurements revealed that the sizes of all polyplexes were below 250 nm, and the PDI values were < 0.3. For any given polymer, the polyplex size decreased with increasing polymer/DNA ratios (Figure 33**).** Also, p(PEG-*co*-(MDO-*co*-DMAEMA)) copolymers resulted in somewhat smaller complexes after quaternization of the nitrogen atoms (compare e.g. samples T1 vs. T5; S1 vs. S5). Apart from these trends, no major size differences were observed, with all complexes being well in the size range of cellular internalization. Likewise, the zeta potentials of all the synthesized polymer complexes were positive even at the lowest polymer/DNA mass ratio (Figure 34), and thus in the range

necessary for cellular uptake.[71,72] As expected, zeta potentials increased with higher polymer/DNA mass ratios, and there was a trend towards higher zeta potentials in the complexes based on quaternized polymers when compared to their unquaternized counterparts (compare T1-T3 with T5-T7; S1-S3 with S5-S7). Likewise, there was a trend towards higher zeta potentials in complexes based on polymers with PEG 6 kDa blocks as compared to their PEG 2 kDa block counterparts (compare T1-T3 vs. S1-S3; T5-T7 vs. S5-S7).

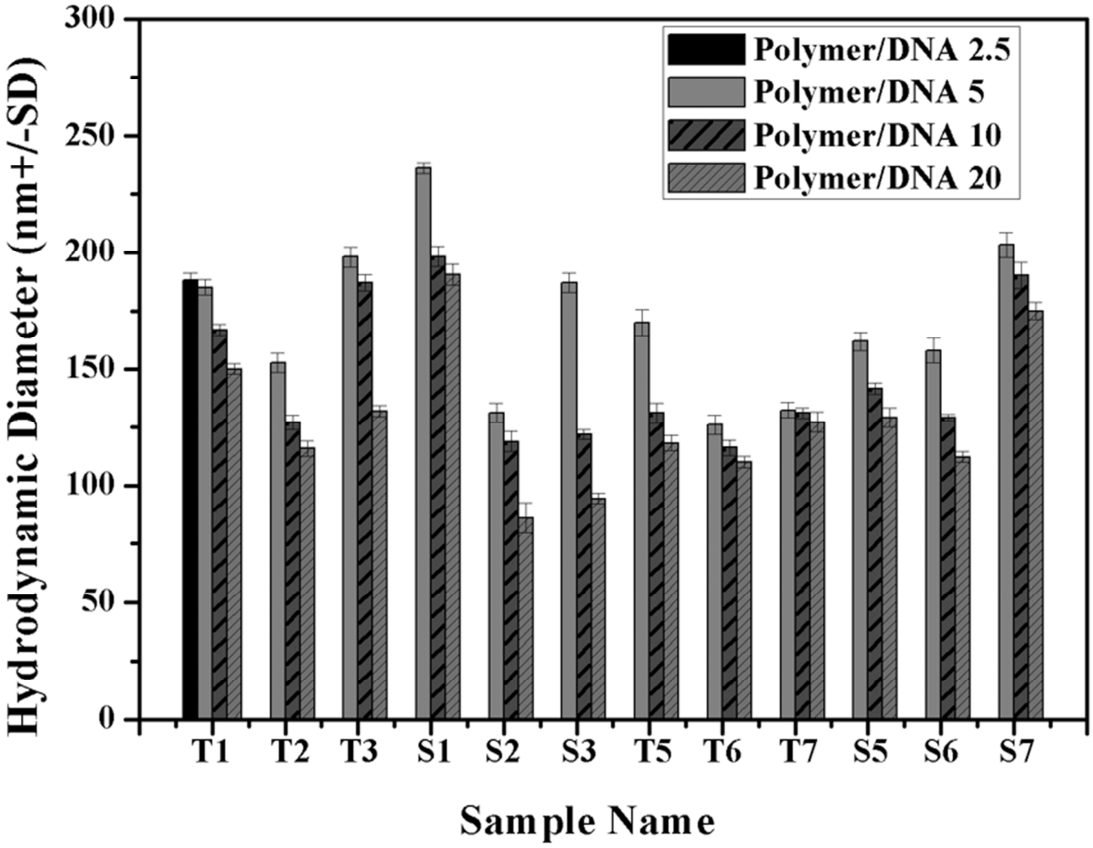

Figure 33: Size of polyplexes, formed with the various copolymers and plasmid DNA at different polymer/DNA ratios, as determined by dynamic light scattering (DLS) measurement.

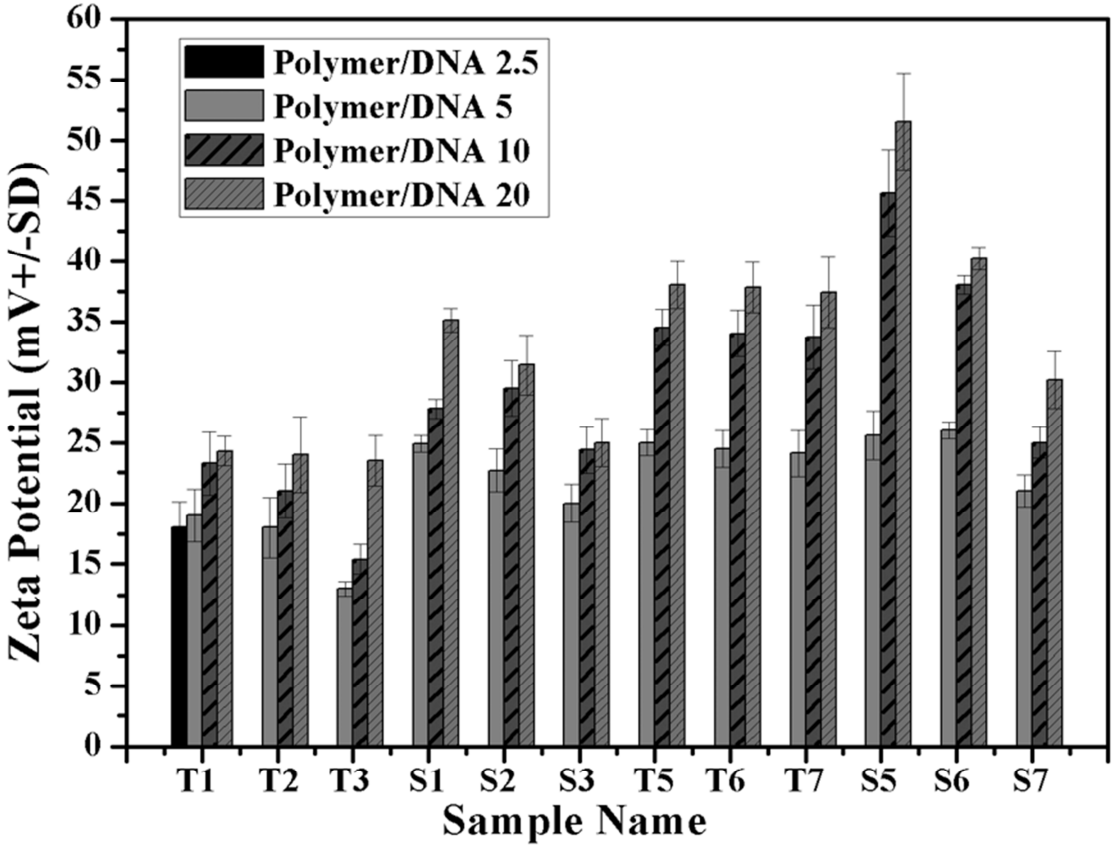

Figure 34: Zeta potential of polyplexes, formed with the various copolymers and plasmid DNA at different polymer/DNA ratios. Values are the means of 6 runs.

Complexation efficiency with DNA. The complexation efficiency with DNA is one crucial property for gene delivery vectors, since complete complex formation is an essential pre-requisite for cellular uptake. DNA complexation efficiencies were dependent on the DMAEMA percentage as well as on quaternization. More specifically, in the case of unquaternized PEG6000-based polymers, a 10-fold shift to higher mass ratios was observed between S1 (50% DMAEMA) and S3 (19% DMAEMA) (Figure 35 a vs. b). Likewise, while no major differences were observed between 91% and 66% DMAEMA in PEG2000-based polymers (T1 / T2), a > 100-fold shift to higher mass ratios was detected in T3 (26% DMAEMA) (Figure 35, c vs. d). Quaternized polymers showed generally higher complexation efficacies. This was especially true for the direct comparison of quaternized / unquaternized polymers with lower DMAEMA percentages, where 10 - 100-fold higher complexation efficacies were observed upon quanternation (Figure 35, b vs. e).

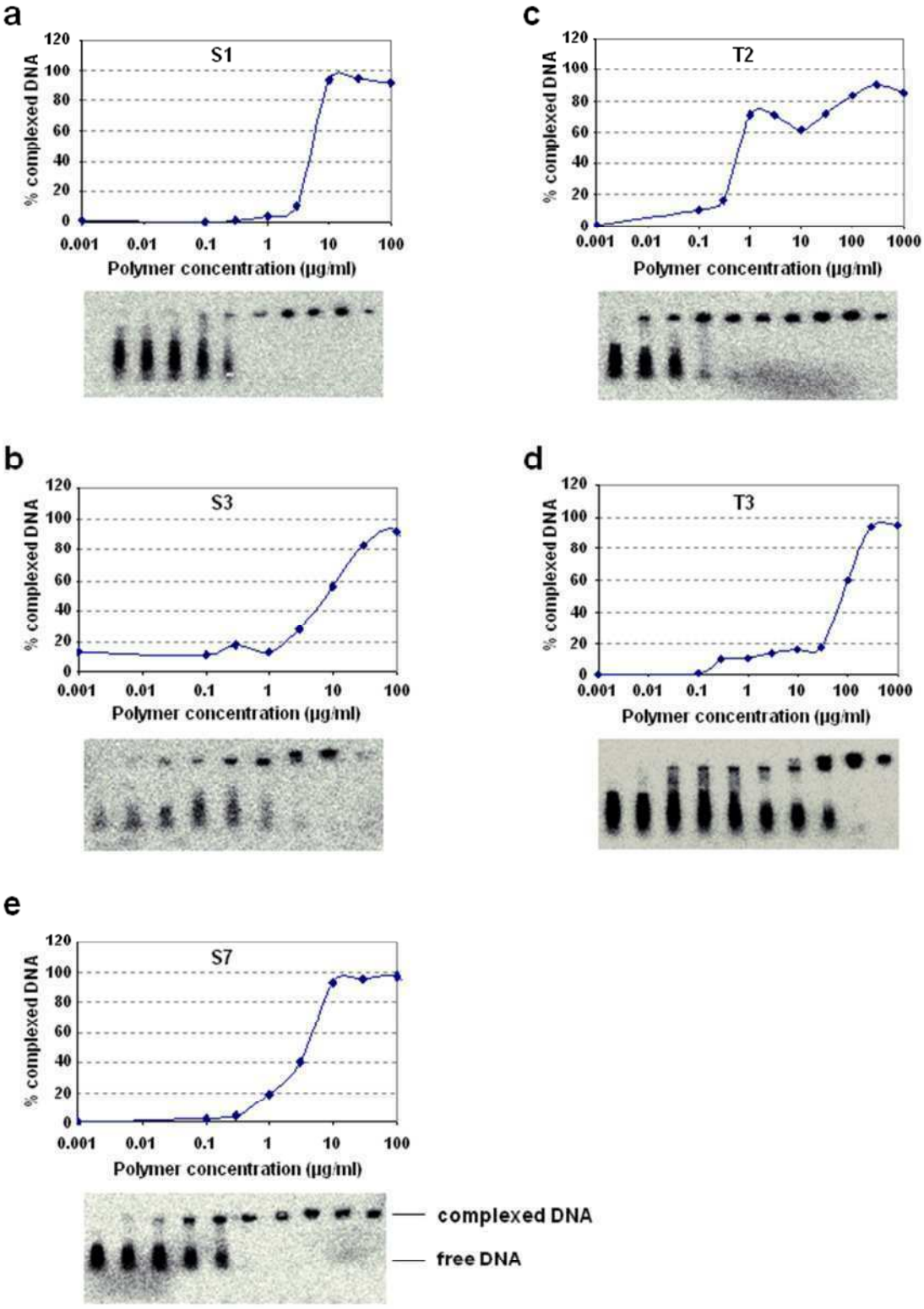

Figure 35: Complexation efficacies of selected copolymers S1 (a), S3 (b), T2 (c), T3 (d) and S7 (e) with DNA. Gel bands represent complexed and free DNA, respectively.

Beyond biological efficacies, the suitability of the polymers as gene delivery vectors is determined by their (absence of) toxicity. Therefore, we assessed the *in vitro* cytotoxicity of the polymers in cell viability assays (Figure 36). Dependent on the polymer, cytotoxicity was observed only at concentrations > 1 - 10 µg/ml, with T2 being the only exception. All quaternized polymers showed lower cytotoxicity than their unquanternized counterparts. Also, while no clear correlation was found between cytotoxicity and DMAEMA percentage, PEG6000-based polymers were less cytotoxic than polymers containing PEG2000. Particularly biocompatible were S5 and S6, but S1, T1 and T7, which showed best transfection efficacies (see below), displayed only low to moderate cytotoxicity as well.

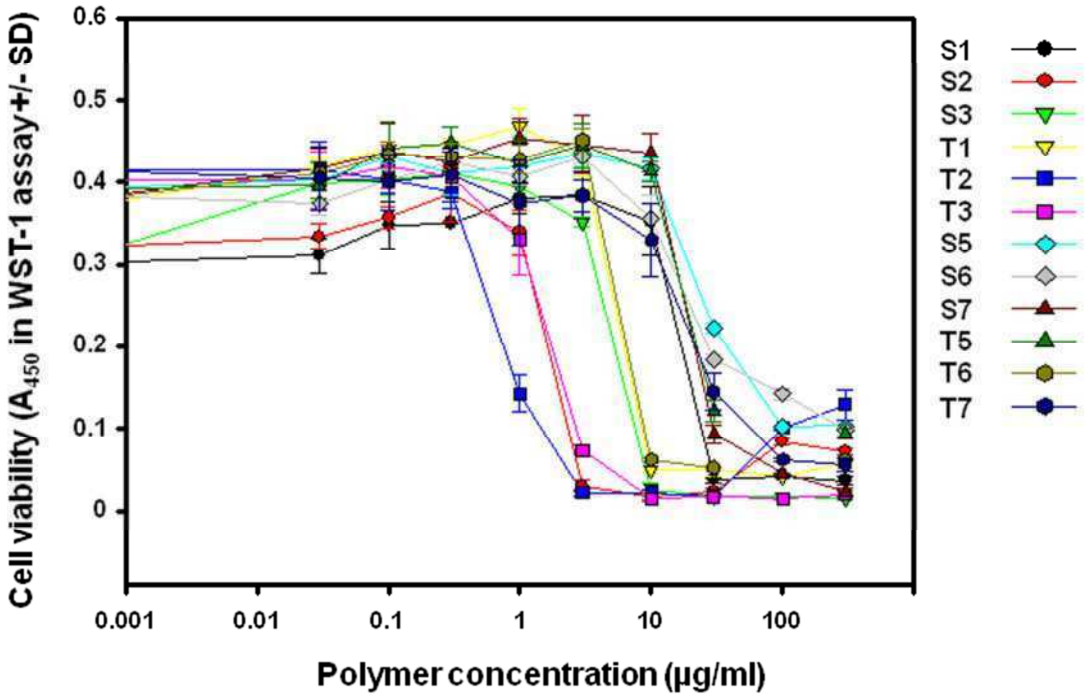

Figure 36: Dose-dependent cytotoxicity of the various copolymers. SKOV-3 ovarian carcinoma cells were incubated with the indicated polymer at various concentrations for 24 h, prior to the determination of cell viability.

Plasmid-DNA transfection efficacy . DNA transfection efficacies in the presence of serum were tested for the various polymers at different polymer/DNA ratios and with different complex amounts. Among the MDO ester group-containing biodegradable polymers, highest luciferase expression was observed upon transfection with complexes based on copolymer T7 (Figure 37). At the lowest mass ratio tested (mass ratio 5), luciferase activity was strongly dependent on the DNA amount transfected, with 3 µg DNA leading to the highest RLU values. However, profound luciferase expression was also observed at higher mass ratios, which also allowed to employ smaller DNA amounts (see e.g. Ratio 10, 0.25 µg DNA). Above mass ratio 60 / 0.25 µg DNA, cell death was determined by microscopy, corresponding with the absence of luciferase activity, while at lower mass ratios no major impairment of cell viability was observed. Notably, quaternization markedly improved biological activity since the corresponding, unquaternized polymer T3 did not show appreciable transfection efficacy (data not shown). This is in contrast to previous results with other CKA (BMDO instead of MDO)-based polymers, where higher activity was observed in the unquaternized polymer (early publication).[64] It probably reflects the fact that the BMDO radical is less reactive, thus leading to a lower percentage of (hydrophobic) ester groups in these polymers which in turn translates into a higher rigidity and higher hydrophilicity with no beneficial effect of quaternization.

.

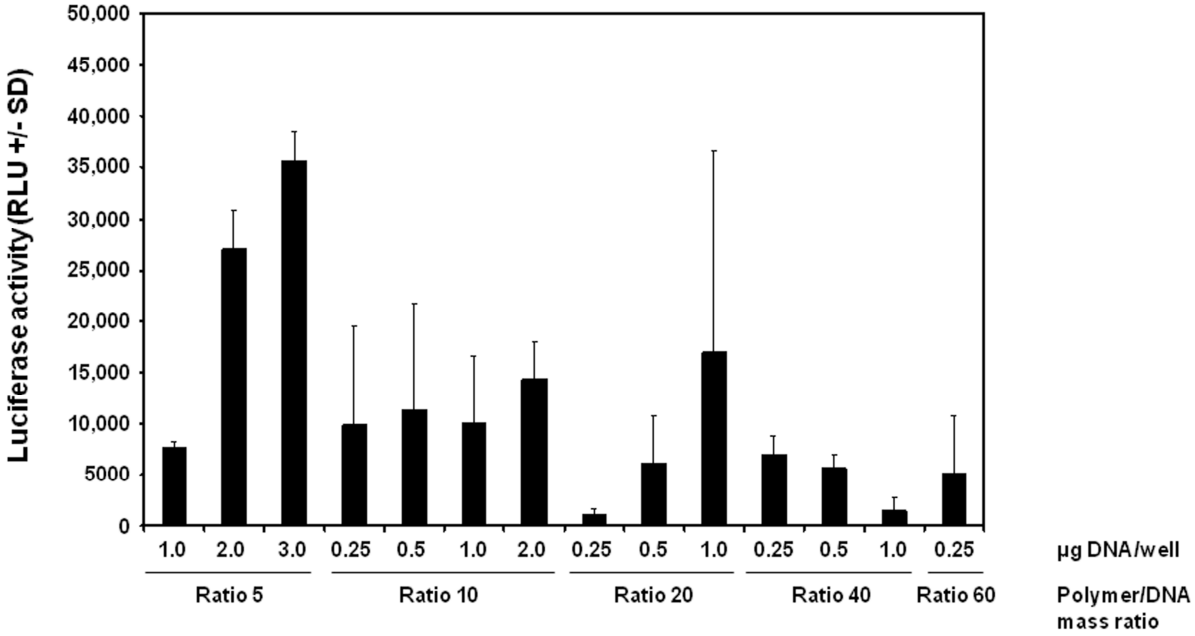

Figure 37: Transfection efficacies of complexes comprising the quaternized 57:43 (MDO:DMAEMA) copolymer with plasmid-DNA and prepared at different polymer/DNA ratios, as determined by luciferase activities in SKOV-3 ovarian carcinoma cells.

2.3.3 Conclusion

The aim of this study was to synthesize novel degradable, water soluble polymeric DNA transfection vectors with low toxicity. Degradable and biocompatible poly(PEG-*co*-(MDO-*co*-DMAEMA) were obtained via free radical polymerization using PEO macro-azo-initiator. The presence of MDO units onto the polymer backbone led to hydrolytic degradability. The water solubility is an essential prerequisite for their use as DNA delivery agents, and after quaternization, the solubility of the polymers as well as their complexation efficacies were greatly improved. Beyond favorable physicochemical data of the polymer/pDNA complexes with regard to hydrodynamic diameter and zeta potential, we demonstrate high biocompatibility and positive results in reporter gene transfection experiments in the presence of serum, and identify T7 as particularly efficient. Our poly(PEG-*co*-(MDO-*co*-DMAEMA) copolymers may thus represent promising vectors for in vivo applications with regard to the delivery of DNA or other therapeutic nucleic acids (Figure 38).

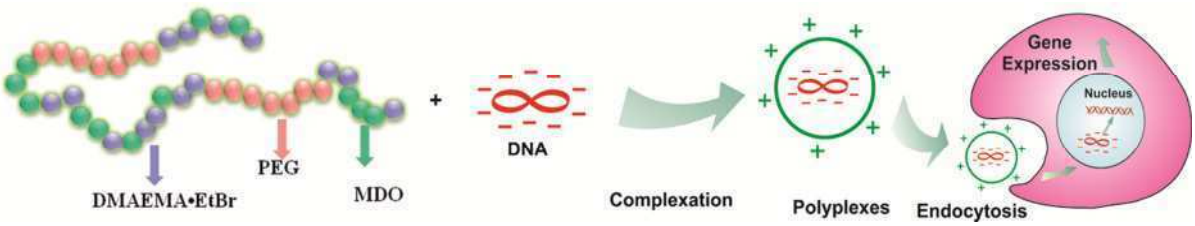

Figure 38: Illustration of poly(PEG-*co*-(MDO-*co*-DMAEMA) forms polyplex with plasmid DNA and shows positive gene expression.

Chapter III: Degradable Polymers for Drug Delivery

3.1 Biocompatible and Degradable Poly(2-Hydroxyethyl Methacrylate) based Polymers for Drug Delivery Applications

Zhang, Yi; Chu, Dafeng; Zheng, Mengyao; Kissel, Thomas; Agarwal, Seema; *Polymer Chemistry* **2012,** DOI:10.1039/c2py20403g

3.1.1 Introduction

Poly (2-hydroxyethyl methacrylate) (PHEMA) is a widely used and researched biocompatible polymer. Every repeat unit of PHEMA has one hydroxyl (-OH) group which makes the polymer highly hydrophilic and shows less or practically no tendency to adhere to proteins. It is an outstanding material for many different biomedical applications like scaffolds for tissue engineering, soft contact lenses, artificial skin and drug delivery systems for water soluble drugs etc..[81–83] However, PHEMA has a C-C backbone and is therefore neither hydrolysable nor enzymatically degradable. For many biomedical applications degradability is important. There are some efforts in literature to provide degradability to PHEMA gels. This is done by primarily by using degradable cross-linkers. For example, the use of disulfide –S-S- cross-linkage has been reported by Galaev et al.[84] S-S- linkages are stable under oxidizing conditions, but can be broken down into thiol groups in a reductive environment. They used a water soluble disulfide cross-linker, *N,N*'-bis(methacryloyl)-L-cystine for cross-linking PHEMA chains and showed disintegration of the gel with a reducing agent like dithiothreitol. The use of hydrolytically and enzymatically degradable oligomeric polycaprolactone (PCL), as a cross-linker for PHEMA chains was also prepared.[85] Peptide based cross-linkers have also been used to provide degradability to PHEMA gels. Enzymatically degradable hydrogels

based on HEMA and poly (ethylene oxide) PEO cross-linker having tripeptide like Gly-Gly-Leu have been researched by *Mésini* et al.[86] The cross-linked gels were degraded by the enzyme subtilisin in about 50 days.

In all these representatively cited examples, the PHEMA chain remained as such after degradation. In the last few years, we have provided many new materials like degradable thermoplastic elastomers, ionomers, gene transfection systems etc. by introducing ester linkages onto the vinyl polymer C-C backbone.[12,87–89] Radical-ring-opening copolymerization of cyclic ketene acetals like 2-methylene-1,3-dioxepane (MDO) and 5,6-benzo-2-methylene-1,3-dioxepane (BMDO) with vinyl monomers has been a promising method for introducing degradable ester linkages into the C-C polymer backbones. Cyclic ketene acetals (CKA) are the isomers of the corresponding cyclic lactones and can undergo radical addition at the vinyl double bond with subsequent ring-opening leading to the formation of esterbonds in the polymer backbone. Utilising similar radical ring-opening polymerization chemistry of CKAs, biocompatible PHEMA could also be made degradable i.e. simply by copolymerization of HEMA and CKAs.

The main question of this work is whether it is possible that ester linkages be randomly brought onto the PHEMA backbone and if so, how this can be done. If this can be successfully done, this would provide a new hydrophilic hydroxyl functionalised degradable polymer for biomedical applications. The initial efforts of copolymerizing HEMA with CKA like BMDO for introducing degradable ester linkages on its backbone were not successful. Detailed analysis has shown that the proton (from HEMA) addition to the double bond of BMDO was preferred in contrast to the expected ring-opening BMDO HEMA copolymerization. Therefore, protection-deprotection chemistry at hydroxyl (-OH) group of HEMA has been used for copolymerization with BMDO. The resulting PHEMA has ester

linkages randomly distributed on the backbone. The polymers were shown to be biocompatible and degradable. The exemplary use of resulting polymers for drug encapsulation has also been shown.

3.1.2 Experimental Part

Instrumentation. One dimensional NMR 1H (300 MHz) and 13C (100 MHz) spectra were recorded on a Bruker DRX-300 spectrometer. Tetramethylsilane was used as internal standard. 1H–13C correlation experiments were performed on a Bruker DRX-500 spectrometer, with a 5 mm multinuclear gradient sample and using gs-HMQC (heteronuclear multiple quantum coherence) and gs-HMBC (heteronuclearmultiple bond coherence) pulse sequences. The HMQC experiment was optimized for C-H coupling of 140 Hz, with decoupling applied during acquisition, while the HMBC experiment was optimized for coupling of 8 Hz, with decoupling during acquisition.

The molecular weight and the polydispersity of the synthesized polymers were measured with Gel Permeation Chromatography (GPC) using a Knauer system at 25 °C using DMF with LiBr as eluting solvent. Molecular weights were calculated using PMMA calibration; toluene was used as an internal standard. The GPC had a 50 × 8 mm2 precolumn and three linear 10 μm polyester columns (GRAM, PSS) 300 × 8 mm2. The injector volume was 50 μL and the polymer concentration was 1 mg/mL. DMF with 5 g/L LiBr was used as eluent at a flow rate of 1 mL/min. The software PSS WinGPC Unity (Build 5403) from Polymer Standards Service GmbH was used for evaluation of the elugramms.

Synthesis of Protected HEMA Monomer (HEMA-TMS). 40 mL HEMA (42.92 g, 0.33 mol) were placed in a 250 mL flask. The flask was cooled with an ice bath and Hydrochinon (100 mg, 0.9 mg) were added. Then 34.4 mL of 1,1,1,3,3,3-hexamethyldisilazane (HMDS) (26.62 g, 0.16 mol) were slowly added to the solution. After addition of HMDS, two drops of TMSCl were added as catalyst. The reaction mixture was stirred at room temperature (18 °C) for 24 h. The reaction was monitored with gas chromatography (GC). In the GC, only one peak could was observed after 24 h. The reaction mixture was dried with MgSO4 for 10 min. Then the

solution was filtered and distilled under high vacuum. The final product was received as a clear liquid.

^{1}H NMR, δ (300 MHz, $CDCl_3$, ppm): 6.10 (s, H_2C=C, 1H), 5.54 (s, H_2C=C, 1H), 4.20 (t, O-CH_2-CH_2-OSi, 2H), 3.80 (t, O-CH_2-CH_2-OSi, 2H), 1.92 (s, CH_3, 3H), 0.10 (s, Si-CH_3, 9H)

Copolymerization of HEMA / HEMA-TMS and BMDO. All the polymerization reactions were carried out under argon using AIBN (azobis isobutyronitrile) as initiator. In a typical polymerization reaction the monomer BMDO (0.99 g, 6.1 mmol) was dissolved in HEMA-TMS (1.18g, 6.1mmol) in a predried Schlenk tube under argon atmosphere. The reaction mixture was degassed by three freeze-pump-thaw cycles. The AIBN (4.95 mg, 0.37 mmol) was added to the still frozen solution. The Schlenk tube was then sealed, evacuated and backfilled with argon (procedure was repeated three times) then immersed immediately in a preheated oil bath at 70 °C for 24 h. Afterwards the Schlenk tube was taken out of the oil bath and shock cooled in an ice bath. The reaction mixture was soluble in chloroform. It was then diluted with chloroform and precipitated in 200 mL pentane. The polymer was recovered by centrifugation, and dried at 40 °C for 48 h. Similar procedure was used for making copolymers with HEMA and HEMA-TMS of different copolymer compositions. For copolymers having more than 50% HEMA in the feed ratio, cold MeOH was used as precipitating agent.

For deprotection of the TMS group, 1 g of the polymer obtained above was dissolved in 25 mL THF, 0.65 g (10.8 mmol) of KF and 0.03 g (0.1 mmol) of Tetra-n-butylammonium fluoride (TBAF) was added. This mixture was stirred for 24 h. THF was partly evaporated and the mixture was then precipitated in n-pentane. The product was redissolved again in THF and the precipitated in 200 mL distilled water containing two drops of HCl. After filtration,

the white polymer was then dried under vacuum at 40 °C for 72 h. The structure of the polymer was then analyzed with ^{1}H and ^{13}C NMR.

Cytotoxicity Studies. The cell cytotoxicity test (MTT (3 (4,5-dimethyl-thiazol-2-yl)-2,5-diphenyl tetrazolium bromide) assay) was performed according to the method of Mosmann.[67] Polymer solutions were prepared in serum supplemented tissue culture medium (Dulbecco's modified Eagle's medium, supplemented with 10% serum, without antibiotic) containing 2×10^{-3} M glutamine and sterile filtered (0.2 µm, Schleicher & Schüll, Dassel, Germany).

24 h before the MTT assay, L929 cells (8000 cells/well) were seeded into 96-well plates (Nunc, Wiesbaden, Germany). On the day of the MTT assay, the culture medium was replaced by 200 µL serial diluted polymer medium solution with different concentration. After a further 24 h incubation at 37 °C, the cell culture medium were replaced with 200 µL medium containing 20 µL sterile filtered MTT (Sigma, Deisenhofen, Germany) stock solution in phosphate buffered saline (PBS) (5 mg/mL) in each well. The final concentration of MTT in each well was 0.5 mg/mL. After 4 h incubating at 37 °C in the dark, the medium was removed and 200 µL DMSO were added in each well to dissolve the purple formazane product. The measurement was performed spectrophotometrically with an ELISA reader (Titertek Plus MD 212, ICN, Eschwege, Germany) at wavelengths of 570 nm and 690 nm. Culture medium without cells was used as reference to set zero point for calibration of the spectrometer. The relative viability (%) related to control wells containing cell culture medium without polymer was calculated by the following equation:

$$\text{Relative cell growth} = \frac{(\text{A } 570)\text{ test} - (\text{A } 690)\text{ test}}{(\text{A } 570)\text{ control} - (\text{A } 690)\text{ control}} \qquad (4)$$

Random poly(*D,L*-lactide-*co*-glycolide) (PLGA) (PLGA 21 kDa, Boehringer Ingelheim, Germany) was used as a positive control. The IC_{50} value was calculated using the Boltzman sigmoidal function from Microcal Origin1 v 7.0 (OriginLab, Northampton, USA). It shows the polymer concentration, which inhibits growth of half of the cells relative to non-treated control cells.

Hydrolytic Degradation. The hydrolysability of the polymers was tested under basic conditions using 5 wt.% KOH water solution. The degradability was followed using mass loss (by gravimetry) and molecular weight determination by GPC. The polymer films were made using a laboratory press (Polystat 200 T, Schwabenthan, Berlin, Germany). The polymers were compressed at 20 bar and 140 °C in 1 mm thick stainless steel molds for 10 min. This system cooled down to room temperature using cold water. The film thickness was 1.02 ± 0.05 mm. It was cut into small pieces with a weight around 300±10 mg/piece. The films were placed separately in a 5 wt.% KOH water solution at 37 °C in a vibrator for different time intervals. After a certain time the film was taken out of the solution and washed with water. Then the film was dried in a freeze dryer for 48 h and the weight lost was determined. For each degradation study three films were used and the average of the weight was then calculated. The molecular weight of the remaining undegraded films was determined with GPC.

Macrophages-mediated Degradation. J774A macrophages were maintained in DMEM containing 4.5 g/L of D-glucose, sodium pyruvate, L-glutamine, 10% of fetal bovine serum, 1% of Antibiotic-Antimycotic Solution (v/v) (PAA, Germany). Cells were passaged every 3-4 days by scraping. The seeding density was approximately 3.6 and 7.2×10^4 cells/cm^2. The volume of the used medium used was 1 mL for each well. The study was divided into three groups for two cell concentration and one control medium (n=3). In group one the

3.6×10^4 cell/cm^2 concentration was used. In group two 7.2×10^4 cells/cm^2 concentrations was used. Polymer films were first sterilized with isopropanol and then placed in the well plates (1 film/well). Macrophages were directly cultured on the surface of the film. For the control group films were not cultured with cells. After 10 days of culturing, the polymer film was first observed via microscopy. Afterwards the polymer film was washed with water. After drying the weights of the residual films were determined.

Nanoparticle Formation. Coumarin-6 loaded nanoparticles (NPs) were prepared by solvent displacement technique. 10 mg of polymer and 10 μg of coumarin-6 were dissolved together in 1 mL acetonitrile or acetone. The resulting polymer solution was injected into a magnetically stirred (600 rpm) aqueous solution of 5 g water (filtered and double distilled) through an injection needle (0.6 x 40 mm) at a constant flow rate (6.0 mL/min). After injection of the organic phase, the resulting suspensions were stirred for 4 h in a fume hood to remove the residual acetone.

Determination of Encapsulation Efficiency. The encapsulation efficiency was calculated by determining the concentration of coumarin-6 in the NPs after centrifugation and freeze drying. Samples of 150 μL were subjected to ultracentrifugation (Airfuge, Beckman Coulter, Krefeld, Germany) for 60 min with a 8000 rpm at room temperature. After centrifugation the supernatant was carefully removed. The NPs were rinsed with 100 μL of distilled water and centrifuged twice. The remaining NPs were freeze-dried (Beta II, Christ, Osterode, Germany). The NPs containing the encapsulated coumarin-6 were dissolved in acetonitrile and the concentration was determined by fluorescence spectroscopy (BMG Labtech, Offenburg, Germany) with excitation wavelength at 457 nm and emission wavelength at 500 nm. The calibration curve was established in the range of 10-50 ng/g ($R^2 > 0.99$). Encapsulation

efficiency (EE) was calculated by comparing the actual and theoretical loading of coumarin-6. Experiments were conducted in triplicates.

Measurement of Particle Size and ζ-potential. The average particle size and size distribution were determined by dynamic light scattering using a Zetasizer NanoZS/ZEN3600 (Malvern Instruments, Herrenberg, Germany). ζ-potential was measured by laser Doppler anemometry using the same device. The analysis was performed at 25 °C. The Dispersion Technology Software V. 6.01 was used to calculate particle mean diameter, the width of the fitted Gaussian distribution, which is displayed as the polydispersity index (PDI) as well as the average ζ-potential values. Measurement of 10 runs each was performed in triplicate after the NPs preparation.

***In Vitro* Coumarin-6 Release Studies.** The release of coumarin-6 from NPs was investigated using a dialysis method (MWCO 100 kDa) at 37 °C under 50 rpm with 0.5 g of coumarin-6 loaded NPs solution against 25 g of 0.01 M phosphate buffer, 140 mM NaCl, pH 7.4 / ethanol (70 : 30, w/w) to create sink condition for poorly water soluble coumarin-6. At certain time points, 1 mL of the release medium was drawn and replaced with fresh medium. The amount of coumarin-6 released in each time interval was determined by fluorescence spectroscopy with excitation wavelength at 472 nm and emission wavelength at 506 nm. The calibration curve was established in the range of 2-100 ng/g ($R^2 > 0.99$). Experiments were conducted in triplicates.

3.1.3 Results and Discussion

Synthesis and Structural Characterization.

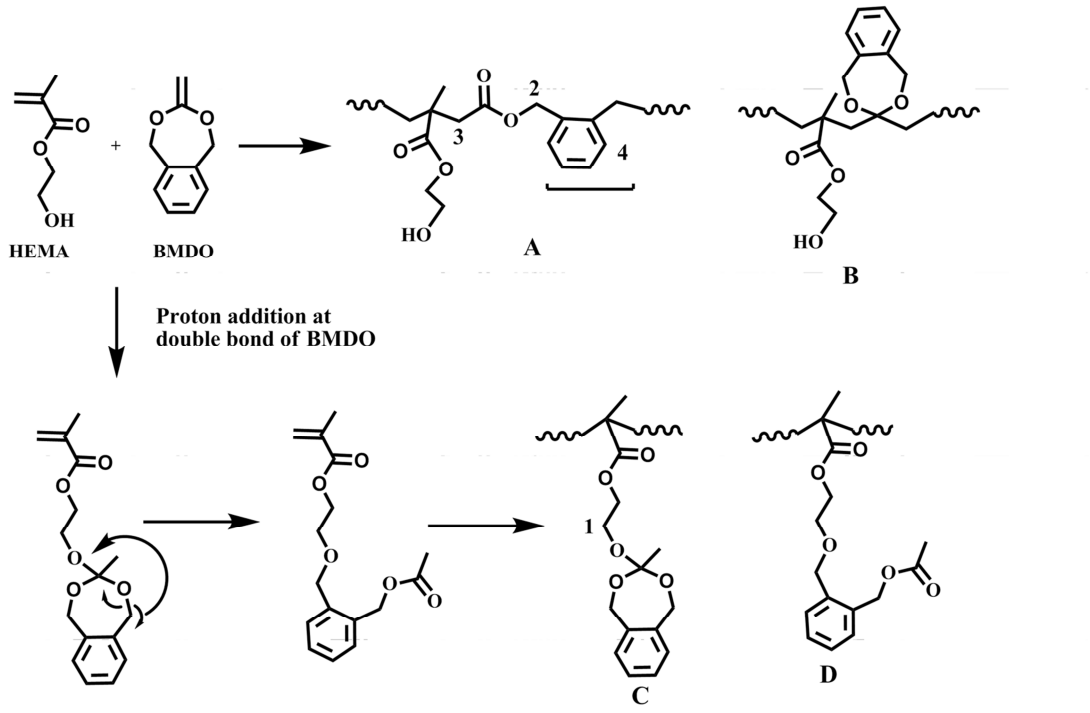

Scheme 3: Different probable polymer structures possible on copolymerization of HEMA and BMDO.

Free-radical copolymerization of HEMA and BMDO was carried out in an effort to make hydroxyl functionalized polymers with hydrolysable ester linkages in the backbone. The initial efforts of copolymerizing HEMA with BMDO by radical polymerization were not successful. Detailed NMR analysis showed the presence of many different moieties of polymer structures as compared to the expected copolymerization (Scheme 3). In general, the copolymerization of BMDO with vinyl monomers provides either the ring-opening reaction with the formation of ester linkages onto the polymer backbone and or copolymerization with ring-retained BMDO structure (polyacetal formation) (Scheme 3, structures A and B). In the present work, in addition to it, we also observed the proton (from HEMA) addition at double

bond of BMDO leading to two new structures with ring-retained and ring-opened BMDO in the polymer side chain (structures C and D; Scheme 3).

2D NMR like HMQC and HMBC were used to analyse the complex polymer structure. ^{13}C NMR of the reaction product showed two strong peaks at 116.0 ppm and 116.3 ppm. These two peaks showed no correlation in 2D HMQC spectrum and therefore proved them to be quaternary carbons (Q-Cs). One of the reasons for the origin of Q-Cs could be acetal structure formation by ring-retaining vinyl polymerization of BMDO at its double bond (structure B, Scheme 3). This is a very common reaction that can occur during copolymerization of CKAs with vinyl monomers depending upon the comonomer, initiator, temperature etc. and is known in the literature.[87] One of these Q-Cs peak at 116.0 ppm showed three strong cross-signals (A, B, C) in 2D HMBC NMR spectrum (Figure 39A) with –OCH2 peaks at 5.1 ppm and 4.7 ppm attached to aromatic ring of BMDO (the correlation of these peaks with aromatic carbonyl was observed in HMBC but not shown here) and the backbone $–CH_2$ at 1.6 ppm. This confirmed the ring-retained structure of BMDO (B, Scheme 3). In addition the other Q-C peak at 116.3 ppm showed a strong correlation with peaks at lower 3.4 ppm (D) and 1.7 ppm (E). The peak at 3.4 ppm derives from $–OCH_2$ group of HEMA type repeat unit (the corresponding peak at 51.5 ppm in ^{13}C NMR as determined by 2D HMQC NMR – not shown here) as there was no correlation with aromatic and carbonyl peaks in ^{13}C NMR. The peak at 3.4 ppm was from $–OCH_2$ proton marked 1 in structure C of HEMA derivative (Scheme 3). This gave the hint about structure C (Scheme 3) formed by proton addition at the double bond of BMDO and further polymerization. This structure was confirmed by observing correlation of the peak at 1.7 ppm (E) ($–CH_3$ group showed a correlation in HMQC with peak at 19.8 ppm) with Q-C peak at 116.3 ppm. The complexity of the reaction product was further seen while analysing carbonyl carbon region in ^{13}C NMR. Two groups of carbonyl signals

were seen that is one group of multi signals between 176.0-178.5 ppm and the second between 169.0-172.0 ppm (Figure 39B). The group of multi signals in the range from 176.0-178.5 ppm were from HEMA carbonyl units as they showed many correlations with -OCH_2, backbone –CH_2 and –CH_3 protons in 2D HMBC NMR spectrum. The other signals between 169.0-172.0 ppm could be from the ring opening of BMDO and were proved by careful analysis of 2D HMBC NMR spectrum. The carbonyl signal at 172.3 ppm correlated with –OCH_2, -CH_2-C(O) and –CH_2-Ar (marked 2, 3 and 4 in Scheme 3 structure A protons of BMDO units after ring-opening and showed respective correlations as H, I and J in Figure 39. The main proof for structure D in Scheme 3 was the correlation of carbonyl peak at 170.8 ppm with –CH_3 group (2.1 ppm) (K in Figure 39) observed in 2D HMBC NMR. The peak from the methyl group peak at 2.1 ppm did not show any other correlation. The proton addition at the double bond of BMDO was also observed previously for the reaction with acrylic acid.[87] It was not possible to determine quantitatively the amount of each species in the polymer because of overlapping peaks in ^{1}H NMR spectrum. The other most common problem during radical homo- and co-polymerization of HEMA like cross-linking due to transesterfication or transfer reactions to polymer and/or monomer was not seen in the present system as the polymers were soluble in common organic solvents.[90,91]

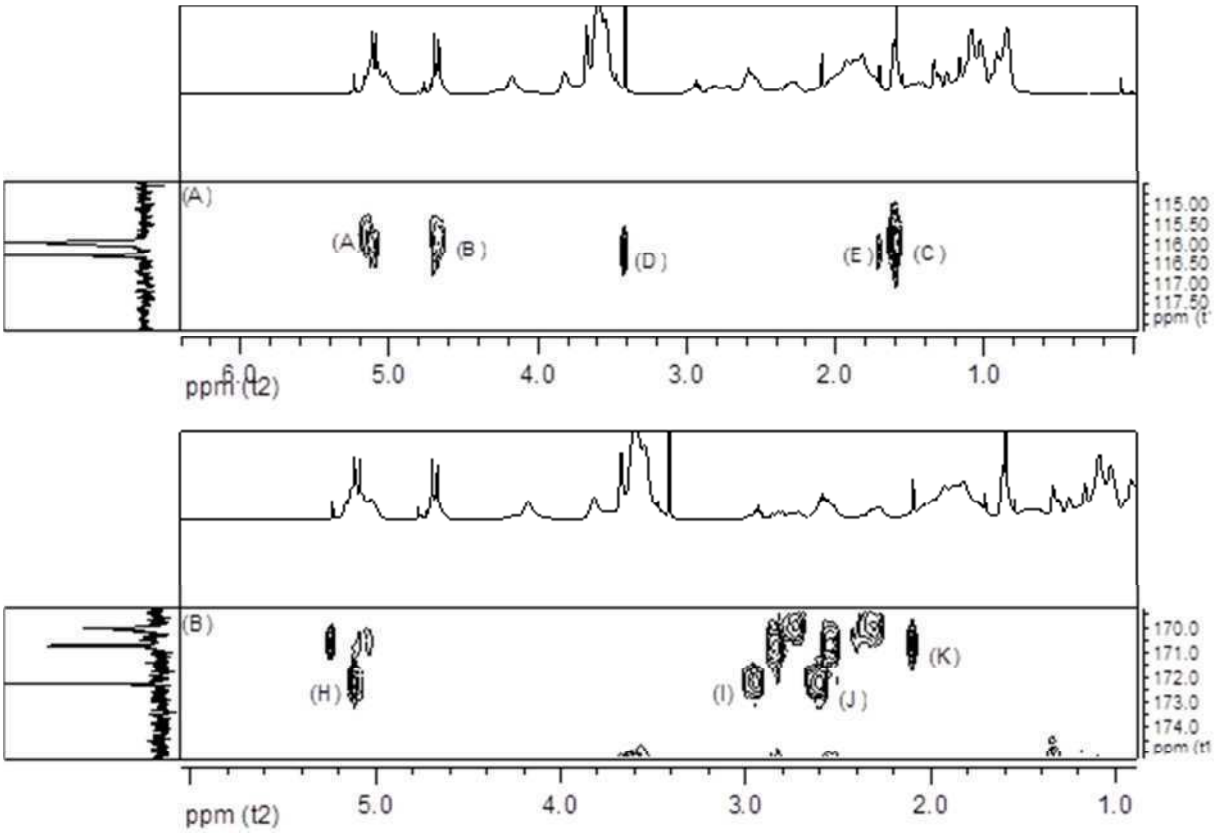

Figure 39: 2D HMBC correlation spectra A) ^{13}C region is from 115.0-118.0 ppm B) ^{13}C region is from 170.0 – 175.0 ppm.

Therefore, in order to achieve the targeted ester containing PHEMA, protection-deprotection chemistry at hydroxyl group of HEMA was employed. A three step reaction was performed as shown in Scheme 4.

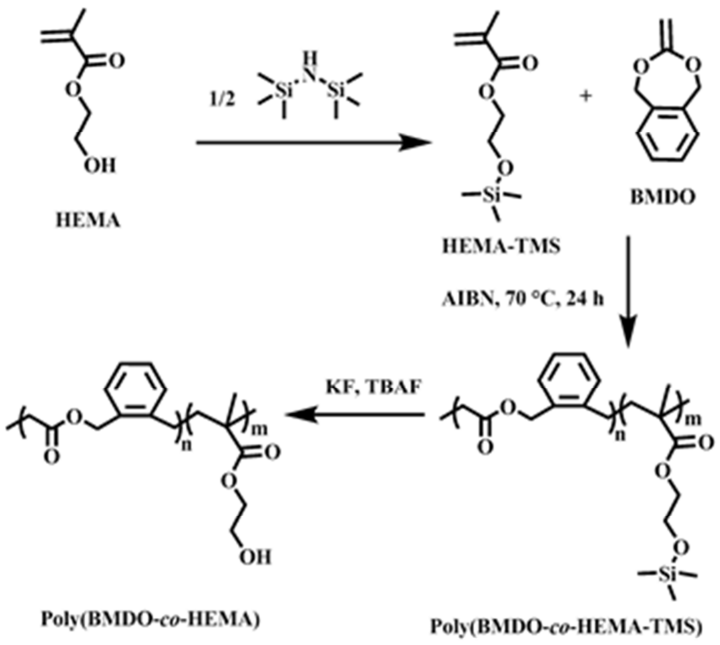

Scheme 4: The synthetic route to the functional degradable polymer: poly(HEMA-*co*-ester).

In the first step, the OH group of HEMA monomer was protected using TMS as a protective group. The protection reaction was followed by gas chromatography (GC) and the protected HEMA (HEMA-TMS) was characterized with ^{1}H NMR and found to be quantitative with more than 99% protection. The copolymerization reaction of BMDO with HEMA-TMS was then performed at 70 °C for 24 h using different feed ratios of the two comonomers (Table 5). The obtained polymers were structurally characterized by NMR. ^{13}C NMR in Figure 40 shows a comparison of the polymers obtained after reaction of BMDO with protected HEMA (HEMA-TMS) to the reaction product with unprotected HEMA (described above). No peak was observed around 116 ppm in all the copolymers using protected HEMA (HEMA-TMS) showing quantitative ring-opening and no ring-retained structures from BMDO (therefore structures B and C of Scheme 3 were ruled out). A representative ^{1}H NMR of one of the copolymers is shown in Figure 41. All characteristic peaks of ring-opened BMDO and HEMA TMS were observed. The signal from methyl group at around 2.0 ppm showing only correlation with carbonyl carbon in HMBC as seen and explained above for polymer product

with unprotected HEMA (HMBC not shown here). This ruled out the presence of the structure D of Scheme 3 also and showed formation of copolymers with ester linkages from ring-opening reaction of BMDO in the back bone, which means successful formation of poly(BMDO-co-HEMA-TMS) (Structure A Scheme 3).

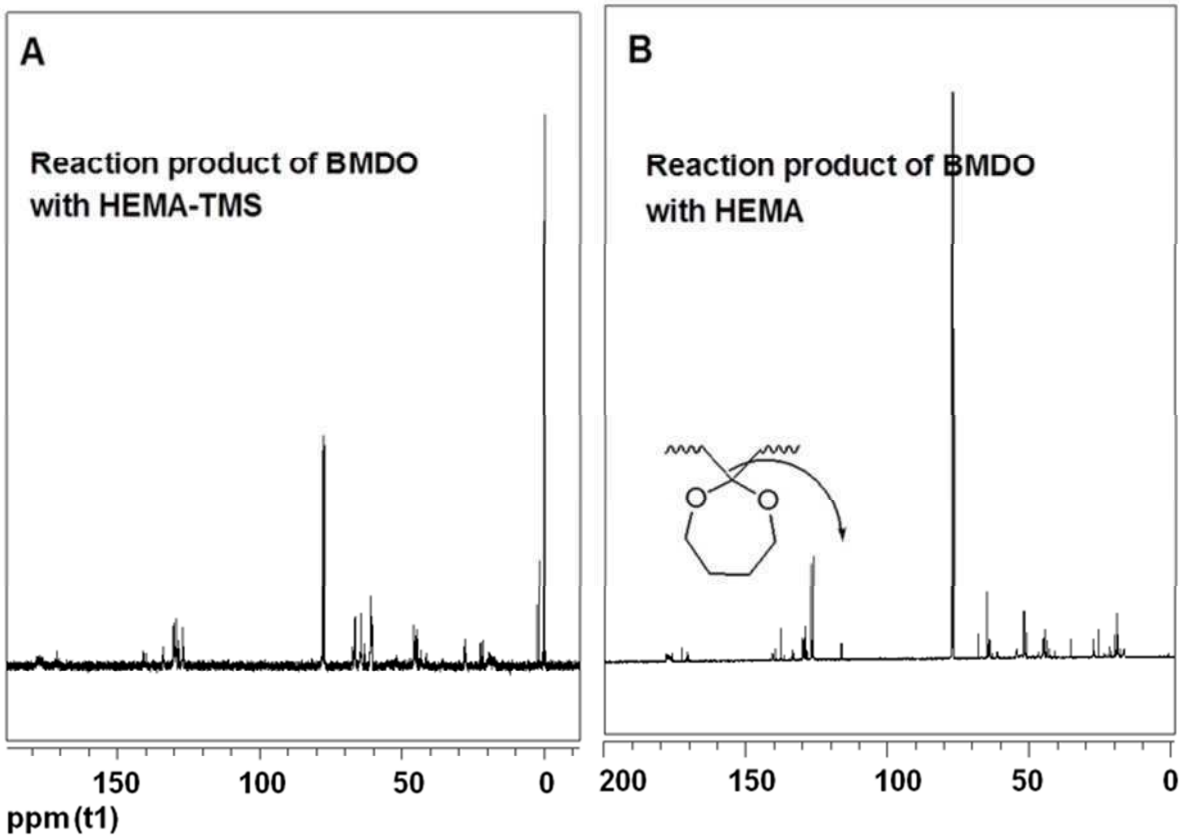

Figure 40: A comparison of ^{13}C NMR spectra of reaction product of BMDO with A) protected HEMA (HEMA-TMS) and B) unprotected HEMA. Ring-retained structures are visible in spectrum B.

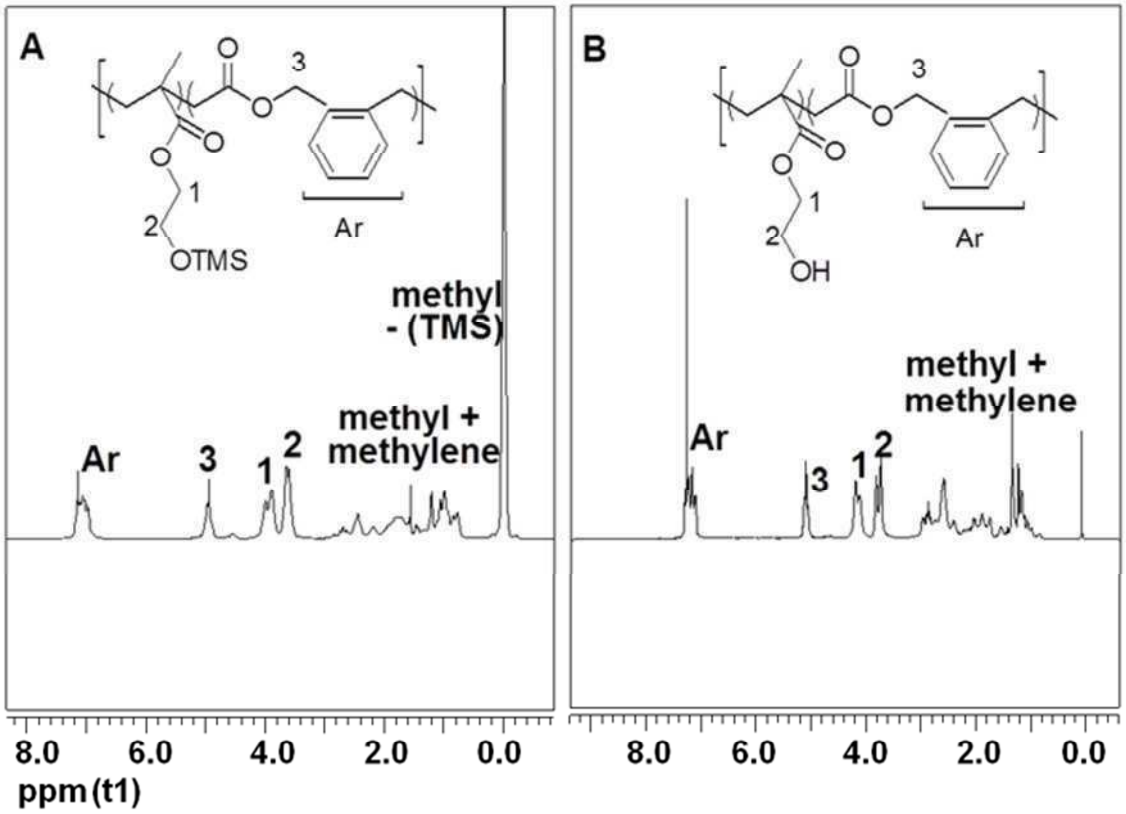

Figure 41: ^{1}H NMR spectra A) of poly(BMDO-*co*-HEMA-TMS) (sample R2 Table 1) and B) same polymer after deprotection.

Moderate molecular weight copolymers with unimodal GPC curves could be made depending on the copolymer composition (Table 5). The molecular weights were determined using DMF-LiBr as eluent relative to PMMA standard using UV detector. Although they do not represent true molecular weights but were appropriate in giving rough approximation of the chain lengths. The real molecular weight is approximately half of the value determined by GPC in DMF-LiBr eluent (PMMA as calibration standard) as shown by Matyjaszewski et al. for PHEMA and MMA-HEMA block copolymer.[90,92] The copolymer composition was determined by taking the ratio of peak areas under the peak at 5.0 ppm (characteristic of BMDO units) and 3.6 ppm (characteristic of HEMA units). Different copolymers with varied amounts of ester units could be made by changing the feed ratio (Table 5).

Table 5: Reaction conditions and copolymer characterization: free radical copolymerization was carried out using AIBN (0.25 mol-%) as initiator and different molar ratios of HEMA-TMS and BMDO at 70 °C for 24 h.

Sample name	Feed composition HEMA-TMS:BMDO	Copolymer composition[a] HEMA-TMS:BMDO	M_n Poly(BMDO-*co*-HEMA-TMS)	PDI M_w/M_n	M_n Poly (BMDO-*co*-HEMA)	PDI M_w/M_n	Yield %
R1	25:75	57:43	26000	1.9	20000	1.8	39
R2	50:50	67:33	42000	1.8	30000	1.7	55
R3	70:30	82:18	86000	2.0	63000	1.9	62
R4	90:10	93:7	340000	3.3	220000	2.5	79

[a] as determined from ^{1}H NMR

To get an insight into the copolymerization behavior, for one specific initial feed (HEMA-TMS:BMDO = 1:1) polymerization reactions at five different intervals of time were investigated (Table 6). Both HEMA and BMDO content continuously increased with increasing reaction time. The yield and the copolymer composition remained constant after about 18 h of reaction time. The incorporation of HEMA-TMS was much faster in the copolymers than BMDO (Table 6; Figure 42).

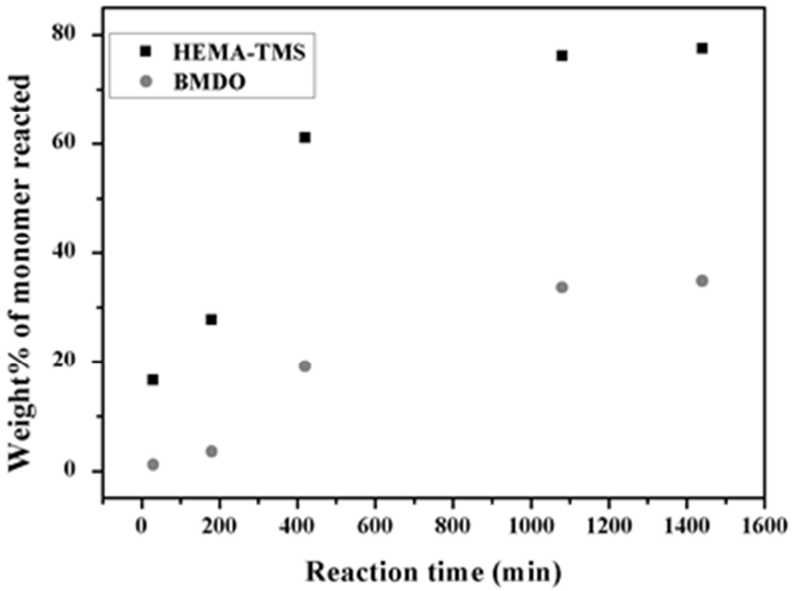

Figure 42: Caption Comparison of monomer (HEMA-TMS and BMDO) reactivity during free radical polymerization at 70 °C; (HEMA-TMS:BMDO 1: 1 molar ratio in feed, AIBN = 0.25 mol %)

The change of the copolymer composition over time showed the formation of random copolymers with long sequences of HEMA-TMS at the beginning followed by more randomization at the end of the polymerization. This was also supported by determination of reactivity ratios. Five copolymerizations with different monomer feed ratios were carried out at 70 °C till low conversions to determine the reactivity ratios (Table 7). All the conversions were between 8 and 12%. The reactivity ratios were calculated using Kelen-Tüdos method applicable for higher conversions (Figure 43) and showed r HEMA-TMS = 7.6±1.6 and r BMDO = 1.2±0.4.[93] The error of the reactivity ratio was calculated with 95% joint-confidence interval.[94]

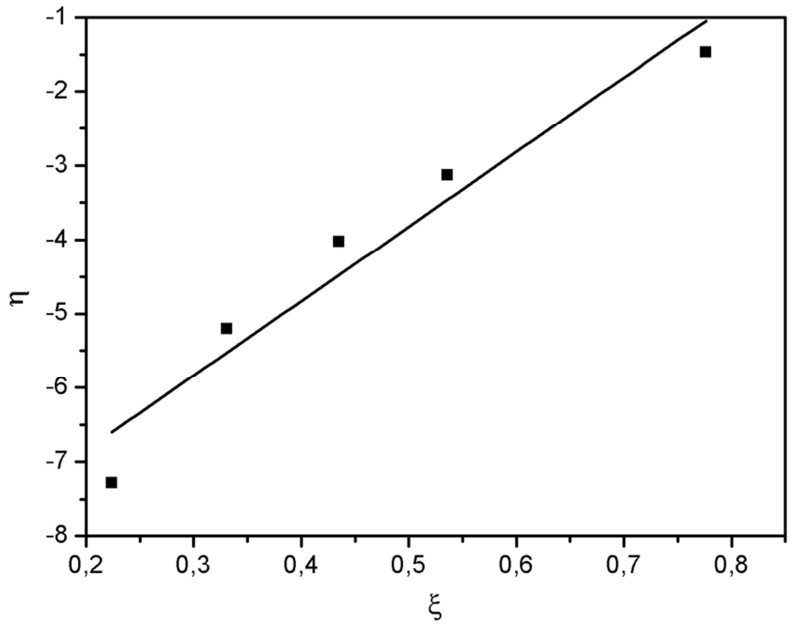

Figure 43: Kelen-Tüdos plot for poly (BMDO-*co*-HEMA-TMS) (values based on Table 3).

Table 6: Free radical bulk copolymerization of HEMA-TMS and BMDO (1:1 molar ratio) using AIBN as initiator for different time intervals temperature of polymerization = 70 °C, AIBN = 0.25 mol %).

Sample Name	Reaction Time min	Copolymer Composition HEMA-TMS mol%	Copolymer Composition BMDO mol%	Conversion %	Fraction of Monomer Reacted[a)] HEMA-TMS wt.%	Fraction of Monomer Reacted[a)] BMDO wt.%	M_n KDa	PDI
T1	30	84.8	15.3	9	17	1	68	1.4
T2	180	80.6	19.4	16	28	4	45	1.5
T3	420	74.1	25.9	39	61	19	41	1.8
T4	1080	66.5	33.5	56	77	35	35	2.1
T5	1440	66.7	33.3	55	76	34	32	2.1

Table 7: Free radical bulk copolymerization of HEMA-TMS and BMDO using AIBN as initiator with different feed compositions. Reactions were stopped at low conversions for reactivity ratio calculations by Kelen-Tüdos method (temperature of polymerization = 70 °C, AIBN = 0.25 mol %).

Sample Name	Feed Ratio		Yield	Copolymer Composition	
	HEMA-TMS mol%	BMDO mol%	%	HEMA-TMS mol%	BMDO mol%
K1	75	25	9	94	6
K2	50	50	12	85	15
K3	40	60	10	80	20
K4	30	70	11	74	26
K5	20	80	8	67	33

TMS-deprotection of the polymers was done using KF and Tetra-n-butylammonium fluoride (TBAF) as described in the experimental section. Quantitative deprotection of the hydroxyl groups (as seen by 1:1 peak ratio of $-OCH_2$ protons of HEMA at 4.1 ppm and 3.8 ppm in ^{1}H-NMR) was possible without cleaving backbone ester linkages (Figure 41B). The molecular weights after deprotection for all the samples are tabulated in the Table 5. Figure 44 shows the comparison of GPC chromatograms before and after deprotection for one of the representative sample (R2). There was a decrease in molecular weight due to TMS removal but polydispersity remained almost same before and after deprotection. Also, no tailing was seen in GPC chromatograms and therefore also ruled out degradation of polymer backbone during deprotection of TMS.

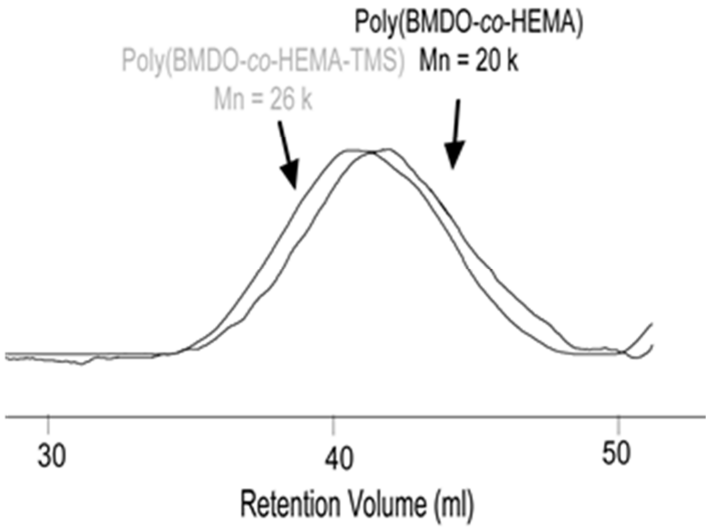

Figure 44: Comparison of GPC chromatograms of Sample R2 before and after deprotection of TMS group.

The hydrolytic degradation behavior of poly(BMDO-*co*-HEMA) was studied under basic (5 wt.% KOH) conditions and proved the random distribution of ester linkages onto the polymer backbone. The polymer was compressed at 20 bar and 140 °C using a 1 mm thick stainless steel mold for 10 min to a 1 mm thick film. This film was treated with 5 wt.% KOH for 48 h. The mass loss and the molecular weight of the polymer film were determined (Figure 45). After 17 h the film lost more than 50% mass, after 48 h only 20% polymer film remained (Figure 45A). The remaining films were completely soluble in chloroform and showed a reduced molecular weight (M_n = 2 kDa), which indicated the degradation of the polymer due to randomly distributed ester linkages (Figure 45B). The deprotected polymers were used further for cytotoxicity, degradation and drug release studies.

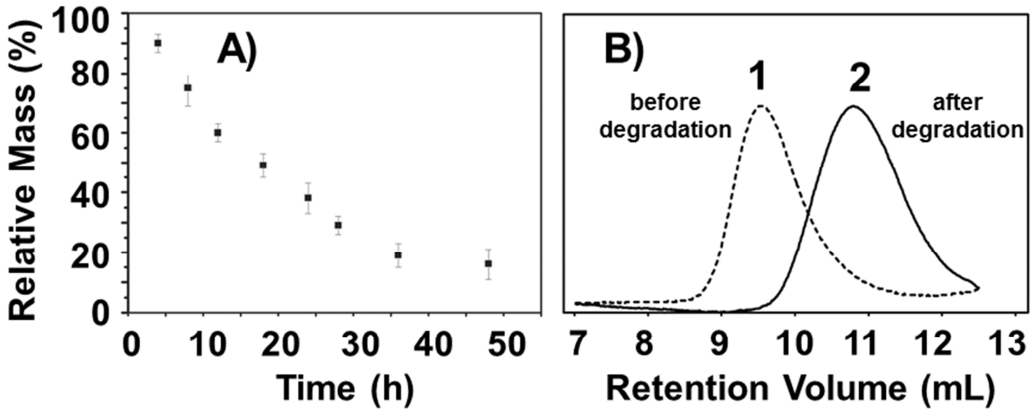

Figure 45: A) Mass loss profile of the poly (HEMA-*co*-BMDO) film (deprotected T3) after incubation with 5 wt.% KOH at 37 °C for different time intervals; B) GPC elugramms of 1) poly (HEMA-*co*-BMDO) film (deprotected T3, before degradation) and 2 after degradation in 5 wt.% KOH).

Cytotoxicity Test with MTT Assay. To evaluate the cytotoxicity of the synthesized copolymers, MTT assay was performed with L929 cells. The cell viability of the synthesized copolymers was compared with the well-known biocompatible polymer PLGA, which is usually used for drug delivery applications. The polymer concentrations between 0.01 mg/mL and 100 mg/mL were tested. The cell viability diagrams are shown in Figure 46. The polymers made in this work showed very high cell viabilities, even at high concentrations (100 mg/mL), the poly(BMDO-*co*-HEMA) had cell viability higher than 90%.

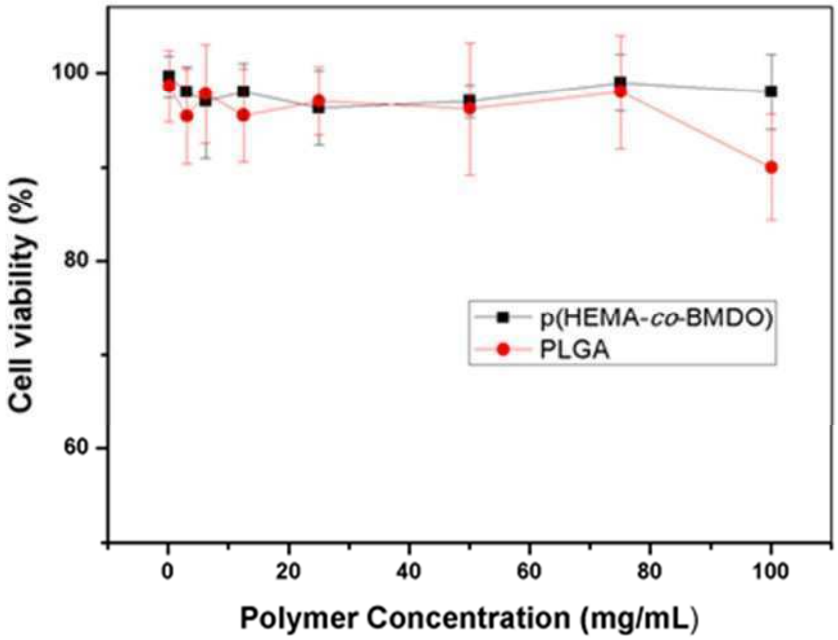

Figure 46: Cytotoxicity of polymer (deprotected R2) in comparison to well-known biocompatible PLGA studied by MTT assay. L929 cells were incubated with polymer of different concentrations for 24 h

Degradation Test with J774A Macrophages Cells. The macrophages mediated degradation of poly(BMDO-*co*-HEMA) was also tested and analyzed with Microscope. J774A macrophages cells were used and cultured on the polymer film for 14 days with two different concentrations 3.6 $\times 10^4$ cells/cm^2 and 7.2 $\times 10^4$ cell/cm^2. After treating the polymer film with cell medium for 2 weeks, holes were visible indicating degradation (Figure 47A). The black color in the microscopic pictures was the polymer film. The mass loss of the polymer film is shown in Figure 47B and increased with the cell concentration. With 3.6×104 cell/cm^2 the polymer film lost around 35% mass. The polymer film lost 54% mass with 7.2×104 cell/cm^2. The remaining film with low cell concentration was not soluble in chloroform. The DMF GPC showed almost no change in the molecular weight which indicated the surface erosion of the films. In contrast, when the polymer film is incubated with high cell concentration, the

remains of the polymer film were soluble in chloroform and showed drastic change in the molecular weight (Figure 47C). A multimodal distribution showing dispersity in molecular weight after degradation could be observed. The signal at elution volume of 11 mL had a molecular weight of 6 kDa and the other signal at 9 mL volume had a molecular weight of 17 kDa. This indicates that the degradability of the copolymers depends on the cell concentration.

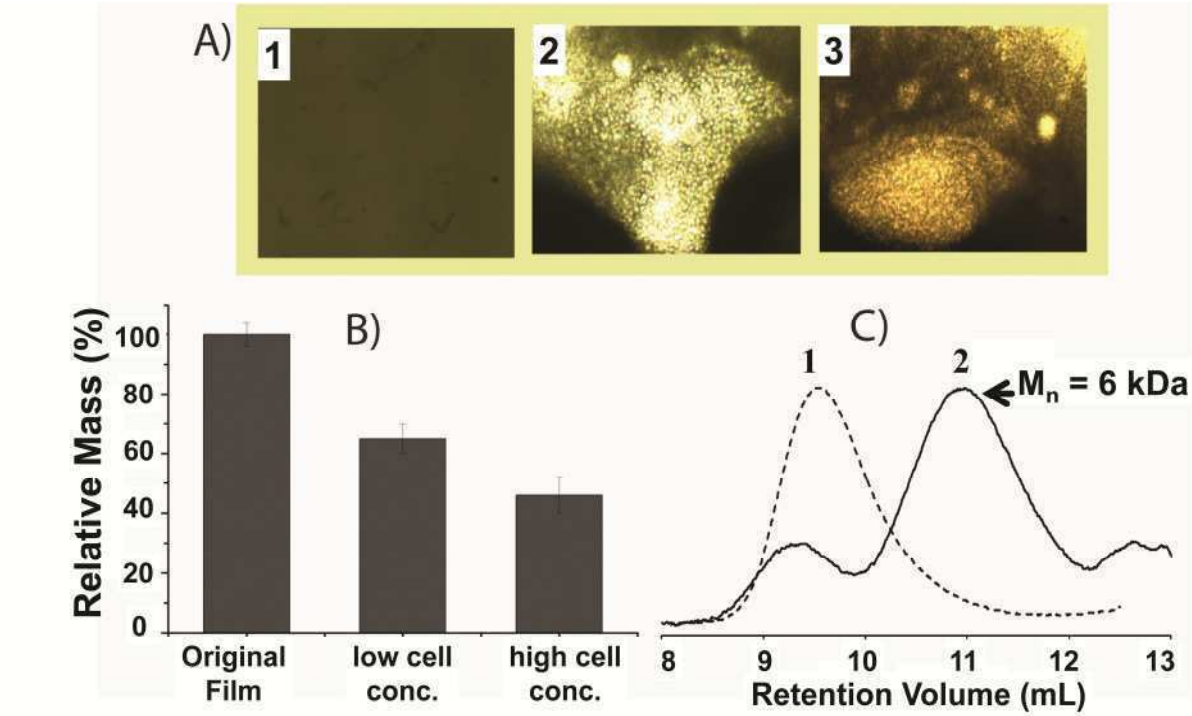

Figure 47: J774A macrophages mediated degradation data for poly(BMDO-*co*-HEMA) film (deprotected T3) after 10 days of culturing A) Microscope pictures; a) original film b) cultured with 3.6×10^4 cell/cm^2 cells, c) 7.2×10^4 cell/cm2; B) relative mass after 10 days of cell culturing with low cell concentration of cells (3.6×10^4 cell/cm^2) and high concentration of cells (7.2×10^4 cell/cm^2); C) GPC profiles showing degradability; 1) original sample 2) after 10 days of cell culturing with 7.2×10^4 cell/cm^2.

Preparation and characterization of Nanoparticles (NPs) and in vitro drug delivery.

Nanoparticle preparation loaded with coumarin-6 was performed by solvent displacement method without any additional surfactant (Figure 48A).[68,95] The properties of coumarin-6 loaded NP are summarized in Table 8. The polymer formed NPs with narrow PDI in the desired size range below 200 nm and negatively charged surface. Almost all the coumarin-6 was entrapped in the NPs which can be explained by extreme hydrophobicity of coumarin-6 and also the good NP forming nature of the polymer. Release profile was determined using membrane dialysis which is a valuable system for drug release studies from nanocarriers.[96] The nanocarriers can be easily separated from the release buffer, without any shear forces affecting the particle integrity. To achieve sink condition for the poorly water-soluble compound, 30 vol% ethanol was added as a co-solvent. A retarded drug release was observed and about 36%, 60% and 83% of the drug were released, after 1 h, 3 h, 8 h, 16 h and 24 h, respectively. The release was completed (>90%) after 24 h (Figure 48B), which will be sufficient for drug delivery and targeting to specific regions. Comparable experiments were carried out using only coumarin-6. A burst release was observed and more than 80% was released in 2 h.

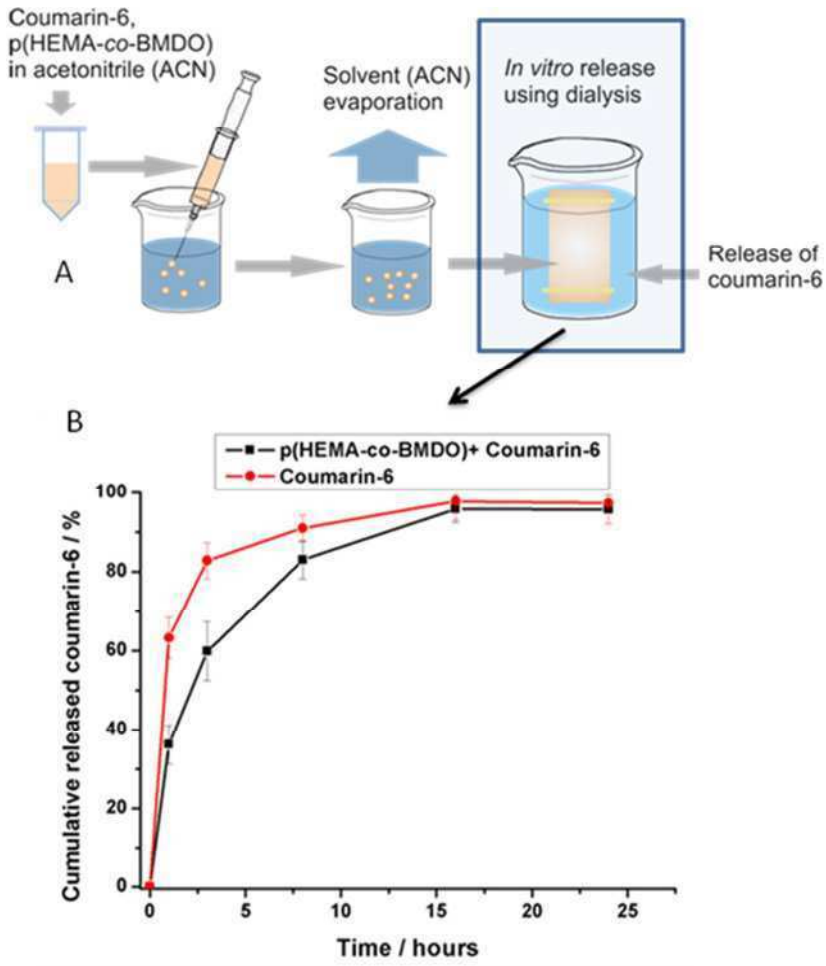

Figure 48: A) Procedure of making coumarin-6 encapsulated NPs by solvent displacement method from deprotected T3 sample and in vitro release studies B) release profile in PBS/ethanol (70/30, w/w), pH 7.4 at 37 °C.

Table 8: Physicochemical characterization of coumarin-6 loaded NPs. Values were presented as the mean±standard deviation (n=3).

Size (nm)	PDI	ζ-potential (mV)	Encapsulation efficiency (%)
81.9 ± 4.7	0.091 ± 0.021	-30.2 ± 1.8	98.2 ± 0.7

3.1.4 Conclusion

Biocompatible and degradable functional polymers based on HEMA could be synthesized successfully by radical polymerization. The structure of the resulting polymers was unambiguously proved by 2D NMR techniques. The cell viabilities were over 80% even for very high polymer concentrations (100 mg/ml). The hydroxyl functionalized polymers synthesized in this work were hydrolytically degradable under basic conditions and also showed surface erosion and bulk degradation using macrophages. Degradation using macrophages was concentration dependent. We have also demonstrated promising positive results for the use of such polymers for drug encapsulation. Although further modification of this system to tune the sustained delivery rate is under progress in our laboratory, we have already provide a new, well characterized biocompatible and degradable hydroxyl functionalized polymer suitable for many different biomedical applications.

Chapter IV: Antibacterial Application

4.1 Design and Synthesis of Antibacterial Hydrogel

4.1.1 Introduction

Hydrogels like crosslinked poly(2-hydroxyethyl methacrylate) (PHEMA) are widely used for biomedical applications.[97] Therefore, microbial contamination is a major concern in fields such as medical treatment, because bacterial contamination leads to severe infections and serious threats to human health. Another drawback of this kind of superabsorber is the non-degradability of the polymer backbone.

The aim of this study was to synthesize and characterize a degradable hydrogel with antibacterial properties (Figure 49).

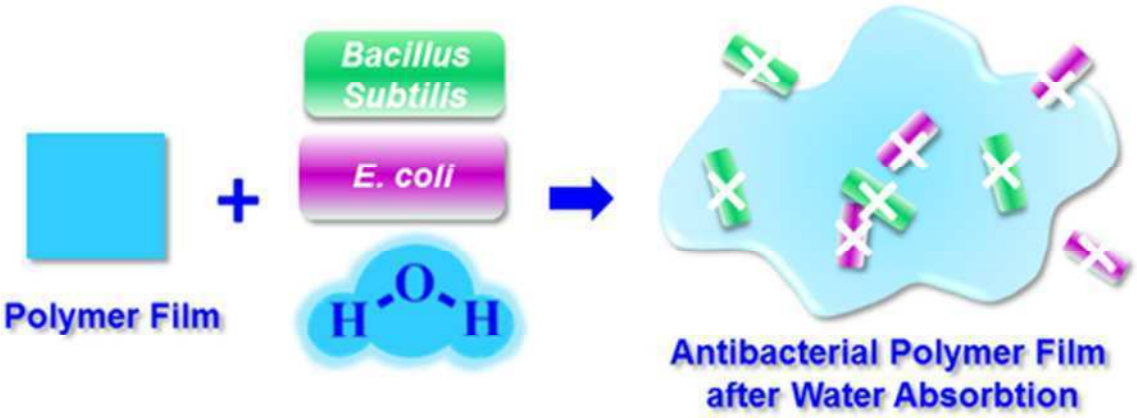

Figure 49: Illustration of a poly(BMDO-*co*-HEMA-*graft*-DMAEMA) film for water absorption and antibacterial (both *Bacillus Subtilis* and *E. coli*) applications.

For the design of an antibacterial polymer the differences of the bacterial cell membranes and walls have to be considered. While Gram-positive bacteria possess a cell wall composed of a single phospholipid bilayer covered by a up to 80 nm thick layer of murein, Gram-negative bacteria exhibit two phospholipid bilayers in their cell membrane with a 3 nm thin layer of

murein in between.[98] Antibacterial polycations targeting the cell membrane are therefore often more active against Gram-positive bacteria, although the polymer needs to penetrate the thick murein layer (Figure 50).

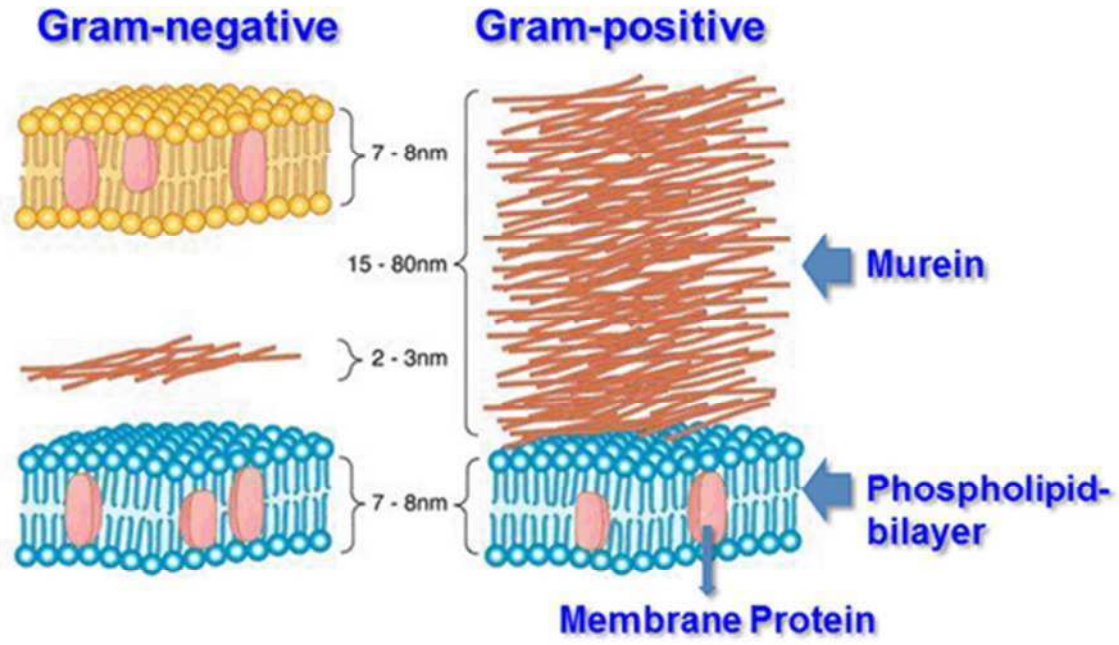

Figure 50: Illustration of the differences of the grambacterial cell membranes and walls.[98]

Poly(2-dimethylaminoethyl methacrylate) (PDMAEMA) is well known as antimicrobial material, which inhibits growth of both Gram-positive and Gram-negative bacteria.[99] PDMAEMA is able to diffuse through the thick layer of murein to reach the cell membrane. Due to its polycationic character it can adsorb onto the negatively charged cell membrane. The hydrophobic part of PDMAEMA can then enter the cell membrane and bind membrane lipids to itself, which are then extracted from the membrane leaving a hole, which ultimately kills the bacterium.

For optimal antibacterial activity, the molecular weight and the amphiphilic balance are very important structural factors. To achieve a tunable polymer chain length and macromolecular architecture, controlled polymerization methods like Atom Transfer Radical Polymerization

(ATRP) and Reversible Addition Fragmentation Chain Transfer (RAFT) were intensively investigated for the polymerization of PDMAEMA.[100,101] Recent studies used different lengths of the alkyl chain of alkyloxylethylammoniun ionenes to optimize the hydrophilic and hydrophobic balance.[102]

The strategy of this work is based on a combination of an antibacterial polymer and a hydrogel moiety synthesized via ATRP. A degradable polymer poly(HEMA-*co*-BMDO), which contains hydroxyl groups in the side chain, was used as polymer backbone. The hydroxyl groups subsequently can be partially functionalized as ATRP initiator moieties, which enables grafting of antibacterial PDMAEMA side chains with different chain lengths. The remaining hydroxyl groups which were not converted into ATRP initiator functionalities can be further on used as crosslinking sites for the transesterfication reaction between poly(HEMA-*co*-BMDO) side chains.[103] This eventually resulted in an antibacterial hydrogel.

4.1.2 Experimental Part

Material. DMAEMA (Acros, 99%) was passed through a basic alumina column to remove the inhibitor. PMDETA and anisole were dried using molecular sieves overnight (4 Å) and distilled before use. All other solvents were purified by destillation. Compost was received from Marburger Entsorgungs-GmbH (Marburg, Germany). All other chemicals were obtained from Sigma-Aldrich (Steinheim, Germany) and used as received.

Instrument. ^{1}H-NMR (300 MHz) and ^{13}C-NMR (100 MHz) spectra were recorded on a Bruker DRX-400 spectrometer. Tetramethylsilane was used as internal standard.

Elemental Analysis. Elemental analysis was carried out at the central analytic service of chemistry department at Philipps Universität Marburg. It was performed by combustion analysis, where a sample was burned in an excess of oxygen and the combustion products nitroxide (NO), carbondioxide (CO_2) and water (H_2O) were collected in various traps. The weights of these combustion products were determined and used to calculate the composition of the samples. Br analysis was accomplished by *Schoeniger* oxidation of the sample, followed by titration with $AgNO_3$. The weights of the precipitates (AgBr) were used to calculate the composition of the analyzed sample. The weight fraction (w/w) of carbon (C), hydrogen (H), nitrogen (N) and bromine (Br) was given as result.

Synthesis of the PDMAEMA Grafted Polymer via ATRP Method.

Synthesis of ATRP Macroinitiator. A random copolymer poly(BMDO-*co*-HEMA) with 33 mol% of BMDO, 67 mol % of HEMA and a molar weight of 34 kDa was synthesized as described previously.[104] 0.8 g of poly(BMDO-*co*-HEMA) was mixed with 0.5 mL Et_3N (3.3 mmol) and a catalytic amount of DMAP in 20 mL absolute THF at 0 °C. 0.5 mL of 2-bromo-2-methylpropiomyl bromide (3.3 mmol) was added slowly to the reaction mixture.

This reaction mixture was stirred overnight at rt. After centrifugation at rt for 30 min at 10000 rpm, the liquid phase was then precipitated in *n*-pentane. Purification of the precipitated polymer was performed by dissolving the crude product in $CHCl_3$ and reprecipitating in *n*-pentane. The polymer was lyophilized for 2 days at the freeze dryer. The yield was 71%. ^{1}H-NMR (300 MHz, $CDCl_3$), δ□ppm: 7.0-7.5 (Ar, m, 4H), 5.0 (C*H*$_2$-Ar, m, 2H), 3.8-4.2 (COOC*H*$_2$C*H*$_2$, m, 4H from HEMA), 2 ((C*H*$_3$)$_2$CBr, s, 6H), 1- 3 (m, other methyl and methylene). Elemental analysis (wt.%) C : H : Br = 50.2 : 5.6 : 21.6. That means 95 mol% of OH groups from HEMA were converted into ATRP initiator.

Polymerisation of DMAEMA. A typical polymerization reaction is described for sample 2: 33.7 mg of macroinitiator (0.1 mmol, 0.06 mmol of bromine active initiator part) and 2 mL of DMAEMA (12 mmol) monomer were dissolved in 2 mL absolute anisole in a Schlenk tube.[105] 12 µL of PMDETA (0.06 mmol) was added to the reaction solution, which was degassed three times by freeze-pump-thaw cycles. 8.5 mg of copper(I)-bromide (0.06 mmol) were added to the frozen mixture. The reaction flask was quickly evacuated and purged with argon three times. The reaction was then carried out for 2 h in an oil bath at 90 °C.[106] Afterwards, the reaction was stopped by shock cooling with liquid nitrogen. The reaction vessel was opened and excess water was added. The final product was then purified by dialysis (MWCO 20 kDa) against deionized water. (Yield: 78%, 43 wt.% PDMAEMA in graft polymer, Elemental analysis (wt.%) C : H : N = 62.7 : 8.4 : 3.8).

For sample 1, 1 mL of DMAEMA (6 mmol) monomer was dissolved in 1 mL absolute anisole. (Yield: 75%, 32 wt.% of PDMAEMA in graft polymer, Elemental analysis (wt.%) C : H : N = 63.0 : 8.1 : 2.9).

For sample 3, 3 mL of DMAEMA (18 mmol) monomer were dissolved in 3 mL absolute anisole. (Yield: 70%, 58 wt.% of PDMAEMA in graft polymer, Elemental analysis (wt.%) C : H : N = 62.2 : 8.7 : 5.2).

Swelling Measurements. 50 mg of the polymer was added to 50 mL of different water solutions. The weight of the polymer was determined before and after different times.

For the pH dependent test, pH 5, pH 7 and pH 9 buffers were used. For the temperature influence test, distilled water at temperatures of 4 °C, rt and 50 °C was tested. For the repetitive water uptake, 50 mg polymer was treated with 50 mL of pH 7 buffer solution for 24 h. Then, the polymer weight was determined and dried afterwards.

Each analysis was performed in the same manner three times. Results were visualized including the calculated errors using Microcal Origin1 v 7.0 (OriginLab, Northampton, U.S.A.).

Compostability Test. The polymer film (0.5 mm × 0.5 mm) was placed in compost in a plastic container (500 mL size) at 45 °C for several days. This compost was ventilated each day for 5 min. 2 mL water was added to the container each two days. After 30, 60 and 90 days the film was recovered, washed with distilled water and then dried using a freeze dryer for three days. The weight loss of the film was determined gravimetrically. This procedure was carried out with three polymer films.

Preparation of Bacteria Suspension. For the Gram-negative antibacterial test, a single colony of *Escherichia coli* (*E. coli*) (DSM No. 1077, K12 strain 343/113), was transferred from the stem nutrient agar plate to liquid nutrient (tryptic soy broth, Sigma Aldrich, aqueous solution c = 30 g/L) using an inoculation loop. The suspension was incubated at 37 °C with shaking until the optical density at 578 nm indicated that a concentration of 10^8 cfu/mL *E. coli* was obtained $\Delta OD_{578} = 0.125$. The suspension was diluted to an approximate concentration of 10^6 cfu/mL for further tests; the exact amount of bacteria was determined by spreading serial tenfold dilution on nutrient tryptic soy agar plates followed by colony counting after incubation for 24 h at 37 °C.[107]

For the Gram-positive strain, *Bacillus Subtilis* (DSM No. 1088), peptone meat extract medium was used as nutrient (Sigmal-Aldrich, aqueous solution meat extract c = 5 g/L, peptone from soybean meal, enzymatic digest. C = 3g/L). *Bacillus Subtilis* inocula were prepared analogously to the procedure described for *E. coli*.

Minimum Inhibitory Concentration (MIC)/ Minimum Bactericidal Concentration (MBC). To determine the MIC (as described in DIN 58940-6), a suspension of the biocide in liquid nutrient was prepared with different concentrations. In a microcentrifuge tube, each 500 µL solution as well as a blank control were inoculated with 500 µL *E. coli* or *Bacillus Subtilis* inoculum. After incubation for 24 h at 37 °C, bacteria growth was monitored visual evaluation of the test solutions for turbidity. The lowerst polymerconcentration, which inhibited bacteria growth, i.e. remained clear was taken as MIC.[107]

The solutions which showed no bacteria growth were spread on nutrient agar plates and incubated for 24 h at 37 °C. The lowest polymer concentration which did not lead to colony formation was taken as MBC.

Time Dependent Antibacterial Activity. To determine the time dependence of the antibacterial activity, 2 mL inoculum was incubated at rt with different amounts of poly(BMDO-*co*-HEMA-*graft*-DMAEMA) in microcentrifuge tubes. Serial tenfold dilutions of 100 µL aliquots in sterile phosphate buffer, drawn after different contact times, were spread on nutrient agar plates and incubated for 24 h at 37 °C. The number of viable cells after each immersion period was determined by colony counting.[102]

4.1.3 Results and Discussion

Synthesis of the PDMAEMA Grafted Polymer via ATRP Method.

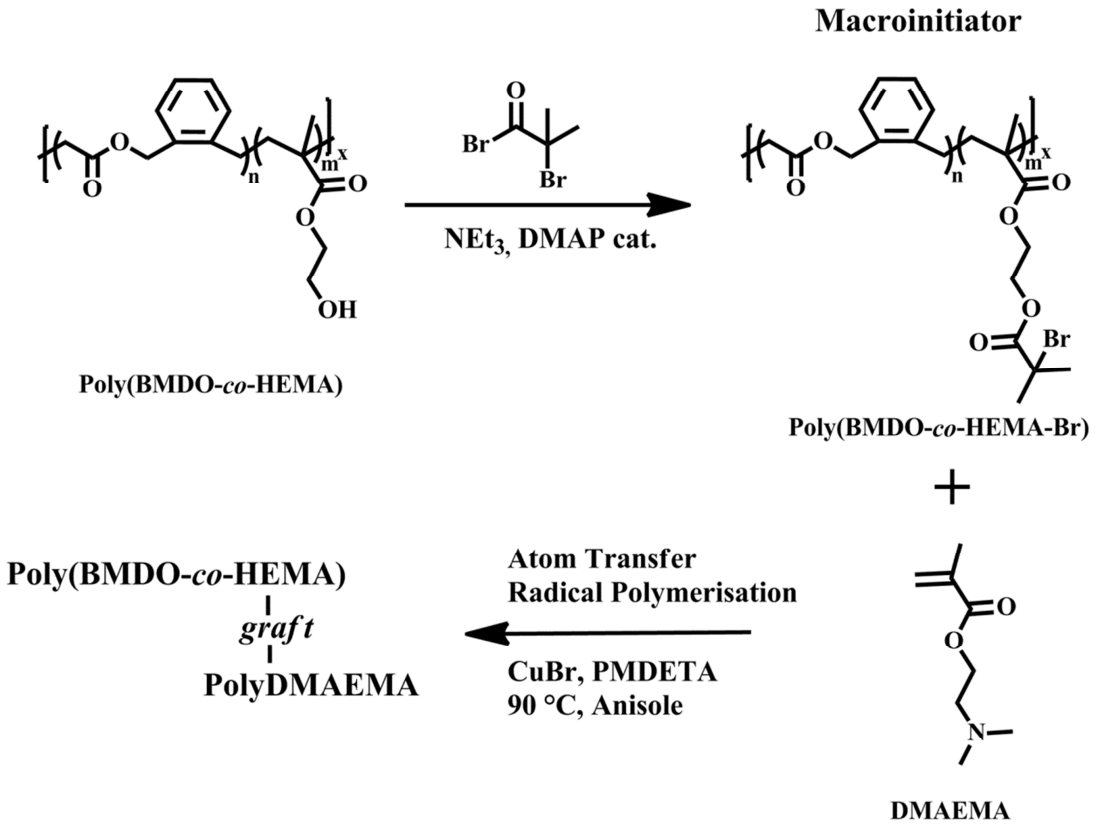

Scheme 5: Synthetic route to PDMAEMA grafted copolymer poly(BMDO-*co*-HEMA-*graft*-DMAEMA).

The synthetic route is based on the degradable linear polymer poly(BMDO-*co*-HEMA) with a molecular weight of 33 kDa, 67 mol% HEMA and 33 mol% BMDO content. The synthesis method of poly(HEMA-*co*-BMDO) was described in an earlier publication.[104] In the first step, the macro ATRP initiator poly(BMDO-*co*-HEMA-Br) was synthesized. A bromine content of 21.6 wt.% was determined via elemental analysis. 21.6 wt.% of Br were detected by elemental analysis. Conclusively, 95 mol% of hydroxyl groups from HEMA were converted into ATRP initiator. In the next step, DMAEMA was grafted onto the side chain of the ATRP macro initiator using copper(I) bromide as catalyst and PMDETA as ligand (Scheme 5).

By controlling the amount of the monomer DMAEMA, the amount of PDMAEMA in the final product poly(BMDO-*co*-HEMA-*graft*-DMAEMA) was adjusted. Since the polymer is not soluble in any solvent, the PDMAEMA content in the product was determined by elemental analysis. PDMAEMA was grafted with 32 wt.%, 43 wt.% and 58 wt.% on the side chain.

Swelling Studies

Reduction of Hydrogen Bond Formation. The synthesized polymer poly(BMDO-*co*-HEMA-*graft*-DMAEMA) (43 wt.% PDMAEMA) shows high water uptake efficiency. It can absorb about 2600 wt.% of water. Within 25 min, the polymer could reach around 84% of the maximum water uptake efficiency (Figure 51).

The water uptake efficiency was reduced to about 40% in the present of potassium thiocyanate, a hydrogen bond breaker.

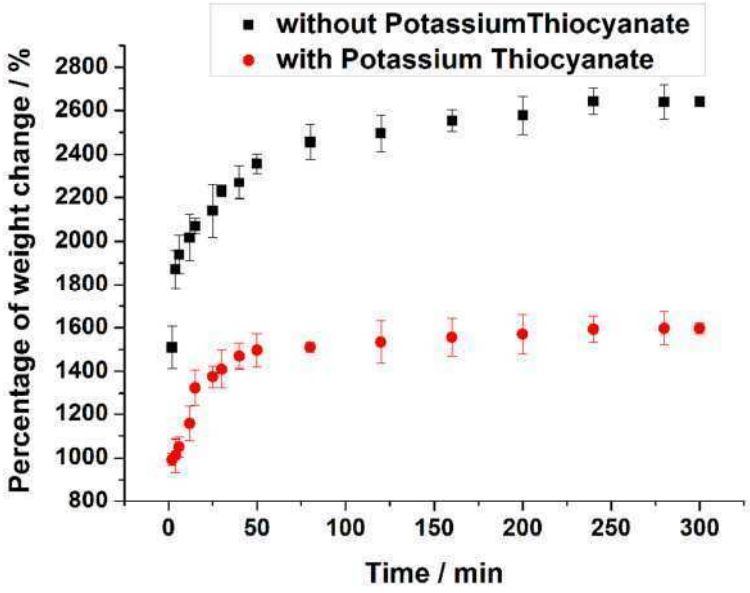

Figure 51: Water uptake efficiency of poly(BMDO-*co*-HEMA-*graft*-DMAEMA) (43 wt.% PDMAEMA) with and without potassium thiocyanate influence.

Effect of Amount of PDMAEMA on Swelling Properties. Different amounts of PDMAEMA grafted on the poly(HEMA-*co*-BMDO) also influence the water uptake efficiency (Figure 52). It is known that water absorption is highly influenced by the crosslinking grade. The polymer with 43 wt.% of PDMAEMA on the side chain has shown the highest water uptake result. The polymer with the highest PDMAEMA content (58 wt.%) showed the lowest water uptake efficiency. However, it could still absorb more the 1600 wt.% of water.

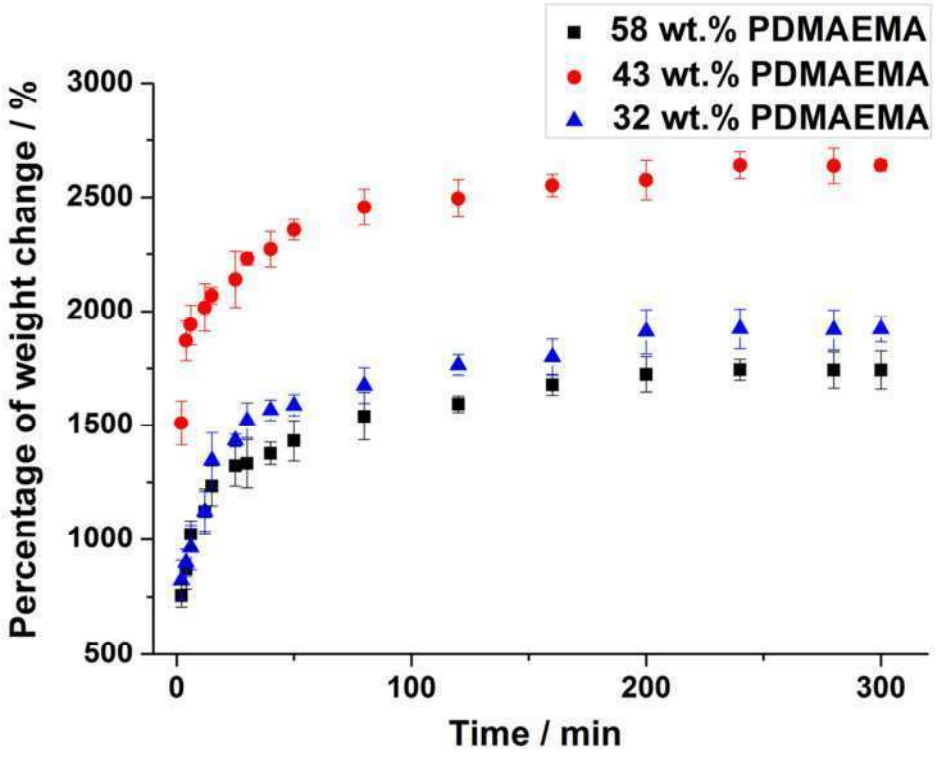

Figure 52: Water uptake efficiency of p(BMDO-*co*-HEMA-*graft*-DMAEMA) (32 wt.%, 43 wt.% and 58 wt.% PDMAEMA) with different PDMAEMA length.

Temperature Effect on Water Uptake Efficiency. Temperature can influence the water uptake efficiency as well. Experiments were carried out with sample 2 (43 wt.% PDMAEMA in graft polymer) at 4 °C, 25 °C and 50 °C (Figure 53). At 4 °C, poly(BMDO-*co*-HEMA-*graft*-DMAEMA) showed about 5% reduction in the maximum water uptake efficiency. The

water uptake speed is much faster at 25 °C and 50 °C than at 4 °C. At rt and 50 °C the polymer sample showed similar water uptake results, however water uptake was fastest at 50 °C. After only 2 min the water uptake was at 1630 wt.%. After 4 min it showed 2060 wt.% of water uptake.

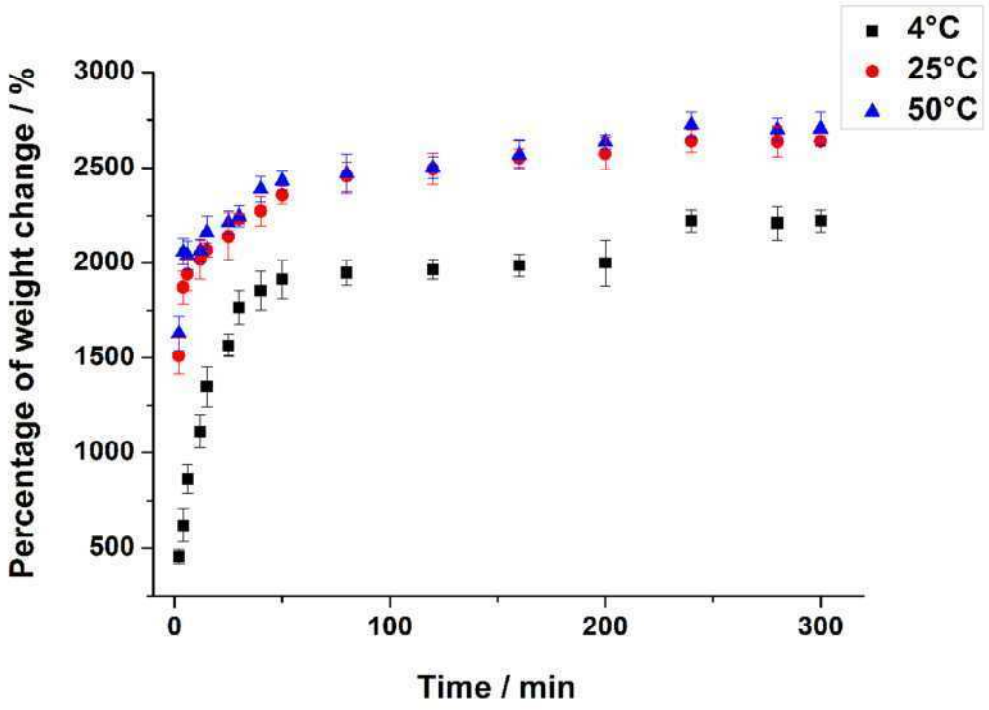

Figure 53: Water uptake efficiency of poly(BMDO-*co*-HEMA-*graft*-DMAEMA) (43 wt.% PDMAEMA) at different temperatures.

PH Depending Water Uptake. The pH dependent water uptake efficiency was tested using buffer solutions with different pH values (Figure 54). The test results showed that the water uptake efficiency can be controlled by different pH values. The water uptake increased with decreasing pH (Figure 55). At pH 5 the polymer could reach a maximum water uptake of 4430 wt.%. Within 2 min it could reach a water uptake of 2190 wt.% at pH 5. At pH 9 it was only 430 wt.% of water uptake after 2 min. The lower pH provides a high water uptake at a high speed. Figure 55 shows the same amount of poly(BMDO-*co*-HEMA-*graft*-DMAEMA) in buffer solutions with different pH values after 2 min. It is clearly visible, that the polymer at lower pH has the largest volume.

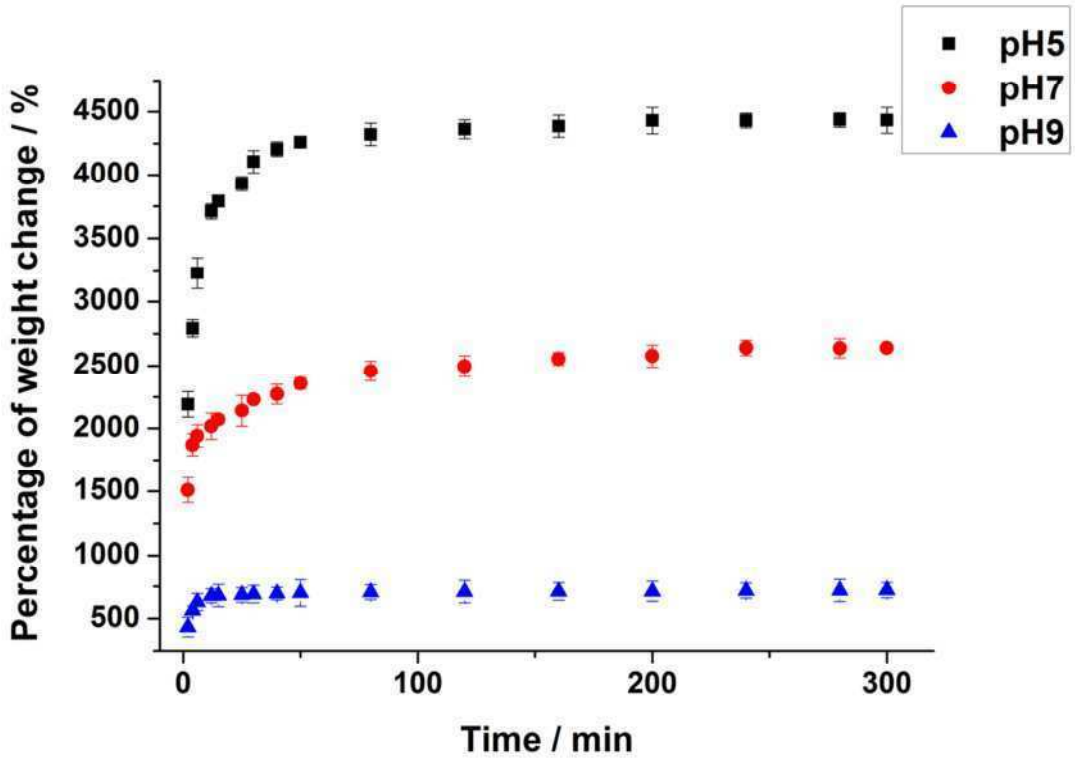

Figure 54: Water uptake efficiency of p(BMDO-*co*-HEMA-*graft*-DMAEMA) (43 wt.% PDMAEMA) in buffer solution with different pH values.

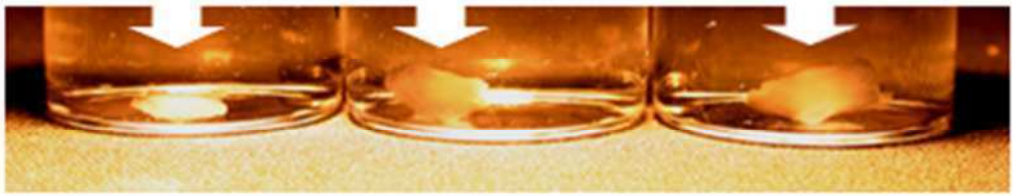

Figure 55: The morphology of poly(BMDO-*co*-HEMA-*graft*-DMAEMA) (43 wt.% PDMAEMA) in buffer solutions with different pH values after 2 min (pH value from left to right: 9, 7, 5).

The higher water absorption ability at lower pH is explained in Figure 56. At lower pH more of the amine groups on the polymer side chain are protonated than at higher pH. More hydrogen bonds can be formed between water and protonated amine groups. Because of this, water can be absorbed in the gaps between the side chains of the polymer. At lower pH the polymer chains are more stretched due to the water between the side chains and show a bigger volume than at higher pH.

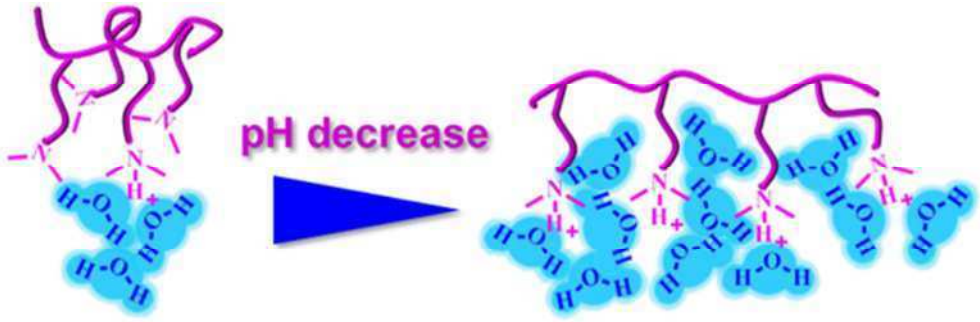

Figure 56: Illustration of water uptake efficiency at different pH values.

Repetitive Water Uptake. To further test the water uptake efficiency, experiment was performed using the same sample for 5 cycles. The sample was dried after treatment with buffer solution and treated again with the buffer solution (Figure 57). It showed a minimal reduction of water uptake efficiency after the first cycle. Then it reached a stable plateau. This shows, that the material can be reused as a water absorber.

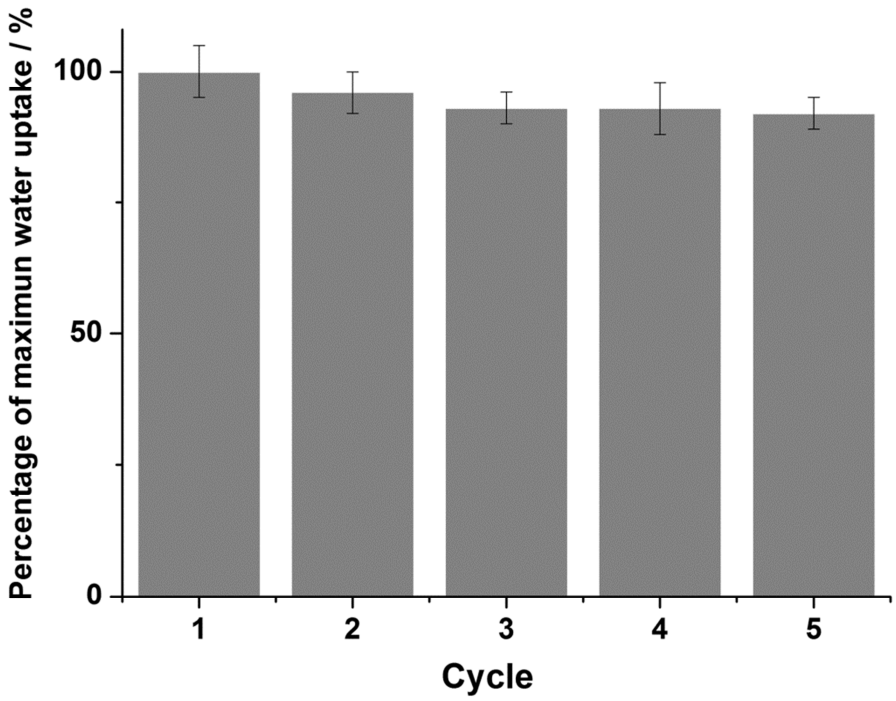

Figure 57: Water uptake efficiency repetition of poly(BMDO-*co*-HEMA-*graft*-DMAEMA) (43 wt.% PDMAEMA) in pH 7 buffer solution at rt for 5 cycles.

Compostability Test. The degradation of the graft polymer film was tested using the compost method. The weight loss was determined after 30, 90 and 120 days. The polymer film lost 3% weight after 30 days, after 90 days about 7%, after 120 days 9%. The images of the polymer film (43 wt.% PDMAEMA) before and after 120 days degradation (after drying) are shown in Figure 58. Conclusively, the polymer can be slowly degraded in compost.

Figure 58: Illustration of the polymer film (43 wt.% PDMAEMA) before and after 120 days (after drying) in compost at 45 °C.

Antibacterial Test. All of the grafted polymers poly(HEMA-*co*-BMDO-*graft*-DMAEMA) were tested for their antibacterial activity against representative Gram-negative *E. coli* bacteria and Gram-positive *Bacillus Subtilis*. The MIC and MBC values are shown in Figure 59.

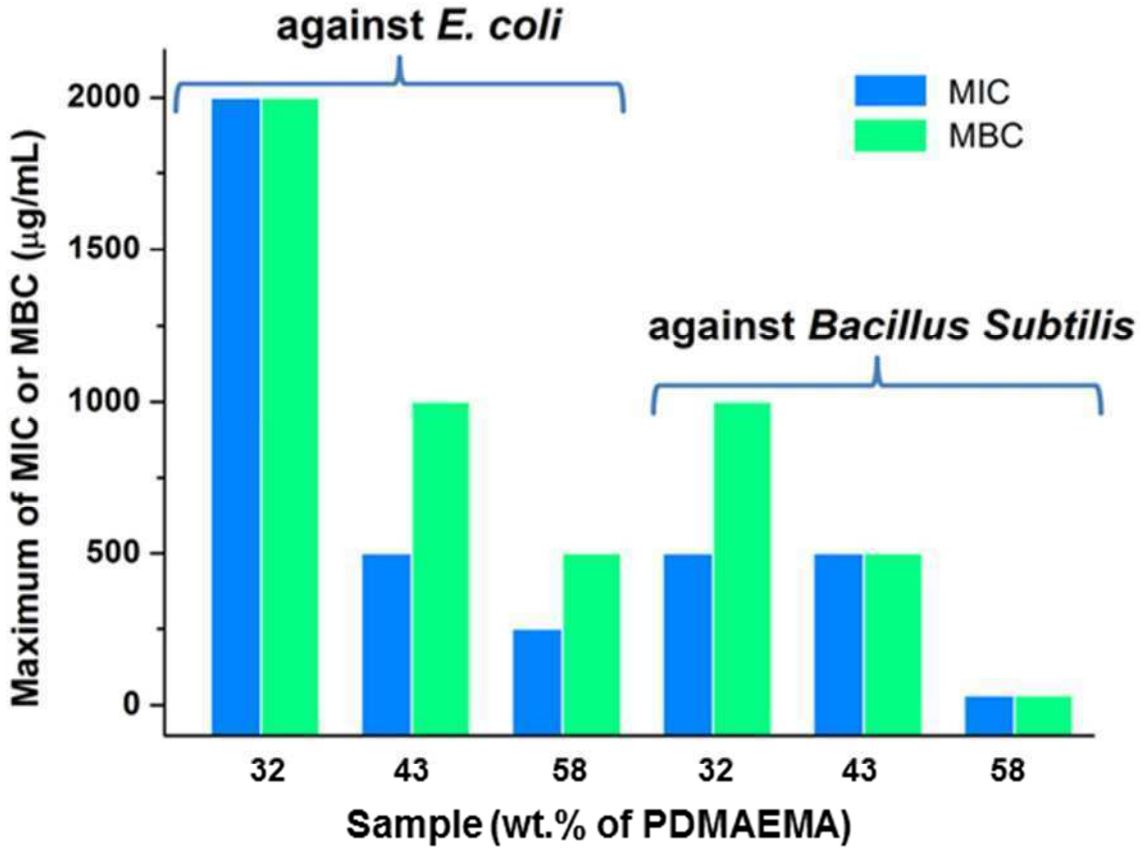

Figure 59: MIC and MBC values of poly(BMDO-*co*-HEMA-*graft*-DMAEMA) (32 wt.%, 43 wt.% and 58 wt.% PDMAEMA (samples 1, 2 and 3)) against *E. coli* and *Bacillus Subtilis*.

The sample 3 with 58 wt.% of DMAEMA showed the best antibacterial activity. It was antibacterial with a MBC against *E. coli* of smaller than 31.25 mg/mL, with a MBC against *Bacillus Subtilis* of also smaller than 31.25 mg/mL. It showed the optimal hydrophilic and hydrophobic balance for killing bacteria. All the polymers are antibacterial against both gram

negative and Gram-positive bacterial strains. The antibacterial activity against *Bacillus Subtilis* was better than against *E. coli* because of the additional membrane that has to be penetrated in Gram-negative bacteria.

The time dependent antibacterial test was performed with a polymer concentration of 2 mg/mL. All the synthesized polymers can kill more than 99.9% against *E. coli* within 1 min. Figure 60 shows that after contact for 1 min with 43 wt.% PDMAEMA grafted polymer, 99.91% of the bacteria were killed, after 30 min 99.99% of the bacteria were killed. Graft polymer with the highest amount of PDMAEMA on the side chain (58 wt.%) has the highest antibacterial effect. After 1 min contact with sample 3 more than 99.99% bacteria were killed.

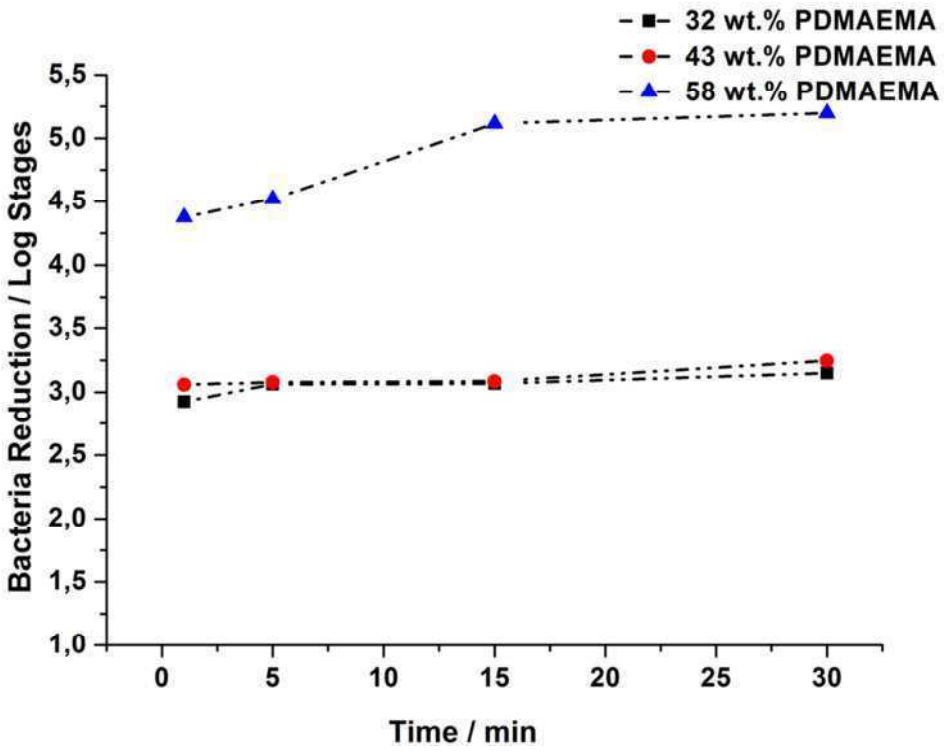

Figure 60: Time dependent antibacterial test against *E. coli*) (32 wt.%, 43 wt.% and 58 wt.% PDMAEMA (samples 1, 2 and 3)).

4.1.4 Conclusion

The aim of this study was to synthesize degradable polymers with high water absorption ability and antibacterial effect. Poly(BMDO-*co*-HEMA-*graft*-DMAEMA) was synthesized using a new macro ATRP initiator and shows up to 4430 wt.% of water uptake. The water uptake efficiency of the copolymers with different side chain PDMAEMA length was tested at different pH and temperature values. At higher temperature and at lower pH the polymer with 43 wt.% of DMAEMA on the side chain shows the highest water uptake efficiency. Poly(BMDO-*co*-HEMA-*graft*-DMAEMA) demonstrated high antibacterial activity against both *E. coli* and *Bacililus Subtilis* up to 31.25 µg/mL. The time dependent antibacterial test showed a 99.9% antibacterial activity within 1 min. Besides the high water absorption ability and high antibacterial activity, the polymers could also be slowly degraded under compost condition.

Chapter V: Summary

5.1 Summary

In this thesis degradable polymers for three different purposes, DNA transfection, drug delivery and antibacterial properties were designed, synthesized and characterized.

In the first part of the DNA transfection application the novel degradable and biocompatible poly(PEG-*co*-(BMDO-*co*-DMAEMA)) and its quaternized derivative poly(PEG-*co*-(BMDO-*co*-DMAEMA·EtBr)) were successfully synthesized and characterized. This copolymer shows a significant solubility improvement by introducing hydrophilic PEG blocks into the polymer backbone. The successful incorporation of ester linkages into the copolymer backbone led to a fast degradation of the copolymer under enzymatic and buffer conditions. All the synthesized copolymers show a low cytotoxicity. The unquaternized copolymers result in higher cell viability than the quaternized copolymers as well as positive results in p-DNA transfection.

In the second part of the DNA transfection application degradable and biocompatible poly(PEG-*co*-(MDO-*co*-DMAEMA)) and the quaternized derivative poly(PEG-*co*-(MDO-*co*-DMAEMA·EtBr)) were obtained also via free radical polymerization using PEG macro-azo-initiator. The presence of the PEG unit in the polymer backbone led to great improvement of the polymer solubility. The more reactive MDO leads to a higher ester content in the copolymer than with BMDO as monomer. After quaternization of poly(PEG-*co*-(MDO-*co*-DMAEMA), the solubility of the polymers as well as their complexation efficiencies were greatly improved. This highly biocompatible polymer shows a positive result in the gene transfection experiments in the presence of serum.

For the drug delivery application, a biocompatible and degradable functional polymer which is based on HEMA could be successfully synthesized by radical polymerization. The structure of the resulting polymers and the reaction kinetics was studied in this work. The cell viabilities were over 80 % even for very high polymer concentrations (100 mg/ml). The hydroxyl functionalized polymers are hydrolytically degradable under basic conditions and also show surface erosion and bulk degradation upon treatment with macrophages. A promising positive result is demonstrated for the use of such polymers for drug encapsulation. This new, well characterized biocompatible and degradable hydroxyl functionalized polymer could be suitable for many different biomedical applications.

For the antibacterial application, poly(BMDO-*co*-HEMA-*graft*-DMAEMA) with different DMAEMA side chain lengths was synthesized using a new macro ATRP initiator. A high water absorption ability of these copolymers can be observed. At higher temperature and lower pH the polymer with 43 wt.% of DMAEMA shows the highest water uptake efficiency. Poly(BMDO-*co*-HEMA-*graft*-DMAEMA) demonstrates great antibacterial activities against both *E. coli* and *Bacillus Subtilis* down to concentrations as low as 31.25 µg/mL. The time dependent antibacterial test shows that 99.9 % of the treated *E. coli* bacteria were killed within 1 minute. This polymer also presents slow degradation ability under compost condition.

5.2 Perspectives

This thesis was done particularly in regard to methods of design, synthesis and characterization and new materials have been made. Basic work for future projects has been carried out. Therefore a variety of possible research directions for further work has been obtained.

For the DNA transfection material project, the MDO and BMDO based polycationic gene vectors show positive results in DNA transfection experiments. An optimization of the different monomer ratios in the copolymer to enhance the transfection efficiency and to lower the cytotoxicity will be of great importance in the future. For further research, it is necessary to investigate DNA and RNA delivery into living cells.[108] The synthesized polymer shows degradation ability under physiological condition. Moreover, it is interesting to determine the *in vivo* degradation in animals.

For the drug delivery material project, the *in vitro* drug delivery efficiency was successfully performed using coumarin as model drug. Furthermore it will be very meaningful to investigate *in vitro* drug delivery tests with anticancer drugs like Paclitaxel. Afterwards it would be important to perform *in vivo* drug delivery tests for treatment of cancer.

For the antibacterial material project, a polymer with excellent water uptake efficiency and high antibacterial activity against gram positive and gram negative bacteria was obtained. These properties can be of use for example for wound dressing as well as hygienic products.[109] For these applications *in vitro* and *in vivo* test are necessary to determine the biodegradation products and to investigate whether it is non-antigenic. Other monomers can be incorporated in the polymer backbone to research their influence on the properties of the

crosslinked polymer, for example poly(*N*-acryloyl glycinamide) (NAGA) to introduce UCST to have a smart, antibacterial super absorber.[110]

5.3 Zusammenfassung

In dieser Arbeit wurden abbaubare Polymere für drei verschiedene Anwendungen designt, synthetisiert und charakterisiert: DNA-Transfektion, Wirkstofffreisetzungen und antibakterielle Materialien.

Im ersten Teil der DNA-Transfektion wurden das neuartige abbaubare und biokompatible Poly(PEG-*co*-(BMDO-*co*-DMAEMA)) und das quaternisierte Poly(PEG-*co*-(BMDO-*co*-DMAEMA·EtBr)) erfolgreich synthetisiert und charakterisiert. Durch die Einführung eines hydrophilen PEG-Blocks in das Polymerrückgrat konnte die Löslichkeit des Polymers in Wasser deutlich verbessert werden. Zusätzlich führte der erfolgreiche Einbau von Estergruppen in das Copolymerrückgrat zu einem schnellen Abbau des Copolymers unter enzymatischen und Pufferbedingungen. Alle synthetisierten Copolymere zeigten eine niedrige Zytotoxizität. Die quaternisierten Copolymere besaßen höhere IC_{50}-Werte mit L929 Zellen als die unquaternisierten Copolymere und lieferten positive Ergebnisse bei Versuchen zu den p-DNA-Transfektionen.

Im zweiten Teil der DNA-Transfektionen wurde das abbaubare und biokompatible Poly(PEG-*co*-(MDO-*co*-DMAEMA)) und das quaternisierte Polymer Poly(PEG-*co*-(MDO-*co*-DMAEMA·EtBr)) mittels radikalischer Polymerisation unter Verwendung des PEG-Makro-Azoinitiators synthetisiert. Die PEG-Einheit in der Polymerkette führte zu einer Verbesserung der Löslichkeit des Polymers. Die Verwendung des reaktiveren MDO an Stelle von BMDO als Monomer führte zu einem höheren Anteil an Esterbindungen im Copolymer. Nach der Quaternisierung von Poly(PEG-*co*-(MDO-*co*-DMAEMA)), zeigten die Polymere eine deutlich bessere Löslichkeit und Komplexierungseffizienz. Das biokompatible Polymer zeigte ein positives Ergebnis im Transfektionsexperiment in Gegenwart von Serum.

Für die Wirkstofffeisetzung wurde ein biokompatibles, funktionales und abbaubares Polymer, welches auf HEMA basiert Poly(BMDO-*co*-HEMA), erfolgreich durch radikalische Polymerisation synthetisiert. Die Struktur des resultierenden Polymers und die Reaktionskinetik wurden in dieser Arbeit untersucht. Die Überlebensrate der Zellen war höher als 80%, selbst bei sehr hohen Polymerkonzentrationen (100 mg/ml). Das hydroxyl-funktionalisierte Polymer wurde hydrolytisch unter basischen Bedingungen abgebaut und zeigte Oberflächenerosion und Bulk-Abbau bei Verwendung von Makrophagen. Ein vielversprechendes positives Ergebnis wurde für die Verwendung solcher Polymere für Wirkstoffverkapselung festgestellt. Dieses neue, gut charakterisierte, biokompatible und abbaubare hydroxyl-funktionalisierte Polymer ist potenziell für viele verschiedene biomedizinische Anwendungen geeignet.

Für die antibakterielle Anwendung wurde Poly(BMDO-*co*-HEMA-*graft*-DMAEMA) mit unterschiedlichen DMAEMA-Seitenkettenlängen unter Verwendung eines neuen Makro ATRP-Initiators synthetisiert. Eine hohe Wasseraufnahmefähigkeit dieses Copolymers konnte beobachtet werden. Bei höheren Temperaturen sowie einem niedrigeren pH-Wert zeigte das Polymers mit 43 wt.% DMAEMA an der Seitenkette die höchste Wasseraufnahmeeffizienz. Poly(BMDO-*co*-HEMA-*graft*-DMAEMA) zeigte eine hohe antibakterielle Aktivität gegen *E. coli* und *Bacililus Subtilis* bei Konzentrationen bis unter 31,25 µg/mL. Die zeitabhängigen antibakteriellen Tests ergaben eine antibakterielle Aktivität gegen *E. coli* von 99,9% innerhalb von 1 min. Dieses Polymer wies auch einen langsamen Abbau unter Kompostbedingungen auf.

6 References

(1) Crank, M.; Patel, M.; Marscheider-Weidemann, F.; Hüsing, B.; Angerer, G. *Techno-economic Feasibility of Large-scale Production of Bio-based Polymers in Europe*; **2005**; 1-260.

(2) Uhrich, K. E.; Cannizzaro, S. M.; Langer, R. S.; Shakesheff, K. M. *Chem. Rev.* **1999**, *99*, 3181-3198.

(3) Zaikov, G. E.; Livshits, V. S. *Pharm. Chem. J.* **1985**, *18*, 288-296.

(4) http://en.european-bioplastics.org/market/ Market _ european-bioplastics (accessed Jul 18, 2012).

(5) Gunatillake, P. a; Adhikari, R. *European cells & materials* **2003**, *5*, 1-16.

(6) Ikada, Y.; Tsuji, H. *Macromol. Rapid Commun.* **2000**, *21*, 117-132.

(7) Pouton, C. W.; Akhtarb, S. *Advanced drug delivery reviews* **1996**, *18*, 133-162.

(8) Shuai, X.; Merdan, T.; Unger, F.; Wittmar, M.; Kissel, T. *Macromolecules* **2003**, *36*, 5751-5759.

(9) http://www.bioplastics.basf.com/faq.html#1 ecoflex (accessed Jul 18, 2012).

(10) Lucas, N.; Bienaime, C.; Belloy, C.; Queneudec, M.; Silvestre, F.; Nava-Saucedo, J.-E. *Chemosphere* **2008**, *73*, 429-442.

(11) Bailey, W. J.; Ni, Z. *J. Polym. Sci., Part A: Polym. Chem.* **1982**, *20*, 3021-3030.

(12) Agarwal, S.; Kumar, R.; Kissel, T.; Reul, R. *Polym. J.* **2009**, *41*, 650-660.

(13) http://www.ornl.gov/sci/techresources/Human_Genome/medicine/genetherapy.shtml (accessed Jul 18, 2012).

(14) Anderson, W. F. *Science* **1992**, *256*, 808-813.

(15) Dalgleish, A. *Gene Ther.* **1997**, *4*, 629-630.

(16) Knoell, D. L.; Yiu, I. M. *Am J Health Syst Pharm* **1998**, *55*, 1998.

(17) Azzam, T.; Domb, A. J. *Curr. Drug Delivery* **2004**, *1*, 165-193.

(18) Mah, C.; Byrne, B. J.; Flotte, T. R. *Clini pharmacokinet.* **2002**, *41*, 901-911.

(19) Garnett, M. C. *Crit. Rev. Ther. Drug Carrier Syst.* **1999**, *16*, 147-207.

(20) Anwer, K.; Earle, K. a; Shi, M.; Wang, J.; Mumper, R. J.; Proctor, B.; Jansa, K.; Ledebur, H. C.; Davis, S.; Eaglstein, W.; Rolland, a P. *Pharm. Res.* **1999**, *16*, 889-995.

(21) Behr, J. P.; Demeneix, B.; Loeffler, J. P.; Perez-Mutul, J. *Proceedings of the National Academy of Sciences of the United States of America* **1989**, *86*, 6982-6986.

(22) Pertmer, T. M.; Roberts, T. R.; Haynes, J. R. *Journal of virology* **1996**, *70*, 6119-6125.

(23) Brumbach, J. H.; Lin, C.; Yockman, J.; Kim, W. J.; Blevins, K. S.; Engbersen, J. F. J.; Feijen, J.; Kim, S. W. *Bioconjugate Chem.* **2010**, *21*, 1753-1761.

(24) Wang, T.; Upponi, J. R.; Torchilin, V. P. *Int. J. Pharm.* **2012**, *427*, 3-20.

(25) Godbey, W. T.; Barry, M. a; Saggau, P.; Wu, K. K.; Mikos, a G. *Journal of biomedical materials research* **2000**, *51*, 321-328.

(26) Chen, T.-H. H.; Bae, Y.; Furgeson, D. Y.; Kwon, G. S. *Int. J. Pharm.* **2012**, *427*, 105-112.

(27) Zheng, M.; Liu, Y.; Samsonova, O.; Endres, T.; Merkel, O.; Kissel, T. *Int. J.Pharm.* **2012**, *427*, 80-87.

(28) Zhu, C.; Zheng, M.; Meng, F.; Mickler, F. M.; Ruthardt, N.; Zhu, X.; Zhong, Z. *Biomacromolecules* **2012**, *13*, 769-778.

(29) Legler, J.; van den Brink, C. E.; Brouwer, a; Murk, a J.; van der Saag, P. T.; Vethaak, a D.; van der Burg, B. *Toxicological sciences* **1999**, *48*, 55-66.

(30) Goldshtein, H.; Hausmann, M. J.; Douvdevani, A. *Annals of clinical biochemistry* **2009**, *46*, 488-494.

(31) http://products.invitrogen.com/ivgn/product/S11494 (accessed Jul 18, 2012).

(32) Ornitz, D. M.; Yayon, A.; Flanagan, J. G.; Svahn, C. M.; Levi, E.; Leder, P. *Mol. Cell. Biol.* **1992**, *12*, 240-247.

(33) Merkel, O. M.; Mintzer, M. A.; Librizzi, D.; Samsonova, O.; Dicke, T.; Sproat, B.; Garn, H.; Barth, P. J.; Simanek, E. E.; Kissel, T. *Molecular Pharmaceutics* **2010**, *7*, 969-983.

(34) Fotakis, G.; Timbrell, J. a *Toxicology letters* **2006**, *160*, 171-177.

(35) Charman, W. N.; Chan, H.-K.; Finnin, B. C.; Charman, S. a. *Drug Dev. Res.* **1999**, *46*, 316-327.

(36) Müller-Goymann, C. C. *European journal of pharmaceutics and biopharmaceutics* **2004**, *58*, 343-356.

(37) Reddy, P. D.; Swarnalatha, D. *Int.J. PharmTech Res.* **2010**, *2*, 2025-2027.

(38) Haag, R. *Angew. Chem. Int. Ed.* **2004**, *43*, 278-282.

(39) Tekade, R. K.; Dutta, T.; Tyagi, A.; Bharti, A. C.; Das, B. C.; Jain, N. K. *Journal of drug targeting* **2008**, *16*, 758-772.

(40) Lee, J. H.; Nan, A. *Journal of drug delivery* **2012**, 1-17.

(41) Torchilin, V. P. *Nature reviews. Drug discovery* **2005**, *4*, 145-160.

(42) Agnihotri, S. a; Mallikarjuna, N. N.; Aminabhavi, T. M. *J. Controlled Release* **2004**, *100*, 5-28.

(43) Soma, C. E.; Dubernet, C.; Bentolila, D.; Benita, S.; Couvreur, P. *Biomaterials* **2000**, *21*, 1-7.

(44) Song, X. R.; Zheng, Y.; He, G.; Yang, L.; Luo, Y. F.; He, Z. Y.; Li, S. Z.; Li, J. M.; Yu, S.; Luo, X.; Hou, S. X.; Wei, Y. Q. *J. Pharm. Sci.* **2010**, *99*, 4874-4879.

(45) Langer, R. *Science* **1989**, *249*, 1527-1533.

(46) Fakhrai, H.; Dorigo, O.; Shawler, D. L.; Lin, H.; Mercola, D.; Black, K. L.; Royston, I.; Sobol, R. E. *Proc. Natl. Acad. Sci. U.S.A.* **1996**, *93*, 2909-2914.

(47) Spear, M. a; Herrlinger, U.; Rainov, N.; Pechan, P.; Weissleder, R.; Breakefield, X. O. *J. NeuroVirol.* **1998**, *4*, 133-147.

(48) Takamiya, Y.; Short, M. P.; Ezzeddine, Z. D.; Moolten, F. L.; Breakefield, X. O.; Martuza, R. L. *J. Neurosci. Res.* **1992**, *33*, 493-503.

(49) Kabanov, A. V.; Felgner, P. L.; Seymour, L. J. In *Self-assembling complexes for gene delivery - From Laboratory to Clinical Trial*; Wiley: NY, 1998; pp. 115-167.

(50) Felgner, P. L.; Heller, M. J.; Lehn, P.; Behr, J. P.; Szoka, J. F. C. In *Am. Chem. Soc*; Oxford University Press: Washington, USA, 1996; pp. 177-190.

(51) Rolland, A. In *Advanced Gene Delivery*; Harwood Academic Publishers: The Netherlands, 1999; pp. 103-190.

(52) Chesnoy, S.; Huang, L. *STP Pharma Sci. 9*, 5-12.

(53) Neu, M.; Fischer, D.; Kissel, T. *J. Gene Med.* **2005**, *7*, 992-1009.

(54) Cherng, J. Y.; Wetering, P. van de; Talsma, H.; Daan, J. A. C.; Hennink, W. E. *Pharm. Res.* **1996**, *13*, 1038-1042.

(55) Arigita, C.; Zuidam, N. J.; Crommelin, D. J. A.; Hennink, W. E. . *Pharm. Res.* **1999**, *16*, 1534-1541.

(56) van de Wetering, P.; Cherng, J.-Y.; Talsma, H.; Hennink, W. E. *J. Controlled Release* **1997**, *49*, 59-69.

(57) Jones, R. a; Poniris, M. H.; Wilson, M. R. *J. Controlled Release* **2004**, *96*, 379-391.

(58) Verbaan, F. J.; Klein Klouwenberg, P.; van Steenis, J. H.; Snel, C. J.; Boerman, O.; Hennink, W. E.; Storm, G. *Int. J. Pharm.* **2005**, *304*, 185-192.

(59) Cherng, J. Y.; Talsma, H.; Verrijk, R.; Crommelin, D. J.; Hennink, W. E. *Eur. J. Pharm. Biopharm.* **1999**, *47*, 215-224.

(60) You, Y.-Z.; Manickam, D. S.; Zhou, Q.-H.; Oupický, D. *J. Controlled Release* **2007**, *122*, 217-225.

(61) Agarwal, S.; Ren, L.; Kissel, T.; Bege, N. *Macromol. Chem. Phys.* **2010**, *211*, 905-915.

(62) Petersen, H.; Fechner, P. M.; Martin, A. L.; Kunath, K.; Stolnik, S.; Roberts, C. J.; Fischer, D.; Davies, M. C.; Kissel, T. *Bioconjugate Chem.* **2002**, *13*, 845-854.

(63) Zheng, M.; Liu, Y.; Samsonova, O.; Endres, T.; Merkel, O.; Kissel, T. *Int. J.Pharm.* **2012**, *427*, 80-87.

(64) Zhang, Y.; Zheng, M.; Kissel, T.; Agarwal, S. *Biomacromolecules* **2012**, *13*, 313-322.

(65) Wickel, H.; Agarwal, S. *Macromolecules* **2003**, *36*, 6152-6159.

(66) Samsonova, O.; Pfeiffer, C.; Hellmund, M.; Merkel, O. M.; Kissel, T. *Polymers* **2011**, *3*, 693-718.

(67) Mosmann, T. *J. Immunol. Methods* **1983**, *65*, 55-63.

(68) Beck-Broichsitter, M.; Thieme, M.; Nguyen, J.; Schmehl, T.; Gessler, T.; Seeger, W.; Agarwal, S.; Greiner, A.; Kissel, T. *Macromol. Biosci.* **2010**, *10*, 1527-35.

(69) Wickel, H.; Agarwal, S.; Greiner, A. *Macromolecules* **2003**, *36*, 2397-2403.

(70) Liu, Y.; Steele, T.; Kissel, T. *Rapid Commun.* **2010**, *31*, 1509-1515.

(71) Kunath, K.; Merdan, T.; Hegener, O.; Häberlein, H.; Kissel, T. *J. Gene Med.* **2003**, *5*, 588-599.

(72) Grayson, A. C. R.; Doody, A. M.; Putnam, D. *Pharm. Res.* **2006**, *23*, 1868-1876.

(73) Grigsby, C. L.; Leong, K. W. *J. R. Soc., Interface* **2010**, *7*, 67-82.

(74) Mao, S.; Neu, M.; Germershaus, O.; Merkel, O.; Sitterberg, J.; Bakowsky, U.; Kissel, T. *Bioconjugate Chem.* **2006**, *17*, 1209-1218.

(75) Merkel, O. M.; Librizzi, D.; Pfestroff, A.; Schurrat, T.; Buyens, K.; Sanders, N. N.; De Smedt, S. C.; Béhé, M.; Kissel, T. *J. Controlled Release* **2009**, *138*, 148-159.

(76) Bronich, T.; Kabanov, A. V.; Marky, L. a. *J. Phys. Chem. B* **2001**, *105*, 6042-6050.

(77) Malek, A.; Czubayko, F.; Aigner, A. *Journal of drug targeting* **2008**, *16*, 124-139.

(78) Agarwal, S.; Kumar, R. *Macromol. Chem. Phys.* **2011**, *212*, 603-612.

(79) Cohen, L. E.; Rocco, A. M. *Journal of Thermal Analysis* **2000**, *59*, 625-632.

(80) Grabe, N.; Zhang, Y.; Agarwal, S. *Macromol. Chem. Phys.* **2011**, *212*, 1327-1334.

(81) Casadio, Y. S.; Brown, D. H.; Chirila, T. V.; Kraatz, H.-B.; Baker, M. V. *Biomacromolecules* **2010**, *11*, 2949-2959.

(82) Dziubla, T. D.; Torjman, M. C.; Joseph, J. I.; Murphy-Tatum, M.; Lowman, a M. *Biomaterials* **2001**, *22*, 2893-2899.

(83) Hsiue, G. H.; Guu, J. a; Cheng, C. C. *Biomaterials* **2001**, *22*, 1763-1769.

(84) Andac, M.; Plieva, F. M.; Denizli, A.; Galaev, I. Y.; Mattiasson, B. *Macromol. Chem. Phys.* **2008**, *209*, 577-584.

(85) Atzet, S.; Curtin, S.; Trinh, P.; Bryant, S.; Ratner, B. *Biomacromolecules* **2008**, *9*, 3370-3377.

(86) Khelfallah, N. S.; Decher, G.; Mésini, P. J. *Macromol. Rapid Commun.* **2006**, *27*, 1004-1008.

(87) Ren, L.; Speyerer, C.; Agarwal, S. *Macromolecules* **2007**, *40*, 7834-7841.

(88) Agarwal, S. *Polymer Chemistry* **2010**, *1*, 953.

(89) Ren, L.; Agarwal, S. *Macromol. Chem. Phys.* **2007**, *208*, 245-253.

(90) Beers, K. L.; Boo, S.; Gaynor, S. G.; Matyjaszewski, K. *Macromolecules* **1999**, *32*, 5772-5776.

(91) Robinson, K. L.; Khan, M. a.; de Paz Báñez, M. V.; Wang, X. S.; Armes, S. P. *Macromolecules* **2001**, *34*, 3155-3158.

(92) Oh, J. K.; Matyjaszewski, K. *J. Polym. Sci., Part A: Polym. Chem.* **2006**, *44*, 3787-3796.

(93) Kelen, T.; Tudos, F.; Turcsanyi, B. *J. Polym. Sci., Part A: Polym. Chem.* **1977**, *15*, 3047-3074.

(94) Kelen, T. *Polymer Bulletin* **1980**, *2*, 71-76.

(95) Oster, C. G.; Wittmar, M.; Bakowsky, U.; Kissel, T. *J. Controlled Release* **2006**, *111*, 371-381.

(96) Park, E. K.; Kim, S. Y.; Lee, S. B.; Lee, Y. M. *J. Controlled Release* **2006**, *112*, 145-146.

(97) Hennink, W. E.; van Nostrum, C. F. *Advanced drug delivery reviews* **2002**, *54*, 13-36.

(98) http://www.sciencephoto.com/media/133827/enlarge (accessed Jul 18, 2012).

(99) Rawlinson, L.-A. B.; Ryan, S. M.; Mantovani, G.; Syrett, J. a; Haddleton, D. M.; Brayden, D. J. *Biomacromolecules* **2010**, *11*, 443-453.

(100) Jin, X.; Shen, Y.; Zhu, S. *Macromol. Mater. Eng.* **2003**, *288*, 925-935.

(101) Xiong, Q.; Ni, P.; Zhang, F.; Yu, Z. *Polymer Bulletin* **2004**, *53*, 1-8.

(102) Mattheis, C.; Zheng, M.; Agarwal, S. *Macromol. Biosci.* **2012**, *12*, 341-349.

(103) Roorda, W. E.; Bouwstra, J. a; de Vries, M. a; Junginger, H. E. *Biomaterials* **1988**, *9*, 494-499.

(104) Zhang, Y.; Dafeng, C.; Mengyao, Z.; Kissel, T.; Seema, A. *Polymer Chemistry* **2012,** DOI:10.1039/c2py20403g.

(105) Gan, L.-huat; Ravi, P.; Mao, B. A. O. W. E. I.; Tam, K.-chiu *J. Polym. Sci., Part A: Polym. Chem.* **2003**, *41*, 2688-2695.

(106) Zhang, X.; Matyjaszewski, K. *Macromolecules* **1999**, *32*, 1763-1766.

(107) Mattheis, C.; Schwarzer, M. C.; Frenking, G.; Agarwal, S. *Macromol. Rapid Commun.* **2011**, *32*, 994-999.

(108) Kumagai, M.; Shimoda, S.; Wakabayashi, R.; Kunisawa, Y.; Ishii, T.; Osada, K.; Itaka, K.; Nishiyama, N.; Kataoka, K.; Nakano, K. *J. Controlled Release* **2012**, *160*, 542-551.

(109) Corkhill, P. H.; Hamilton, C. J.; Tighe, B. J. *Biomaterials* **1989**, *10*, 3-10.

(110) Seuring, J.; Bayer, F. M.; Huber, K.; Agarwal, S. *Macromolecules* **2012**, *45*, 374-384.

7 Appendices

7.1 Abbreviations

AIBN	azobisisobutyronitrile
AMP	adenosine monophosphate
ATP	adenosine triphosphate
BMDO	5,6-benzo-2-methylene-1,3-dioxepane
c	concentration
CAN	acetonitrile
CKA	cyclic ketene acetal
CLSM	confocal laser scanning microscopy
DLS	dynamic light scattering
DMAEMA	*N, N*-dimethylaminoethyl methacrylate
DMSO	dimethyl sulfoxide
DNA	deoxyribonucleic acid
DSC	differential scanning calorimetry
E. coli	Escherichia coli
GPC	gel permeation chromatography
HEMA	(hydroxyethyl)methacrylate
HEPES	2-[4-(2-hydroxyethyl)-1-piperazinyl]ethanesulfonic acid
HMBC	heteronuclear multiple bond coherence
HMQC	heteronuclear multiple quantum coherence
hy	hyperbranched
IC_{50}	half-inhibitory concentration
MBC	minimum bactericidal concentration
MDO	2-methylene-1,3-dioxepane
MIC	minimum inhibitory concentration
min	miunite
M_n	number-average molecular weight
mol%	molar percentage
MTT	3-(4,5-dimethylthiazol-2-yl)-2,5-diphenyltetrazolium bromide

M_w	weight-average molecular weight
N/P ratio	nitrogen to phosphate ratio
NAGA	poly(*N*-acryloyl glycinamide)
NMR	nuclear magnetic resonance
NP	nanoparticle
PBS	phosphate buffered saline
PCL	polycaprolactone
PDI	polydispersity index
p-DNA	plasmid DNA
PEG	polyethylenglycol
PEI	polyethylenimine
pKa	acidic association constant, -lg(Ka)
PLGA	poly(lactic-*co*-glycolic acid)
r	reactivity ratio
RNA	ribonucleic acid
rpm	revolutions per minute
rt	room temperature
siRNA	short interfering RNA
SS	disulfide
T_g	glass transition temperature
TGA	thermogravimetric analysis
TMS	trimethylsilyl
UCST	upper critical solution temperature
wt.%	weight percentage

7.2 Curriculum Vitae

PERSONAL INFORMATION

Name:	Yi Zhang
Address:	Berliner Straße 10 35039 Marburg
Place of Birth:	Beijing, China

EDUCATION

02/10 – 09/12 **Philipps-University Marburg**
PhD thesis in Macromolecular Chemistry in the work group of Prof. Dr. Seema Agarwal

- Title: „ Novel degradable polymeric materials for biomedical and antibacterial applications “

04/04 – 10/09 **Philipps-University Marburg**
Chemistry Study

- Diploma thesis in Macromolecular Chemistry in the work group of Prof. Dr. Seema Agarwal

  Topic: „Untersuchungen zur kontrollierten Ringschlusspolymerisation von DADMAC mittels ATRP und RAFT“
- Degree as a Diploma Chemist
- Prediploma in August 2006

7.3 List of Publications (Yi Zhang)

7.3.1 Articles

1. **Zhang, Y.**; Zheng, M.; Kissel, T.; Agarwal, S., Design and Biophysical Characterization of Bioresponsive Degradable Poly(dimethylaminoethyl methacrylate) based Polymers for *In Vitro* DNA Transfection. *Biomacromolecules* **2012**, *13*, 313-322.
2. Grabe, N.; **Zhang, Y.**; Agarwal, S., Degradable Elastomeric Block Copolymers based on Polycaprolactone by Free-Radical Chemistry. *Macromol. Chem. Phys.* **2011**, *212*, 1327-1334.
3. **Zhang, Y.**; Chu, D., Zheng, M., Kissel, T., Agarwal, S., Biocompatible and Degradable Poly(2-hydroxyethyl methacrylate) based Polymers for Biomedical Applications. *Polymer Chemistry* **2012.** DOI:10.1039/c2py20403g.
4. Agarwal, S., **Zhang, Y.**, Maji, S., Greiner, A., Poly(2-dimethylaminoethyl methacrylate) based Polymer-DNA Nanocomplexes as Promising Gene Delivery Materials. *Materials Today* **2012**. Accepted
5. Mattheis, C., **Zhang, Y.**, Agarwal, S., Thermo-Switchable Antibacterial Activity. *Macromolecular Bioscience* **2012.** Accepted
6. Chu, D., Curdy, C., Riebesehl, B., **Zhang, Y.**, Beck-Broichsittera, M., Kissel, T., Mechanisms of Surface Degradation of Poly(ethylene carbonate) Probed by Cholesterol Esterase, Superoxide Anion Radicals and Macrophages. *Biomaterials* **2012**. Submitted
7. **Zhang, Y.**, Aigner, A., Agarwal, S., Synthesis and Characterization of *N,N*-Dimethylaminoethyl Methacrylate based Degradable and Biocompatible Polymers as DNA Transfection Agents. Prepared

7.3.2 Poster Presentations

Seema Agarwal, Normen Grabe, **Yi Zhang**: *Degradable Elastomeric Polycaprolactone Using Free-radical Chemistry*. Europolymer conference, University of Milan, Gargnano, Italy, May 29th- June 3rd 2011

Yi Zhang, Seema Agarwal: *Synthesis of New Degradable and Biocompatible Polymers for Medical Applications.* Bayer AG PhD Student Course, Bayer AG, Leverkusen, Germany. July 10th-14th 2011

Yi Zhang, Seema Agarwal: *Novel Degradable Polymers for Gene Transfection.* Materialforschungstag Mittelhessen. Philipps-Universität Marburg, Germany, July 10th 2012

8 Acknowledgment

At first I wish to sincerely thank my doctoral advisor Prof. Dr. Seema Agarwal.

I want to thank her for the provision of this greatly interesting and interdisciplinary topic and for the intensive care and support during my PhD thesis. Above all I thank her for the full support and the trust during the construction of the biolab. Without it many of the experiments necessary for this dissertation would have not been possible. I am also very grateful for the opportunity to participate in international conferences, exhibitions and meetings with representatives of industry. This allowed me to gain new experiences and establish many contacts. Furthermore I thank her for the appliance of the first survey.

I wish to thank Prof. Dr. Joachim H. Wendorff for the appliance of the second survey.

I would also like to express my gratitude to Prof. Dr. Andreas Greiner for the numerous fertile discussions and constructive suggestions.

I am thanking Prof. Dr. Thomas Kissel for the fruitful cooperation and the energetic support. Thanks to him I could expand my expertise towards biology and pharmacy. Additionally I thank his whole group for the exceptionally hospitable admission at the institute. A special thanks goes to Mrs. Eva Mohr and Dr. Susanne Rösler for transfer of skills concerning the handling of cell cultures.

Prof. Dr. Achim Aigner, thank you for the successful cooperation within the framework of the MDO project, in particular for carrying out the cell culture experiments and the interpretation of results.

I thank all members of the work groups Agarwal and Greiner for the pleasant working environment, nice conversations and effective teamwork.

A special thanks goes to Dr. Michael Bognitzki for his advice regarding synthetic problems.

I thank Christian Heel for performing the chloroform GPC measurements and proofreading my work.

Thanks to Fabian Mitschang for DMF GPC measurements.

Hui Wang, Claudia Mattheis and Kathrin Becker, thank you for performing the antibacterial tests.

I thank my current and former laboratory colleagues Tina Krieg, Johanna Otto, Dominic Keller, Oliver Hauenstein, Mats Knoop, Licheng Tan and Samarendra Maji for the wonderful time in the lab 4411 and their great team spirit.

I want to acknowledge Uwe Justus, Lisa Hamel, Martina Gerlach and Edith Schmidt for their expert assistance in infrastructural, organizational and technical matters.

I thank the electrical, glass and precision mechanic's workshop for their willingness to help with small and big problems.

I thank Catarina Nardi Tironi and Melissa Koehn for the great time at work.

Thanks to Ilka Paulus, Catarina Nardi Tironi, Dr. Ronald Wagner, Oliver Hauenstein, Holger Pletsch and Claudia Mattheis for proofreading of my thesis.

My special thanks goes to my mother Luju Li and the rest of the family, who always unconditionally supported and encouraged me. I hope that I can give them back something in the future.